

**MATERIAL DESIGN FOR ORGANIC
THIN FILM TRANSISTORS**

**MATERIAL DESIGN AND INTERFACIAL ENGINEERING
FOR HIGH-PERFORMANCE ORGANIC
THIN FILM TRANSISTORS**

By PING LIU

**A Thesis Submitted to the School of Graduate Studies
in Partial Fulfillment of the Requirements for
the Degree of Doctor of Philosophy**

McMaster University © Copyright by Ping Liu, December 2011

DOCTOR OF PHILOSOPHY (2011) **McMaster University**
(CHEMICAL ENGINEERING) **Hamilton, Ontario**

TITLE: Material Design and Interfacial Engineering for
High-Performance Organic Thin Film Transistors

AUTHOR: Ping Liu
M. Sc. (Queen’s University, Kingston, Ontario)
Member of Researcher Staff (Xerox Research
Centre of Canada)

SUPERVISORS: Dr. Shiping Zhu (McMaster University)
Dr. Yiliang Wu (Xerox Research Centre of
Canada)
Dr. Beng S. Ong (Xerox Research Centre of
Canada)

NUMBER OF PAGES: 134

Abstract

Organic thin film transistors (OTFTs) have attracted great attention in the last couple of decades due to their potential of cost reductions in manufacturing low-end electronic devices through solution processes. Currently, one of the major challenges facing the field of OTFTs is lack of high performance functional organic materials including both organic semiconductors and gate dielectrics for effective device integrations by solution deposition technologies. This thesis focuses on material designs, interfacial compatibilities, and device integrations for high performance OTFTs.

Research progresses in the following areas are presented in this thesis. First, novel liquid-crystalline organic semiconductors, 2,5'-bis-[2-(4-pentylphenyl)vinyl]-thieno(3,2-*b*) thiophene and 2,5'-bis-[2-(4-pentylphenyl)vinyl]-(2,2')bithiophene for OTFT applications were developed. Mobilities of the OTFTs fabricated from these semiconductors reached 0.15 cm²/V.s with high environmental stability. Such high performance is attributed to their ability to form highly ordered molecular structures. Second, a simple effective approach was developed for tuning solubility of a high mobility polythiophene system through engineering its molecular structure. OTFTs fabricated with the newly developed copolythiophenes from an environmentally benign non-chlorinated solvent showed excellent performance with mobility up to 0.18 cm²/V.s. Third, an effective approach to a solution processed gate dielectric

design was developed for all solution-processed flexible OTFTs. This was achieved through a dual-layer dielectric structure design comprised of a bottom layer with a UV-crosslinked poly(4-vinyl phenol-co-methyl methacrylate), (PVP-PMMA), and a top layer with a thermally crosslinked polysiloxane. This solution-processed dual-layer dielectric structure enabled all solution-processed high performance flexible OTFTs. Finally, flexible OTFTs were successfully integrated on plastic substrates (PET) from non-chlorinated solvents by using the copolythiophenes and the dual-layer dielectric. The integrated flexible devices showed good OTFT characteristics with mobility up to about $0.1 \text{ cm}^2/\text{V}\cdot\text{s}$, well defined linear and saturated regions, and a close to zero turn-on voltage.

Preface

This thesis is presented in a ‘**sandwich thesis**’ format with three published papers in the following refereed journals and one manuscript prepared for publication in the journal *Materials Science and Engineering B*.

Paper 1

Reprinted with permission from *Chem. Mater.* **2009**, *21*, 2727–2732.

Copyright 2009, American Chemical Society.

Novel High-Performance Liquid-Crystalline Organic Semiconductors for Thin-Film Transistors, P. Liu, Y. Wu, H. Pan, Y. Li, S. Gardner, B. S. Ong, S. Zhu, *Chem. Mater.* **2009**, *21*, 2727–2732.

Paper 2

Reprinted with permission from *Macromolecules*, **2010**, *43*, 6368–6373.

Copyright 2010, American Chemical Society.

High-Performance Polythiophene Thin-Film Transistors Processed with Environmentally Benign Solvent, P. Liu, Y. Wu, H. Pan, B. S. Ong, S. Zhu, *Macromolecules*, **2010**, *43*, 6368–6373.

Paper 3

Reprinted with permission from *J. Am. Chem. Soc.* **2006**, *128*, 4554–4555.

Copyright 2006, American Chemical Society.

Enabling Gate Dielectric Design for All Solution-Processed, High-Performance, Flexible Organic Thin-Film Transistors, P. Liu, Y. Wu, Y. Li, B. S. Ong, S. Zhu, *J. Am. Chem. Soc.* **2006**, *128*, 4554–4555.

Manuscript

Integration of Solution Processed Flexible OTFTs from Non-Chlorinated Solvents

To be submitted for the journal of *Materials Science and Engineering B*

The results presented in this thesis were obtained during my Ph.D. studies under the supervision of Dr. Beng. S. Ong (Sept 2005 to March 2007), Dr. Yiliang Wu, and Dr. Shiping Zhu from September 2005 to December 2011. To the best of my knowledge, the research approaches and results presented in this thesis are unique and original.

I was primarily responsible for the molecular structure design, synthetic work, material characterization, and manuscript preparation presented in this thesis. My supervisors Dr. Yiliang Wu, Dr. Beng S. Ong, and Dr. Shiping Zhu provided valuable supervision and support for my research work and they also helped me in revision of the manuscripts. Dr. Yiliang Wu gave me great assistance and guidance for the fabrication and characterization of OTFTs. Dr. Hualong Pan and Ms Sandra Gardner helped me with single-crystal and thin-film XRD analyses. Dr. Yuning Li provided valuable discussions for the material synthetic work, while he was working at Xerox Research Centre of Canada.

Acknowledgements

This dissertation would not have been possible without the support from many people. I would like to express my deep gratitude to Xerox Research Centre of Canada (XRCC), especially Hadi Mahabadi, Paul Smith, Patricia Burn, and Nan-Xing Hu for providing me the opportunity to pursue a doctoral degree at McMaster University on a part-time basis. I would like to thank my supervisory committee, Dr. Shiping Zhu, Dr. Carlos Filipe, Dr. Yiliang Wu, and Dr. Beng S. Ong for their professional guidance and support throughout my graduate study. Dr. Zhu as the chair of the supervisory committee has provided me with inspiration and mentorship for my research endeavor. Dr. Carlos Filipe provided his continuous support and invaluable discussions. Dr. Yiliang Wu and Dr. Beng S. Ong provided their support and guidance throughout my thesis work at XRCC. My special thanks go to Dr. Jim Britten in the Department of Chemistry at McMaster University for helping me analyze my samples for the structure conformation with his expertise in XRDs. Many thanks go to my project teammates and friends at XRCC for giving me the support when I needed it most. I enjoyed many discussions with my friend Yu Qi and I appreciate her willingness to share her thoughts with me. My special thanks also go to Sandra Gardner, Rosa Duque, Sonja Hadzidedic, Asfaw Biritawit, and Gail Song for their assistance with my sample analysis and characterization. I would also like to thank XRCC librarian Gordana

Pavlovic for her assistance on the literature search and the publication release for my thesis papers. I would also like to thank many friends in Dr. Zhu's research lab, especially Hualong Pan, Mary Jin, Helen Gu and Wei Feng for their great friendship and assistance. Finally, I am grateful to my family, my husband Yue and my son, Richard and Peter, for their understanding and support throughout my graduate study.

Table of Contents

Abstract	iii
Preface	v
Acknowledgements	vii
Table of Contents	ix
List of Figures	xii
List of Tables	xv
Declaration of Academic Achievements	xvi
Chapter 1 Introduction	1
1.1 Background	1
1.2 Organic Thin Film Transistors	4
1.2.1 Device Geometry and Operating Principle	4
1.2.2 Characterization of Organic Thin Film Transistors	6
1.2.3 A Brief Literature Review on Organic Thin Film Transistors	8
1.2.3.1 Organic Semiconductors	9
1.2.3.1.1 Small Molecular Organic Semiconductors	10
1.2.3.1.2 Polymeric Semiconductors	12
1.2.3.1.3 Summary	16
1.2.3.2 Gate Dielectric and Interface Compatibility	18
1.2.3.2.1 Introduction to OTFT Gate Dielectric Materials	18
1.2.3.2.2 Inorganic Dielectrics and Surface Modification	19
1.2.3.2.3 Polymeric Dielectrics and Effect of Interface Compatibility	22
1.2.3.2.4 Summary	27
1.3 Research Objective and Thesis Outline	28
1.4 Contributions to the Field	30
1.5 References	32

Chapter 2 Materials, Instrumentation and Measurement	35
2.1 Introduction	35
2.2 Materials	35
2.3 Instrumentation and Measurement	35
2.3.1 NMR	35
2.3.2 UV-Vis	35
2.3.3 GPC	36
2.3.4 DSC	36
2.3.5 CV	36
2.3.6 XRD	36
2.4 General Procedures for OTFT Fabrication and Characterization	37
2.4.1 General Procedures for OTFT Fabrication	37
2.4.2 Characterization of OTFTs	39
Chapter 3 Novel Stable Liquid Crystalline Organic Semiconductors	41
3.1 Introduction	41
3.2 Main Text of Paper 1: Novel High-Performance Liquid-Crystalline Organic Semiconductors for Thin-Film Transistors	42
3.3 Supporting Materials for the Paper	66
3.4 Summary	67
Chapter 4 Novel Copolythiophene Semiconductors	68
4.1 Introduction	68
4.2 Main Text of Paper 2: High-Performance Polythiophene Thin-Film Transistors processed with Environmentally Benign Solvents	69
4.3 Supporting Materials for the Paper	93
4.4 Summary	94

Chapter 5 Robust Gate Dielectric Design	95
5.1 Introduction	95
5.2 Main Text of Paper 3: Enabling Gate Dielectric Design for All Solution-processed, High-Performance, Flexible Organic Thin-Film Transistors	96
5.3 Supporting Materials for the Paper	108
5.4 Summary	112
Chapter 6 Integration of Solution Processed Flexible OTFTs from Non- Chlorinated Solvents	113
6.1 Introduction	113
6.2 Manuscript: All Solution Processed Flexible Organic Thin-Film Transistors from Non-Chlorinated Solvents	114
6.3 Summary	128
Chapter 7 Summary and Outlook	129
7.1 Summary	129
7.2 Outlook	131

List of Figures

Chapter 1

- Figure 1. Schematic illustrations of OTFT configurations. 4
- Figure 2. Illustrations of OTFT characterizations: (a) output curves; (b) transfer curves. 7
- Figure 3. Chemical structures of pentacene and α -sexithiophene. 10
- Figure 4. Chemical structures of functionalized pentacene derivatives. 11
- Figure 5. Schematic illustrations of (a) Regiorandom poly(3-alkylthiophene); (b) Regioregular poly(3-alkylthiophene). 14
- Figure 6. Structure of solution-processable regioregular poly(3,3''-dialkyl quaterthiophenes), PQT. 15
- Figure 7. Chemical structure of poly(2,5-bis(3-alkylthiophene-2-yl)thieno[3,2-*b*]thiophene), PBTFT. R=C₁₀H₂₁, C₁₂H₂₅, C₁₄H₂₉. 16
- Figure 8. Schematic illustrations of the progress of most significant organic semiconductors developed during the last two decades. 17
- Figure 9. Chemical structures of some polymers used as OTFT dielectrics. 22
- Figure 10. Schematic illustration of the carrier localization enhancement due to polar insulator interface. 25
- Figure 11. Thermal ring-opening and successive 4+2 Diels-Alder cycloaddition/polymerization BCB monomer. 26

Chapter 2

- Figure 1. Photograph of Keithley 4200 SCS semiconductor characterization system. 39

Chapter 3

- Figure 1. UV-Vis spectra of compounds **7** and **8**. **a** and **b** represent **7** and **8** in chlorobenzene solution, respectively; **c** and **d** represent their thin films of **7** and **8** on glass substrates, respectively. 46
- Figure 2. Thermal ellipsoid plots (prepared at the 30% probability level) of single-crystal structure of **8** (viewed down thiophene plane). 47

- Figure 3. Schematic view of the molecular packing of compound **8** as seen down the b-axis. (Hydrogen atoms are not shown for clarity.) 48
- Figure 4. X-ray diffraction patterns of 100-nm thin films: (a) thin film of compound **8** at room temperature; (b) to (e) compound **7** with substrate temperature at room temperature, 40, 60, 80 °C, respectively. 49
- Figure 5. DSC thermograms of compound **7** and **8**. **7** (black line); **8** (red line). 50
- Figure 6. Polarized optical microscopic images of compound **8** at (a) 50 °C, (b) 150 °C, (c) 170 °C, (d) 220 °C, (e) 260 °C, respectively; and compound **7** at (f) 220 °C, (g) 325 °C, respectively. 52
- Figure 7. OTFTs characteristics of an exemplary with vacuum-deposited compounds **7** and **8** as channel semiconductors (substrate at 60 °C, channel length 90 μm and channel width 5000 μm): (a) Output curves at various gate voltages for compound **7**; (b) a transfer curve for compound **8** in the saturated regime at a constant $V_{DS} = -40$ V and the square root of the absolute value of the current as a function of the gate voltage. 54
- Supporting Materials for the paper**
- Figure S1. Cyclic voltammetric curves of **7** (a) and **8** (b). 66
- Figure S2. Transfer curves of an OTFT device with compound **7** as the semiconductor layer. The device has a channel length of 190 μm and a channel width of 1000 μm. Red curve, fresh device which showed a mobility of 0.15 cm²/V.s; blue curve, aged device stored in the dark under ambient air for 2 years, showing a mobility of 0.077 cm²/V.s. 66
- Chapter 4**
- Figure 1. Coating solution stability of **2** (**PQT**) in dichlorobenzene (0.3 wt%), **3** (**PQT-CH₃**) and copolythiophene **4a** (x=10 mol%, y=90 mol%) in xylene (1.0 wt%). 75
- Figure 2. Single crystal structures of **monomer B** (a, c) and **monomer A** (b, d) (a, b: view along outer thiophene plane; c, d: view along inner thiophene plane.) 76

Figure 3. UV-Vis absorption spectra of thin films spin cast from 2 (blue), 3 (black), and 4a (red).	77
Figure 4. XRDs of 4a , (a) 0.2 μm thin film without annealing; (b) 0.2 μm thin film annealed at 140°C; B. XRDs of 3 , (c) 0.2 μm thin film without annealing; (d) 0.2 μm thin film annealed at 120°C.	78
Figure 5. Phase transition temperatures of 2 (PQT), 3 (PQT-CH ₃) and 4(a-c) on heating.	79
Figure 6. Mobility as a function of the molar percentage of the monomer for 2 (PQT) in the copolythiophene.	81
Figure 7. I-V characteristics of exemplary copolymer 4a TFT device with 90- μm channel length and 5000- μm channel width: (a) output curves at different gate voltages; (b) transfer curve at linear regime.	82
Supporting Materials for the Paper	
Figure S1. ¹ H NMR (CDCl ₃) spectrum for copolymer 4c (x=50 mol%, y=50 mol%).	93
Chapter 5	
Figure 1. Schematic depiction of formation of poly(methyl silsesquioxane) from methyltrimethoxysilane and its incorporation as a dielectric top layer in an all-solution processed organic thin film transistor device on PET.	100
Figure 2. (a) Source-drain current versus source drain voltage at different gate voltages for an OTFT with dual-layer gate dielectric. (b) Source-drain current versus gate voltage at a source-drain voltage of -60 V for OTFTs with different gate dielectrics: dual-layer dielectric, black line; OTS-8-modified UV cured-PVP-PMMA dielectric, blue line; UV-cured PVP-PMMA dielectric, red line. (Channel length = 90 μm ; channel width = 1000 μm).	102
Supporting Materials for the Paper	
Figure S1. Forward and reverse scans of I-V characteristics at a source-drain voltage of -40 V for a typical OTFT with the dual-layer gate dielectric.	112

Chapter 6

Figure 1. Schematic configurations of flexible OTFTs: (a) top-contact; (b) bottom-contact. 116

Figure 2. (a) Source-drain current versus source-drain voltage at different gate voltages; (b) Source-drain current versus gate voltage at a source-drain voltage of -40 v for OTFTs with the 10 mol% of PQT-CH₃ copolythiophene. 122

List of Tables

Chapter 1

Table 1. Field-effect mobility values from vacuum deposited oligothiophenes. 12

Table 2. Performance of pentacene OTFTs with different gate dielectric layers. 20

Table 3. Performance of typical all-organic TFTs from 25 nm α -sexithienyl semiconducting layer with different dielectric materials. 23

Chapter 3

Table 1. Summary of OTFT mobility and current on/off ratio with compounds **7** and **8** as semiconductor at various substrate temperatures. 54

Chapter 4

Table 1. Summary of enthalpy data, OTFT mobility, and current on/off ratio with **2** (PQT), **3** (PQT-CH₃) and **4(a-c)** as a semiconductor layer. 81

Chapter 5

Table 1. Water contact angle and device performance of the OTFTs with different dielectrics. 101

Chapter 6

Table 1. Mobility and current on/off ratio for both top and bottom-contact OTFTs from the copolythiophenes containing 10 mol% and 50 mol% of PQT-CH₃ with both evaporated-gold and printed-silver source/drain electrodes. 123

Declaration of Academic Achievement

This thesis research was focused on the development of functional organic materials and the integration of solution processed flexible organic thin film transistors. The main academic achievements include the following:

First, a class of novel liquid crystalline organic semiconductors was developed for OTFT applications. The OTFTs fabricated with this type of organic semiconductors showed excellent air stability and OTFT performance. In addition, such organic semiconductors have great potentials for electronic device applications where transparent OTFTs are required since their thin film absorption peaks appear mainly in the range of ultraviolet region. Second, a series of new copolythiophenes were successfully developed for improving the solubility of a high performance polythiophene (PQT) system through a judicious structure modification. They showed excellent solubility and allowed the OTFT fabrications from more environmentally friendly non-chlorinated solvents while excellent OTFT properties were still maintained. Third, a robust dual-layer gate dielectric comprising a UV-cured poly(4-vinyl phenol-co-methyl methacrylate) (PVP-PMMA) bottom layer and a thermally cross-linked poly(methyl silsesquioxane) (PMSSQ) top layer was developed for solution processed flexible electronic applications. This high performance dual-layer gate dielectric is robust, resistant to common organic solvents, and comparable with most polythiophene semiconductors and it is particularly suitable for all solution processed flexible

OTFTs on plastic substrates. Finally, this study has demonstrated that all solution-processed flexible OTFTs can be successfully integrated with the developed copolythiophenes and the dual-layer dielectric on PET substrates from non-chlorinated solvents. The integrated top-contact flexible OTFTs have showed good OTFT characteristics with mobility up to about $0.1\text{cm}^2/\text{V}\cdot\text{s}$.

In conclusion, this thesis research made significant contributions in the development of organic semiconductors and gate dielectrics for OTFT applications. More specifically, the developed copolythiophene semiconductors and the cross-linked dual-layer gate dielectric structure enable us to integrate solution-processed flexible OTFTs without using environmentally hazardous chlorinated solvents.

Chapter 1

Introduction

1.1 Background

Field-effect transistor is one of the key fundamental components for integrated circuits, which is widely used in the semiconductor industry for electronic products such as televisions, computers, displays, data storage devices, and sensors. Conventional field-effect transistors use single-crystal silicon as semiconductor material and their electrical performance is excellent. Single-crystal silicon based transistor has high field-effect mobility of about $1000 \text{ cm}^2/\text{V}\cdot\text{s}$, which is suitable for applications of high speed electronic circuits. However, single-crystal silicon based transistors are mechanically brittle, and the device fabrication process requires high temperature, typically up to about $1000 \text{ }^\circ\text{C}$.¹ In addition, single crystal silicon has a limited maximum diameter size only up to about 30 cm (e.g. 12 inch wafer) with high prices, which posts challenge for large-area device integration. Therefore, single-crystal silicon transistor technology is not ideal for today's broad market space in large-area electronic panel displays and low-end electronic devices that only require moderate electronic performance.

The thin-film transistors (TFTs) used in the current flat panel display industry are produced by hydrogenated amorphous silicon (a-Si:H) technology.

Amorphous silicon is manufactured by plasma enhanced chemical vapor deposition process where a mixture of organic silane (SiH_4) and hydrogen in a high vacuum chamber is excited by plasma to form a thin layer of hydrogenated amorphous silicon on a heated substrate. The thin film transistors can be fabricated on a large area substrate with much lower temperature of about $300\text{ }^\circ\text{C}$, compared to the fabrication temperature for single-crystal silicon transistors ($\sim 1000\text{ }^\circ\text{C}$). Such a low fabrication temperature makes it possible for using cheap glasses as substrate materials. The mobility of hydrogenated amorphous silicon thin film transistor is in the order of about $1\text{ cm}^2/\text{V}\cdot\text{s}$, which is much lower than the mobility of about $1000\text{ cm}^2/\text{V}\cdot\text{s}$ for single crystal silicon transistor due to the lack of a long range structure order. However, such level of mobility is sufficient for a broad range of electronic applications. Amorphous silicon thin film transistor addressed active matrix liquid crystal displays (AMLCDs) currently dominate worldwide productions for large screen televisions and computer monitors. As the market of large panel displays accelerated and the technology of AMLCDs advanced, large sized a-Si:H TFT addressed LCD displays up to around 100" have been produced by major electronic companies. For example, Philips announced a 100" LCD television in August 2006² and Sharp made a 108" LCD panel in January 2007.

Although the electronic properties of amorphous silicon thin film transistors can meet the requirements for broad range of electronic applications, especially for high-end electronic products, some challenges still remain. One of

the major concerns is the cost incurred from production in low-end electronic device applications. The manufacturing cost of amorphous silicon TFTs is cheaper than that of single-crystal silicon transistors, however it is still considered to be high for certain ultra low-end electronic products since it involves a high cost plasma-enhanced chemical vapor deposition on a heated substrate (~300 °C) in vacuum. The initial investment for such facilities with ultra clean rooms and high vacuum machinery systems is very high and it increases substantially with the size. Another major concern is that most plastic materials cannot be used as a substrate for flexible electronic applications because most of them cannot be processed at such high temperatures.

Researchers in both academia and industry have been searching for new semiconductors and technologies intensively to reduce the manufacturing cost for thin film transistor fabrications in recent years and organic thin film transistors (OTFTs) have received much attention.⁴⁻⁶ One of the rationality is that organic semiconductors can be designed with desired solubility for solution processes, thus OTFTs can be fabricated at a much lower manufacturing cost using solution processable technologies such as spin coating, roll-to-roll manufacturing solution coating, or even inkjet printing for large-area and low-end electronic applications.⁷⁻⁹ Another rationality is that most OTFTs can be fabricated at much lower temperature compared to silicon transistors, and thus they are likely compatible with plastic substrates for applications in flexible electronic devices such as flexible panel displays, curved displays and electronic papers.¹⁰

1.2 Organic Thin Film Transistors

1.2.1 Device Geometry and Operating Principle

Organic thin film transistors have four basic device geometries as shown in Figure 1, where (a) represents bottom gate with top contact configuration; (b) represents bottom gate with bottom contact configuration; (c) represents top gate with bottom contact configuration; and (d) represents top gate with top contact configuration.

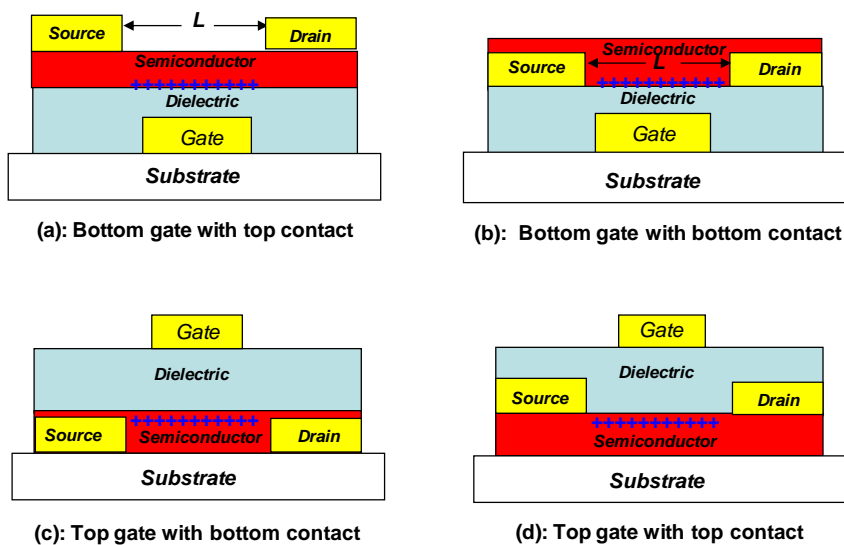


Figure 1. Schematic illustrations of OTFT configurations: (a) Bottom gate with top contact; (b) Bottom gate with bottom contact, (c) Top gate with bottom contact; and (d) Top gate with top contact.

As illustrated in Figure 1, the source and drain electrodes are deposited on the top of semiconductor active layer for the top contact geometries (a) and (d);

while the source and drain electrodes are deposited at the bottom of semiconductor active layer for the bottom contacted geometries (b) and (c). Among these four device geometries, the bottom gate with top contact geometry is most commonly used by researchers since high quality heavily n-doped silicon wafer substrates with a thin layer of thermally grown SiO₂ as gate dielectric layer are commercially available. Thus, organic semiconductors can be easily deposited on the top of thermally grown SiO₂ dielectrics by various deposition techniques including solution depositions for polymeric semiconductors and vacuum depositions for most small organic semiconductors.

OTFTs with top gate and bottom contact geometry (Figure 1c) allow depositions of source and drain electrodes directly on any substrates such as glasses and flexible plastics. This geometry is particularly convenient for use of solution deposition techniques such as inkjet printing for the fabrication of source and drain electrodes with solution-processable conductive inks. OTFTs with top gate and top contact geometry (Figure 1d) allow the deposition of a semiconductor layer on any substrates first. However, the deposition of a dielectric layer directly on the top of a semiconductor layer for top gate OTFTs usually presents a big challenge because certain damages of organic semiconductor layer often occur, especially when dielectrics are solution processed.

A typical organic thin film transistor consists of three basic components: an active semiconductor layer, a dielectric layer, and conductive electrodes. In

general, OTFTs with p-type organic semiconductor layer conduct positive charges in active semiconductor layer. When a negative voltage is applied to the gate electrode, gate-induced positive charge carriers are formed in the organic semiconductor layer close to the interface between dielectric and semiconductor layers. These positive charge carriers can flow through the semiconductor layer, forming a conducting channel near the dielectric-semiconductor interface when the source-drain voltage (V_D) is applied. Thus, a source-drain current (I_D) can be generated. The charge carrier density created in the semiconductor layer for conducting can be modulated by gate voltage (V_G), and the source-drain current (I_D) can be modulated by source-drain voltage (V_D). Therefore, the source-drain current (I_D) is a function of both gate voltage (V_G) and source-drain voltage (V_D).

1.2.2 Characterization of Organic Thin Film Transistors

The electrical properties of OTFTs are illustrated in Figure 2, which shows a typical output curve (a) and a transfer I-V curve (b). The output curve shows a plot of drain current (I_D) vs. drain voltage (V_D) at different gate voltages; and the transfer curve shows a plot of drain current (I_D) vs. gate voltage (V_G) at a constant source-drain voltage (V_D). Among many electronic characteristics, field-effect mobility (μ) and current on/off ratio ($I_{on/off}$) are the two most important parameters for the performance of OTFTs.

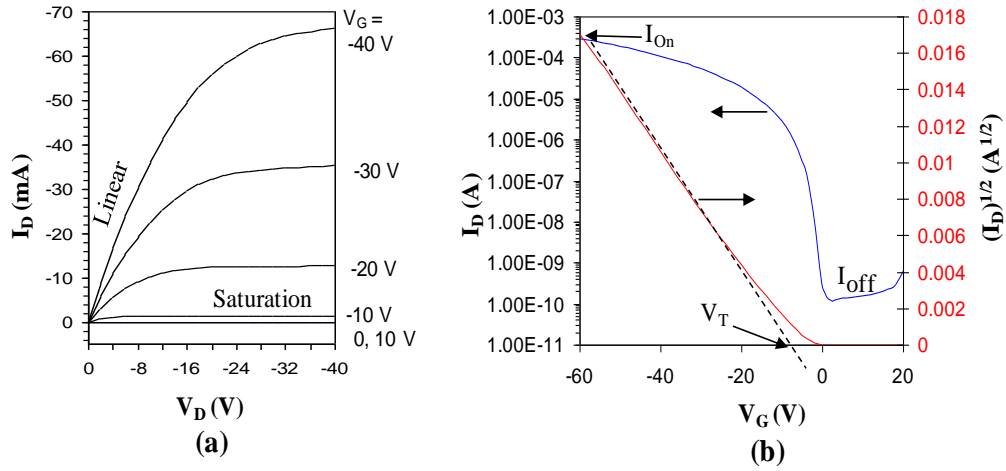


Figure 2. Illustration of OTFT characterization: (a) output curves; (b) transfer curves.

Field-effect mobility (μ) is defined as an average rate of the charge movement in active semiconductor layer through a unit electric field. The higher the mobility value, the higher the switching speed for OTFTs.¹¹ Generally, there are two operating regimes for functional OTFTs including a linear regime and a saturate regime. The field-effect mobility (μ) in the linear and saturated regions can be extracted from the following equations:

$$\text{Linear regime } (V_D \ll V_G): I_D = \mu C_i (W/L)(V_G - V_T)V_D$$

$$\text{Saturated regime } (V_D > V_G): I_D = \mu C_i (W/2L) (V_G - V_T)^2$$

where W and L are channel width and length respectively; V_G and V_D are gate voltage and drain voltage, respectively; C_i is capacitance per unit area of the gate dielectric layer; V_T is threshold voltage that can be determined from the relationship between the square root of I_D at the saturated regime and V_G of the device by extrapolating the measured data to $I_D = 0$.

On-off current ratio ($I_{\text{on/off}}$) is defined as a ratio of current at “on” state (when a gate voltage applied, $V_G \neq 0$) to the current at “off” state (no gate voltage V_G applied, $V_G = 0$). If the semiconductor layer is pure and not oxidized or doped, there are very little mobile charge carriers accumulated in the semiconductor layer, thus I_{off} should be very small. The OTFTs must produce sufficient current (I_{on}) to switch another part of a circuit when a gate voltage is applied, but they must not generate off current (I_{off}) that is large enough to cause an unwanted switching.

At present, single crystalline silicon transistors have mobility of about $1000 \text{ cm}^2/\text{V}\cdot\text{s}$, which is widely used in computer processor and electronic memory. Amorphous silicon ($\alpha\text{-Si}$) has mobility of $0.5\text{-}1.0 \text{ cm}^2/\text{V}\cdot\text{s}$, which is widely used in active matrix liquid crystal displays that dominate large LCD panel display industry. Certain organic semiconductors have reached the level of amorphous silicon. Molecular ordering of organic semiconductors, properties of gate dielectrics and interface compatibilities play critical roles for the high performance of OTFTs.

1.2.3 A Brief Literature Review on Organic Thin Film Transistors

Literatures on the topic of OTFTs are intensive and broad. Here I do not intend to give a broad review of OTFTs. Instead, I would give a brief review on

the literatures more related to my research studies in this thesis including both organic semiconductors and dielectrics on their effects on OTFTs performance.

1.2.3.1 Organic Semiconductors

Organic semiconductors play a dominant role on the performance of OTFTs. Unlike inorganic materials such as metals and crystalline silicon that have excellent ability to conduct electricity, most organic materials are electrical insulators. However, following the initial discovery of polyacetylene conductivity by Shirakawa et al. (1977),¹² organic semiconductor materials have attracted great attentions. Although it has been a great challenge in developing high mobility organic semiconductors with compatible performance to amorphous silicon semiconductor, significant progresses have been made in new organic semiconductors for OTFT applications, especially in the past two decades.^{4-6,13,14} In general, there are two types of organic semiconductor materials, small molecules and polymers. Most small molecule semiconductors have poor solubility and therefore most OTFTs fabricated from small molecule semiconductors were obtained only by vacuum deposition. On the other hand, polymeric semiconductors are more soluble and thus they can be fabricated by solution depositions. The following is a brief review of some important progress in organic semiconductors for OTFT applications in recent years.

1.2.3.1.1 Small Molecular Organic Semiconductors

Small molecular semiconductor materials based on pentacene and thiophene have been intensively studied by several research groups. Figure 3 shows molecular structures of pentacene and α -sexithiophene.

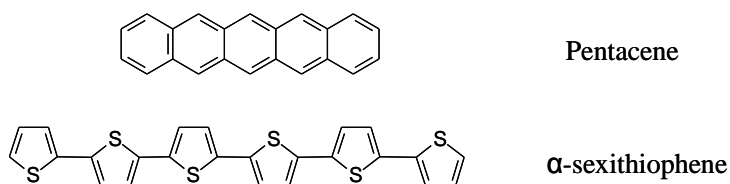


Figure 3. Chemical structures of pentacene and α -sexithiophene.

These molecular structures contain highly conjugated π -orbital systems, which has a significant impact on electrical conductivity because electrons in such conjugated π -orbital systems are mobile.

Pentacene has been one of the most important organic semiconductors for OTFTs since the early 1990s, and it has an excellent potential to achieve high field-effect mobility (μ) because of the presence of a highly conjugated five-fused benzene-ring structure. On the other hand, pentacene has very poor solubility in most organic solvents and thus its thin film was usually fabricated through vacuum depositions. With the extensive studies especially over the last two decade, the mobility (μ) of OTFTs fabricated with a vapor-deposited pentacene semiconductor layer has been improved significantly from $0.002 \text{ cm}^2/\text{V}\cdot\text{s}$ in 1992¹⁵ to about $5 \text{ cm}^2/\text{V}\cdot\text{s}$ in 2003, exceeding the mobility of amorphous silicon.¹⁶

This dramatic enhancement in mobility was achieved through dielectric layer interface modification, which will be discussed later in the section regarding the gate dielectric interface properties.

Furthermore, a class of functionalized pentacene derivatives with significantly improved solubility in certain organic solvents was developed by Anthony's research group as shown in Figure 4.¹⁷ The mobility of OTFTs fabricated with solution deposition from these pentacene derivatives reached 1 cm²/V.s.

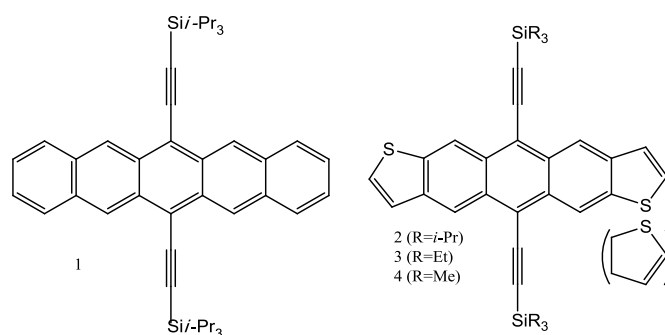
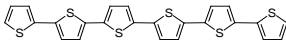
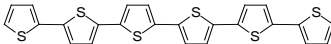
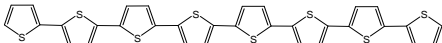
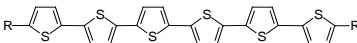


Figure 4. Chemical structures of functionalized pentacene derivatives.¹⁷

Another class of small molecule semiconductors is oligothiophene derivatives, which have attracted much attention over the past two decades.¹⁸⁻²¹ Conjugated oligothiophenes, most notably α -sexithiophene (α -6T) and its derivatives, have been investigated for OTFT applications. Significant improvements on the field effect mobility in OTFTs have been made over the years and the detailed results are shown in Table 1. The dramatic enhancements

on the mobility were achieved through optimizations of chemical structures and the dielectric interface modification leading to highly ordered organic crystalline thin films.

Table 1. Field-effect mobility values from vacuum deposited oligothiophenes.

Year	Oligothiophene semiconductors	Mobility (cm ² /V.s)	I _{on} /I _{off}
1989	 α-sexithiophene (α-6T) ¹⁸	0.001	Not reported
1991	 α-sexithiophene (α-6T) ¹⁹	0.01	Not reported
2000	 α-octithiophene (α-8T) ²⁰	0.3	Not reported
2003	 α,ω-dialkyl thiophene oligomers ²¹	1.1	10 ⁴

1.2.3.1.2 Polymeric Semiconductors

Most small molecule semiconductors such as pentacene and thiophene based derivatives are often difficult to form thin films with good quality by solution depositions. However compared to small molecules, most polymeric materials have advantages in forming more uniform thin films by solution deposition methods such as spin coating, dip coating and printing. This attractive

property is particularly useful for fabricating large area electronics. For high performance OTFTs, polymeric semiconductors must first have good solubility to allow solution processing for low cost manufacturing fabrication. Second, they must have the ability to form highly ordered molecular structures for efficient charge carrier transport, which is essential for high mobility. Furthermore, they must have sufficient stability against oxygen doping to allow the fabrication of OTFTs under ambient conditions. Although it has been a great challenge to find polymeric semiconductors that meet all of these critical requirements, progresses have been made in the recent years. In particular, polythiophene-based polymeric semiconductors have been widely studied by many research groups and the field-effect mobility has been improved significantly over the years since the first field effect transistor was fabricated with polythiophene as semiconductor channel by Tsumura et al in 1986.²²

Regioregular poly(3-hexylthiophene), P3HT, was discovered as the first solution processable polythiophene semiconductor with good mobility ($0.045 \text{ cm}^2/\text{Vs}$) by Bao et al in 1996, where OTFTs were fabricated in the presence of air.²³ Further significant improvement in the performance was made with mobility reaching $0.1 \text{ cm}^2/\text{Vs}$ and current on/off ratio of 10^6 when OTFTs were fabricated in nitrogen atmosphere.²⁴ It has been found that regioregularity of the molecular structure has significant effect on the field-effect mobility. Poly(3-alkylthiophenes) has two structural configurations: regiorandom and regioregular,²⁵ as shown in Figure 5. Regiorandom poly(3-alkylthiophenes) has a

number of irregular linkages at the 2 and 5 positions of the alkyl substituted thiophene ring, referred to head-to-head (H-H), head-to-tail (H-T), and tail-to-tail (T-T) couplings (Figure 5a). In contrast, regioregular poly(alkylthiophenes) contains only head-to-tail (H-T) coupling (Figure 5b). It has longer effective π - π conjugation length along the polymer backbone and thus better ability to form much ordered molecular structures in solid states. The regioregular H-T poly(3-alkylthiophene) shows much better OTFT performance.

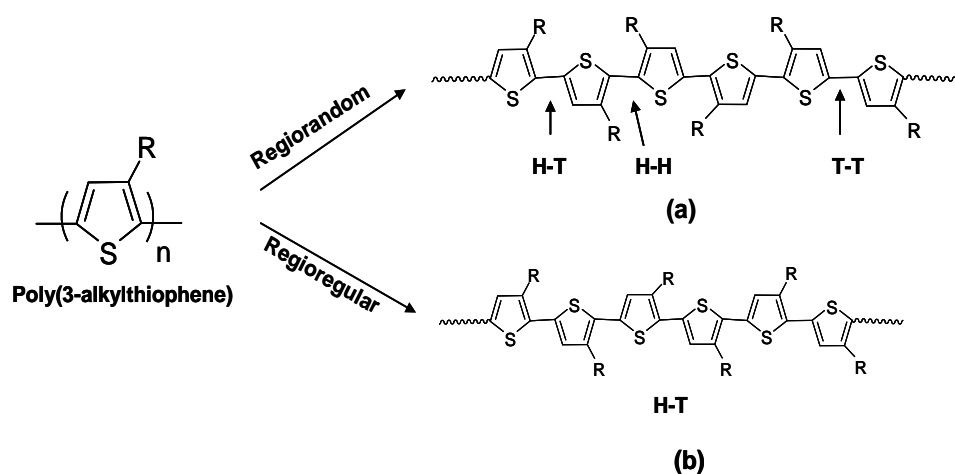


Figure 5. Schematic illustrations of (a) Regiorandom poly(3-alkylthiophene); (b) Regioregular poly(3-alkylthiophene).

Although the mobility of regioregular P3HT could reach to 0.1 when OTFTs were fabricated in nitrogen atmosphere, its mobility and on/off current ratio were significantly lower when the OTFT devices were fabricated in ambient condition and the transistor characteristics degraded rapidly after the devices were exposed to air.²³ Extensive study of regioregular P3HT by optical spectroscopy,

X-ray, and light scattering analyses suggested that all the thiophene rings along polymer backbone are coplanar with π - π stacking in a lamellar structural order through intermolecular side-chain self-alignment.²⁶⁻²⁷ These studies indicated that highly ordered thin films from the regioregular polythiophene-based system are necessary in order to obtain high mobility. On the other hand, this highly ordered conjugated coplanar conformation in the thin film could also cause a rapid degradation of OTFT performance in ambient condition.

A much more stable high performance polythiophene-based semiconductor, poly(dialkylquaterthiophene) (PQT) was developed at Xerox in 2004,²⁸ and the structure of PQT is shown in Figure 6. OTFTs from solution processed PQT-12 (where R is dodecyl) as semiconductor layer exhibited excellent OTFT characteristics with high mobility of $0.15 \text{ cm}^2/\text{V}\cdot\text{s}$ and current on/off ratio of 10^6 , where OTFTs were fabricated under ambient conditions with excellent stability. The improved stability against oxidative doping in ambient condition was achieved through proper control of the effective extended π -conjugation length along polymer backbone.

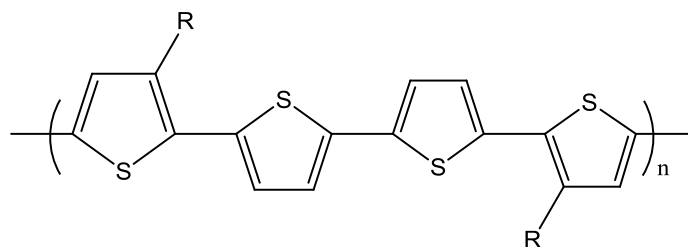


Figure 6. Structure of solution-processable regioregular poly(3,3''-dialkylquaterthiophenes), PQT.

More recently, another high performance regioregular polythiophene, poly(2,5-bis(3-alkylthiophene-2-yl)thieno[3,2-b]thiophene), PBTTT, was developed at Merck by McCulloch et al.(2006),²⁹ and the structure of PBTTT is shown in Figure 7. The chemical structure of PBTTT is very similar to PQT, except that a fused thiophene (thieno) unit was incorporated in the middle of the repeating unit. The field effect mobility of this type of polythiophenes reached as high as 0.2–0.6 cm²/V.s in nitrogen atmosphere. The enhancement in the field effect mobility was achieved through both of its highly conjugated structure and highly ordered polycrystalline morphology in the thin film.

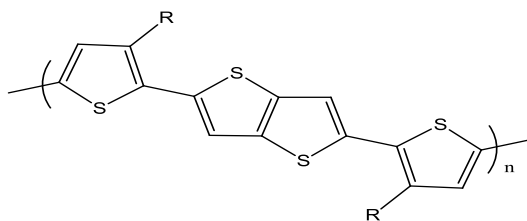


Figure 7. Chemical structure of poly(2,5-bis(3-alkylthiophene-2-yl)thieno[3,2-b]thiophene), PBTTT. R=C₁₀H₂₁, C₁₂H₂₅, C₁₄H₂₉.

1.2.3.1.3 Summary

Over the last two decades, the performance of organic semiconductors has significantly improved, as shown in Figure 8. Among small molecular semiconductors, pentacene, oligothiophenes, and their derivatives give the best performance and their mobilities are comparable to those of amorphous silicon semiconductors. However, there are certain challenges for the device fabrication

by solution processes. Among the polymeric semiconductors, polythiophene-based semiconductors have shown high potentials for solution-processable low-cost OTFTs applications. The field-effect mobility of OTFTs fabricated from some solution-processable polythiophenes and pentacene-based derivatives is approaching to the mobility of amorphous silicon TFTs. However, a great number of challenges still remain including device stability in ambient conditions and effective fabrication process from environmentally friendly solvent system. Further improvements on both mobility and stability of polymeric semiconductors are essential in order to achieve better OTFTs performance for practical electronic industrial applications.

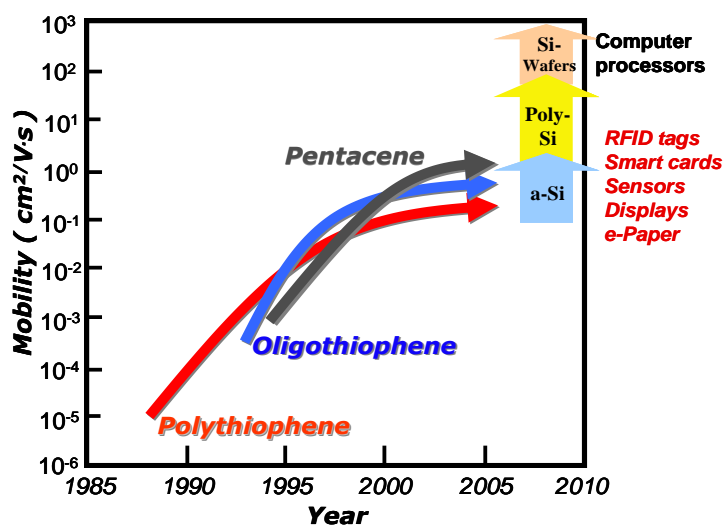


Figure 8. Schematic illustrations of the progress of most significant organic semiconductors developed during the last two decades.

1.2.3.2 Gate Dielectric and Interface Compatibility

1.2.3.2.1 Introduction to OTFT Gate Dielectric Materials

The properties of gate dielectric materials and the interface between dielectric and organic semiconductor layers play an important role for the performance of OTFTs. The most important parameters for dielectric materials include a breakdown voltage and the capacitance per unit area (C_i), which is defined as the following equation:

$$C_i = \epsilon_0(k/d)$$

where k is the dielectric constant; d is the insulator thickness, and ϵ_0 is the vacuum permittivity.³⁰ Capacitance of the dielectric layer is controlled by the dielectric constant of the material and the thickness of the dielectric layer, which often reflects the deposition procedure and quality of the dielectric layer. Uniformity of the dielectric layer is an important property because increased roughness could form valleys in the charge transport channel region, which could act as traps for charge carriers in the interface. Surface roughness also affects morphologies of the organic semiconductor layer, including nucleation densities and polycrystalline domain sizes.³¹ Defects such as pinholes, roughness and cracks would lead to a severe current leakage and dielectric breakdown. Furthermore, dielectric compatibilities at the interface between the dielectric and semiconductor layers play an important role in the performance of OTFTs. Currently, most organic semiconductor OTFT devices are fabricated on silicon wafer substrates with thermally grown silicon oxide (SiO_2) as dielectric layer, which is a very

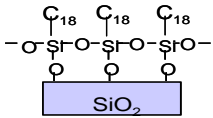
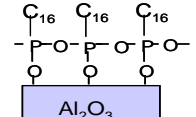
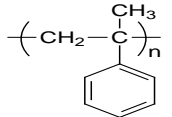
convenient device structure for the performance evaluation of organic semiconductor materials. However, there are several reasons to develop SiO₂ alternative gate dielectric materials. Firstly, fabrication of thermally grown SiO₂ dielectric layer requires high temperature and high vacuum which is not compatible with most plastic flexible substrates and low cost solution deposition processes. Secondly, a thermally grown SiO₂ dielectric layer often requires a surface modification to achieve better compatibilities with a semiconductor layer at the interface. Furthermore, in order to achieve low operating voltage for OTFTs, it is necessary to find suitable dielectrics with a high dielectric constant. The following is a brief review of recent research developments in gate dielectrics including the effects of gate dielectric properties and interface compatibilities on the performance of OTFTs.

1.2.3.2.2 Inorganic Dielectrics and Surface Modification

Currently, a thermally grown SiO₂ dielectric layer on silicon substrates is most widely used in the OTFT research environments because it is commercially available and it is a very convenient device structure for the performance evaluation of organic semiconductor materials. Inorganic gate dielectric such as SiO₂ and Al₂O₃ often possess some hydroxyl groups on their surfaces upon exposure to air, and such a hydrophilic dielectric surface is not compatible with most organic semiconductor layers. Thus inorganic oxide dielectric layer is often modified by such reagents as organosilane, which are capable of forming

chemical bonds to their surface forming self-assembled monolayer (SAM). After the surface modification, the oxide dielectric surface is changed to a more hydrophobic surface and an organic semiconductor layer deposited on such modified dielectric layer would become more uniform, robust, and more ordered in structure,^{30,31} leading to a higher OTFT performance. Examples of significant performance enhancements for pentacene OTFTs through the dielectric surface modifications could be observed in Table 2.

Table 2. Performance of Pentacene OTFTs with different gate dielectric layers

Year	Gate dielectric layer	Mobility (cm ² /V.s)	I _{on} /I _{off}	References
1992	Thermally grown SiO ₂	0.002	Not reported	15
1996	Thermally grown SiO ₂	0.038	140	32
1997	 OTS-modified SiO ₂	1.5	10 ⁸	33
2003	 Phosphonic acid modified Al ₂ O ₃	2.0 – 3.3	10 ⁵	34
2003	 poly(α -methylstyrene)-modified Al ₂ O ₃	3.5 – 5.5	10 ⁶	16

More specifically, Horowitz et al. reported a mobility value of $0.002 \text{ (cm}^2/\text{Vs)}$ for vacuum evaporated pentacene OTFTs in 1992.¹⁵ By 1996, Dimitrakopoulos et al. reported an improved field-effect mobility of $0.038 \text{ cm}^2/\text{Vs}$ with a current On/Off ratio 140.³² In these studies, pentacene films were vacuum deposited directly on a SiO_2 gate dielectric layer. Later, high performance pentacene OTFTs with a field-effect mobility of $1.5 \text{ cm}^2/\text{Vs}$ and on/off current ratio of 10^8 were reported by Lin et al. (1997),³³ where thermally grown SiO_2 dielectric layer was treated by octadecyltrichlorosilane followed by vacuum deposition of pentacene.

Further improved high performance pentacene OTFTs with mobilities ranged from 2.0 to 3.3 (cm^2/Vs) were reported by Kelly et al. who indicated that such enhancement was mainly obtained by the use of a phosphonic acid treated alumina (Al_2O_3) dielectric layer.³⁴ As an extension of their study, Kelly et al. soon reported a further enhancement on the mobility of pentacene OTFTs up to 3.5-5.5 cm^2/Vs using poly(α -methyl)styrene modified alumina (Al_2O_3) dielectrics.¹⁶ They reported that higher ordered pentacene films with larger grain size crystalline domains were formed after modification of the dielectric surface with poly(α -methyl)styrene. Other organosilane agents such as octyltrichlorosilane (OTS-8),²⁸ hexamethyldisilazene (HMDS),^{35,36} and fluorinated trichlorosilane^{37,38} were also widely used for the dielectric surface treatment for polythiophene-based OTFTs.

1.2.3.2.3 Polymeric Dielectrics and Effect of Interface Compatibility

Polymeric dielectrics have great advantages for low-cost OTFT devices by solution fabrication processes. Some critical requirements for polymeric dielectrics include the following. First, they should have good solubility in certain solvents to meet low cost solution processes. Second, they should be capable to form uniform thin film without pinholes to prevent electric leakages. Third, they should be crosslinkable to allow subsequent solution depositions. Finally, they should be compatible with semiconductor layer to facilitate the molecular ordering in the conducting channel for high performance. Some polymeric dielectric materials used in OTFTs are shown in Figure 9.

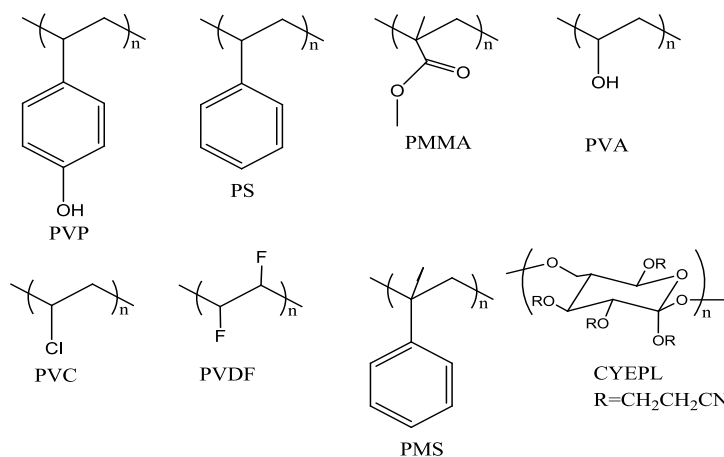


Figure 9. Chemical structures of some polymers used as OTFT dielectrics: PVP (polyvinylphenol), PS (polystyrene), PMMA (polymethylmethacrylate), PVA (polyvinylalcohol), PVC (polyvinylchloride), PVDF (polyvinylidene fluoride), PMS (poly[α-methylstyrene]), CYEPL (cyanoethylpullulan).³⁰

A detailed study of polymeric dielectric materials used in OTFTs was first reported by Peng et al. (1990).³⁹ In the study, a series of organic polymeric dielectric materials were solution coated on a glass substrate as a gate dielectric layer and then organic semiconductor, α -sexithienyl (α -6T), was vacuum evaporated on the prepared dielectric layer. Thus, the effect of the polymeric dielectric materials on the performance of the OTFTs could be evaluated. Strong correlations between the mobility and dielectric constant were found and some of their results were listed in Table 3.

Table 3. Performance of typical all-organic TFTs from 25 nm α -sexithienyl semiconducting layer with different dielectric materials.

Dielectrics	Dielectric constant (ϵ)	Mobility (μ , cm ² /Vs)	Capacitance (C _i , nF/cm ²)
SiO ₂	3.9	2.1 x 10 ⁻⁴	15
PVA	7.8	9.3 x 10 ⁻⁴	10
CYEPL	18.5	3.4 x 10 ⁻²	6
PVC	4.6	-	-
PMMA	3.5	-	-
PS	2.6	-	-

The OTFTs with cyanoethylpullulan (CYEPL) having a high dielectric constant of 18.5, gave the highest field-effect mobility. No mobility values were obtained for PVC, PMMA and PS. The effect of moisture on OTFTs performance

was also evaluated for some of the polymers by heating the devices at 70 °C for about 20 min in vacuum. It was found that there was no change in the device properties with polystyrene (PS,) and PMMA and PVC, which are relatively hydrophobic. The humidity effect for the device with CYEPL was not significant. However, they reported the device with PVA showed huge current leakage after the device was kept about one hour in ambient condition with high humidity.

Recently, Veres et al. (2003) reported that the dielectric does not only affect the morphology of semiconductor layer, but also affect the carrier density of states by local polarization effects.^{40,41} Their results showed that low-k dielectrics achieved better performance than high-k dielectrics, at least for amorphous semiconductors. In order to find out the dielectric polarity effect on OTFT mobility, gate dielectrics with varying polarities, including fluoropolymer ($\epsilon = 2.1$), polypropylene-co-1-butene ($\epsilon = 2.3$), PVP ($\epsilon = 3.5$), PMMA ($\epsilon = 3.8$), PVA ($\epsilon = 10.4$) were used. In their study, amorphous polytriarylamines (PTAA) were selected as semiconductors, thus the morphology effect could be eliminated due to the amorphous characteristics of PTAA. It was found that the mobility was significantly higher when the dielectric constant was below 2.5 indicating that interactions between the dielectric and semiconductor layers play a crucial role in carrier charge transport at the interface. The authors believed that charge carrier localization was enhanced by dielectric layer having a large dielectric constant due to a random dipole field present at the interface as illustrated in Figure 10. The main finding in this study indicated that low polarity dielectric interfaces

could lead to better OTFT performance due to reduced carrier localizations in the dielectric interface.

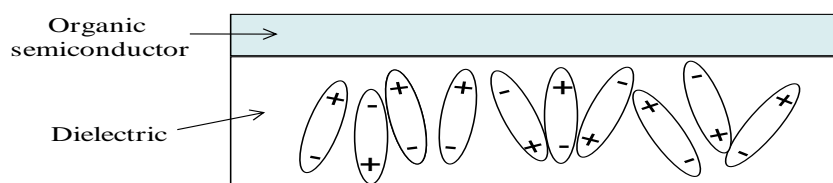


Figure 10. Schematic illustration of the carrier localization enhancement due to polar insulator interface.⁴⁰

Polyimide was used as dielectrics by Bao et al. (1997).⁴² They fabricated the first high-performance plastic OTFT with regioregular poly(3-hexylthiophenes). Polyimide dielectric layer was directly printed through a screen mask onto an ITO-coated poly(ethylene terephthalate) plastic substrate, where ITO acted as gate electrode. The resulted film capacitance was about 20 nF/cm². The semiconductor layer P3HT and the source and drain contacts were also deposited by solution printing process. The field-effect mobility was in the range of 0.01 and 0.03 cm²/Vs. Poly(vinyl phenol) (PVP) was also utilized in plastic electronic circuits.^{8,43,44} For example, functional all-polymer integrated flexible circuits on a polyimide substrate with melamine-crosslinked PVP as dielectric layer and PTV (polythienylenevinylene) as semiconductor were fabricated through solution deposition process by Philips Research Laboratories.⁴³

Recently, an ultra thin siloxane-based gate dielectric layer was reported by Chua et al. (2004).⁴⁵ This dielectric material was obtained using a thermal-

crosslinkable siloxane bisbenzocyclobutene (BCB), as shown in Figure 11. A gate dielectric layer as thin as 50 nm was spin-coated on the semiconductor (poly 9,9-dialkylfluorene-*alt*-triarylamine) for a top gate with bottom contact configuration device. The fabricated OTFT could be operated at a low voltage with a field-effect mobility of $3 \times 10^{-4} \text{ cm}^2/\text{Vs}$. However, this dielectric requires a high thermal curing temperature of 230 °C to 290 °C, which is not suitable for most flexible plastic substrates.

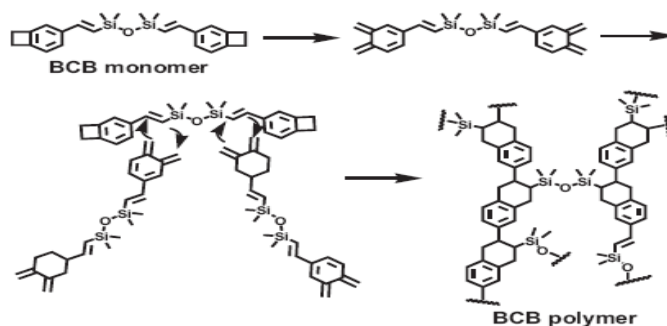


Figure 11. Thermal ring-opening and successive 4+2 Diels-Alder cycloaddition/polymerization BCB monomer. This figure was obtained from reference 45.

More recently, a new class of dielectric materials, crosslinked polymer blends (CPBs), was developed for low operating voltages by Yoon et al. (2005).⁴⁶ The dielectrics were composed of a polymer including polyvinylphenol (PVP) or polystyrene (PS) with a series of siloxane crosslinking agents.⁴⁶ It was reported that uniform and ultra-thin (10-20 nm) gate dielectric layer with high capacitance up to 300 nF/cm^2 could be generated from these dielectric materials, thus resulting in extremely low operating voltages. The crosslinked polyvinylphenol blends

showed good adhesions to various conducting substrates such as ITO-glass, ITO-Mylar, and aluminum foil according to their report and they did not undergo delamination and cracking when substrates were bent or even sonicated in organic solvents for about 30 seconds. In contrast, delamination or complete dissolution was observed for the polystyrene blends. This is understandable since chemical bonds can be formed between poly(vinylphenol) and silane crosslinker, resulting in a strong crosslinked network structure. Pentacene OTFTs with such a crosslinked PVP blend dielectric showed mobility of $0.1 \text{ cm}^2 / \text{V.s}$ and current on/off ratio of 10^4 at a gate voltage of only 4 volts.

1.2.3.2.4 Summary

Numerous studies on the effects of dielectric layer materials and interface properties on OTFT performance were published in the literature. However, their interactions at the interface between dielectric and organic semiconductor layers are rather complicated. Thus, further understanding of the effects of dielectric interface properties on the performance of OTFTs is necessary. Dielectric surface treatments using organosilane agents to form self-assembled monolayers (SAMs) have been widely used, especially for oxide dielectrics such as SiO_2 and Al_2O_3 , which can increase the molecular ordering in semiconductor layer for better device performances. For polymeric dielectrics, a uniform and cross-linked dielectric layer is essential, particularly when a subsequent solution deposition on its surface is followed. In addition, polarity of the dielectric layer has big effect

on the performance of OTFTs. It seems that most organic semiconductors such as thiophene and pentacene based semiconductors exhibit higher mobility when they are deposited on more hydrophobic dielectric surface.²⁸ General explanations may be summarized as follows. Firstly, hydrophobic interface may enhance surface mobility, which helps to increase organic semiconductor crystalline domain size. Secondly, hydrophobic interface reduces the energetic carrier disorder caused by the random dipole field present at the interface. Finally, hydrophobic interface can reduce impurities and water moisture trapped by polar groups in the interface.

1.3 Research Objective and Thesis Outline

Organic thin film transistors present great potentials as alternatives for conventional silicon semiconductor technologies for the applications in low-end electronic devices such as various sensors, radio frequency identifications (RFIDs) and displays. Some major challenges facing the field of OTFTs today are lacking sufficient high performance functional materials including organic semiconductor and dielectrics. In addition to the functional organic materials, great challenges also exist in all solution-processed OTFTs to reduce the manufacturing cost of device fabrications for low-end electronic device applications.

The objectives of this thesis research work are focused on the following areas: firstly, developing new organic semiconductors and dielectrics which can be used in the application of OTFTs; secondly, demonstrating that functional

flexible OTFTs can be fabricated with the new organic semiconductors and dielectrics developed in this study.

The outline of the thesis includes seven chapters. Chapter 1 gives a brief introduction to organic thin film transistors and literature reviews in the organic semiconductors and dielectrics for the applications in OTFTs. Research objectives, thesis outline, and contributions to the field are also included. Chapter 2 describes materials, instrumentation and measurements including details of the instruments and analytical techniques used for the material characterizations. In addition, a general procedure for OTFT fabrication and evaluation is also provided. Chapter 3 and 4 are focused on the development of functional organic semiconductor materials including novel stable liquid crystalline small molecule semiconductors and novel copolythiophenes for the application of OTFTs, respectively. Chapter 5 presents a robust dual-layer gate dielectric design for all solution processed flexible OTFTs and chapter 6 demonstrates that functional flexible OTFTs can be fabricated from non-chlorinated solvents using the developed polymeric semiconductors and dual-layer dielectric approach. Finally, a brief summary and outlook in this field are given in Chapter 7.

1.4 Contributions to the Field

The research work presented in this thesis has made significant contributions to the field of OTFTs. Firstly, several new organic semiconductor materials have been developed for the application of OTFTs. These developed materials include a novel class of high performance liquid-crystalline organic semiconductors based on 2,5'-bis-[2-(4-pentylphenyl)vinyl]-thieno(3,2-*b*)thiophene and 2,5'-bis-[2-(4-pentylphenyl)vinyl]-(2,2')bithiophene and a series of high performance solution processable copolythiophenes. Secondly, a robust dual-layer gate dielectric structure design and fabrication process has been developed and enabled us to fabricate high performance all solution-processed flexible OTFTs. The work has resulted in three scientific papers published in refereed journals and one more manuscript in preparation for future publication.

The mobility of the developed liquid crystalline organic semiconductors reached $0.15 \text{ cm}^2/\text{V}\cdot\text{s}$ with the current on/off ratios of 10^6 . This high performance is attributed to their ability to form highly ordered structures through molecular packing. In addition, high environmental stabilities in ambient condition with the fabricated OTFTs containing this class of liquid crystalline organic semiconductors have been demonstrated. A series of copolythiophenes developed in this study showed excellent OTFT performance when fabricated from a non-chlorinated organic solvent. Unlike other high performance polythiophene-based semiconductors, which usually require non-environmentally friendly chlorinated solvents for their device fabrications, the solubility of these copolythiophenes is

improved dramatically, and thus they do not require chlorinated organic solvents such as chloroform, chlorobenzene, and dichlorobenzene for the fabrications of OTFTs. The results indicate that the OTFT performance and semiconductor solubility properties could be tuned through strategic molecular designs and structure modifications.

1.5 References

1. Printed Organic and Molecular Electronics, edited by Gamota, P. Brazis, K. Kalyanasundaram and J. Zhang, **2004** (Kluwer Academic Publishers, D. R.)
2. <http://www.newscenter.philips.com/article-15499.html>
3. <http://www.foxnews.com/story/0,2933,242431,00.html>
4. C.D. Dimitrakopoulos, P. R. L. Malenfant *Adv. Mater.* **2002**, *14*, 99-117.
5. H. E. Katz, *Chem. Mater.* **2004**, *16*, 4748-4756.
6. T. B. Singh, N. S. Sariciftci, *Annu. Rev. Mater. Res.* **2006**, *36*, 199-230.
7. H. E. A. Huitema, H. G. Gelinck, J. B. P. H. Van der Putten, K. E. Kuijk, K. M. Hart, E. Cantatore, D. M. de Leeuw, *Adv. Mater.* **2002**, *14*, 1201-1204.
8. H. Sirringhaus, T. Kawase, R. H. Friend, T. Shimoda, M. Inbasekaran, W. Wu, E. P. Woo, *Science*, **2002**, *Vol 290*, 2123 – 2126.
9. P. Calvert, *Chem. Mater.* **2001**, *13*, 3299-3305.
10. Flexible flat panel displays, edited by G. P. Grawford, **2005** (Wiley-SID Series in Display Technology).
11. Printed Organic and Molecular Electronics, edited by Gamota, P. Brazis, K. Kalyanasundaram and J. Zhang, **2004** (Kluwer Academic Publishers, D. R.)
12. H. Shirakawa, E. J. Louis, A. G. MacDiarmid, C. K. Chiang and A. J. Heeger, *J.C.S.Chem. Comm.* **1977**, 578-580.
13. Z. Bao, *Adv. Mater.* **2000**, *12*, 227-230.
14. H. Sirringhaus, *Adv. Mater.* **2005**, *17*, 2411-2425.
15. G. Horowitz, X. Peng, D. Fichou, F. Garnier, *Synth. Met.* **1992**, *51*, 419-424.
16. T. W. Kelley, D. V. Muyres, P. F. Baude, T. P. Smith, and T. D. Jones, *Mater. Res. Soc. Symp. Proc.* **2003**, *771*, 169-179.
17. M. M. Payne, S. R. Parkin, J. E. Anthony, C. C Kuo, and T. N. Jackson, *J. Am. Chem. Soc.* **2005**, *127*, 4986-4987.
18. G. Horowitz, D. Fichou, X. Peng, Z. Xu, and F. Garnier, *Solid State Comm.* **1989**, *72*, 381- 384.

19. F. Garnier, G. Horowitz, X. Z. Peng, and D. Fichou, *Synthetic Metals*, **1991**, *45*, 163-171.
20. G. Horowitz and M. E. Hajlaoui, *Adv. Mater.* **2000**, *12*, 1046-1050.
21. M. Halik, H. Klauk, U. Zshieschang, G. Schmid, S. Ponomarenko, S. Kirchmeyer, and W. Weber, *Adv. Mater.* 2003, *15*, 917-922.
22. A. Tsumura, H. Koezuka, T. Ando *Appl. Phys. Lett.* **1986**, *49* (18), 1210-1212.
23. Z. Bao, A. Dodabalapur, and A. J. Lovinger, *Appl. Phys. Lett.* **1996**, *69*, 4108-4110.
24. H. Sirringhaus, P. J. Brown, R. H. Friend, M. M. Nielsen, K. Bechgaard, B. M. W. Langeveld-Voss, A. J. H. Spiering, R. A. J. Janssen, E. W. Meijer, P. Herwig and D. M. de Leeuw, *NATURE*, **1999**, *401*, 685-688.
25. Handbook of Organic Conductive Molecules and Polymers Edited by H. S. Halwa, **1997**.
26. R. D. McCullough, S. Tristram-Nagle, S. P. Williams, R. D. Lowe and M. Jayaraman *J. Am. Chem. Soc.* **1993**, *115*, 4910-4911.
27. T. Yamamoto, D. Komarudin, M. Arai, B. L. Lee, H. Sugauma, N. Asakawa, Y. Inoue, K. Kubota, S. Sasaki, T. Fukuda, and H. Matsuda *J. Am. Chem. Soc.* **1998**, *120*, 2047-2058.
28. B. S. Ong, Y. Wu. , P. Liu, S. Gardner, *J. Am. Chem. Soc.* **2004**, *126*, 3378-3379.
29. I. Mcculloch, M. Heeney, C. Bailey, K. Genevicius, I. Macdonald, M. Shkunov, D. Sparrowe, S. Tierney, R. Wagner, W. Zhang, M. L. Chabiny, R. J. Kline, M. D. Mcgehee AND M. F. Toney, *Nature Materials*, **2006**, *5*, 328-333.
30. A. Facchetti, M-H.Yoon, and T. J. Marks, *Adv. Mater.* **2005**, *17*, 1705-1725.
31. J. Veres, S. Ogier, and G. Lloyd, *Chem. Mater.* **2004**, *16*, 4543-4555.
32. D. Dimitrakopoulos, A. R. Brown, and A. Pomp, *J. Appl. Phys.* **1996**, *80*, 2501-2508.

33. Y.-Y. Lin, D. J. Gundlach, S. F. Nelson, and T. N. Jackson, *IEEE ELECTRON DEVICE LETTERS*, **1997**, *18*, 606-608.
34. T. W. Kelley, L. D. Boardman, T. D. Dunbar, D. V. Muyres, M. J. Pellerite, and T. P. Smith, *J. Phys. Chem. B*, **2003**, *107*, 5877-5811.
35. H. Sirringhaus, N. Tessler, R. H. Friend, *Science*, **1998**, *280*, 1741-1744.
36. A. Zen, D. Neher, K. Silmy, A. Hollander, U. Asawapirom and U. Scherf, *Japanese Journal of Applied Physics*, **2005**, *44*, 3721-3727.
37. A. Salleo, M. L. Chabiny, M. S. Yang, and R. A. Street, *Appl. Phys. Lett.*, **2002**, *81*, 4383-4385
38. S. Kobayashi, T. Nishikawa, T. Takenobu, S. Mori, T. Shimoda, T. Mitani, H. Shimotani, N. Yoshimoto, S. Ogawa, Y. Iwasa, *Nat. Mater.* **2004**, *3*, 317-322.
39. X. Peng, G. Horowitz, D. Fichou, F. Garnier, *Appl. Phys. Lett.* **1990**, *57*, 2013-2015.
40. J. Veres, S. D. Ogier, S. W. Leeming, D. C. Cupertino, and S. M. Khaffaf, *Adv. Funct. Mater.* **2003**, *13*, 199-204.
41. J. Veres, S. Ogier, S. Leeming, D. Cupertino, S. M. Khaffaf, and G. Lloyd, *Proc. SPIE* **2003**, *5217*, 147-158.
42. Z. Bao, Y. Feng, A. Dodabalapur, V. R. Raju, and A. J. Lovinger, *Chem. Mater.* **1997**, *9*, 1299-1301.
43. C. J. Drury, C. M. J. Mutsaers, C. M. Hart, M. Matters, and D. M. de Leeuw, *Appl. Phys. Lett.*, **1998**, *73*, 108-110.
44. Y. Wu, P. Liu, and B. S. Ong, *Appl. Phys. Lett.*, **2006**, *89*,
45. L.-L. Chua, P. K. H. Ho, H. Sirringhaus, and R. H. Friend, *Appl. Phys. Lett.* **2004**, *84*, 3400-3402
46. M.-H. Yoon, H. Yan, A. Facchetti, and T. J. Marks, *J. Am. Chem. Soc.* **2005**, *127*, 10388-10395.

Chapter 2

Materials, Instrumentation and Measurement

2.1 Introduction

This chapter describes the general materials, instrumentations and procedures used for OTFTs fabrications and evaluations in this thesis.

2.2 Materials

All the chemical materials including the starting materials, solvents and catalysts were obtained from Aldrich and used without further purification.

2.3 Instrumentation and Measurement

2.3.1 NMR

NMR spectra were obtained using Bruker DPX 300 NMR spectrometer with tetramethylsilane as an internal reference at room temperature.

2.3.2 UV-Vis

UV-Vis absorption spectra were obtained on a Varian Cary-5 UV-Vis-NIR spectrophotometer for the semiconductor materials synthesized including solutions and thin films.

2.3.3 GPC

Molecular weights and molecular weight distributions were obtained by GPC using a Waters 2690 separation module with polystyrene as standards.

2.3.4 DSC

Thermal properties of semiconductors were characterized from a differential scanning calorimeter (DSC) using TA Instrument (DSC2910) with a scanning rate of 10°C/min under nitrogen.

2.3.5 CV

Cyclic voltammetric analysis was carried out using a BAS volumetric system with a three-electrode cell in a solution of tetrabutylammonium perchlorate (Bu_4NClO_4) in dichloromethane (0.1 M) at a scanning rate of 40 mV/s. using Ag/AgCl as reference electrode. The HOMO levels (ionization potential) of certain semiconductors were estimated from the equation $E_{\text{HOMO}} = E_p + 4.38 \text{ eV}$, where E_p represents the onset potential for oxidation relative to the Ag/AgCl as reference electrode.

2.3.6 XRD

Single-crystal X-ray diffraction was used to analyze the structure conformations for small molecule semiconductor materials including bond angles,

bond lengths, and their arrangements. It was carried out on a Bruker D8 three-circle diffractometer with a Cu RA X-ray source (1.5418 Å) at room temperature.

X-ray powder diffraction technique was used to analyze polycrystalline properties for thin films and powders of semiconductor materials and they were carried out on a Rigaku MiniFlex diffractometer using Cu K α . X-ray source ($\lambda = 1.5418 \text{ \AA}$) with a θ - 2θ scan configuration at room temperature.

2.4 General Procedures for OTFT Fabrication and Characterization

2.4.1 General Procedures for OTFT Fabrication

Detailed procedures for the fabrication of OTFTs in Chapter 3, 4, 5 and 6 are described in each chapter accordingly. Here are the general descriptions regarding how the OTFTs were fabricated.

Both top-contact and bottom-contact OTFTs with bottom-gate were fabricated on n-doped silicon wafers with a thin layer of about 110 nm thermally grown silicon dioxide (SiO₂, ~100 nm) for characterization of the developed liquid-crystalline small organic semiconductors (Chapter 3). The heavily doped silicon wafer functioned as a gate electrode and the thin layer of SiO₂ functioned as a dielectric. In general, silicon wafers were cleaned with plasma, isopropanol and dried with air, and then treated with octyltrichlorosilane (OTS-8) before use. For the top-contact OTFTs, a thin layer of the small semiconductor (~100 nm) was deposited by vacuum deposition on an OTS-8 treated silicon wafer substrate. Gold source and drain electrodes were then vacuum-deposited on the top of the

semiconductor layer through a shadow mask with various channel lengths and widths. For the bottom-contact OTFTs, gold source and drain electrodes were vacuum-deposited through a shadow mask first on the OTS-8 modified silicon wafer. After modification with octanethiol, a thin layer of the small molecule semiconductor was then deposited by vacuum-deposition.

For the convenience of characterization purposes, bottom-gate with top-contact OTFTs with a series of solution processable polythiophenes developed in the study (Chapter 4) were fabricated on n-doped silicon wafers with a thermally grown thin layer of SiO₂ (~110 nm) as dielectric. All device fabrications were performed in ambient conditions without any protection from exposure to air. Silicon wafers were treated with OTS-8 before use. All polymeric semiconductors were solution deposited on the top of a treated silicon wafer by spin coating followed by vacuum-deposition of gold source and drain electrodes on the top of the semiconductor layer through a shadow mask with various channel lengths and widths.

All solution processed flexible OTFTs presented in Chapter 5 and 6 were fabricated on polyester substrates. A gate dual-layer dielectric structure developed in this study was applied to all flexible OTFTs through solution process by spin coating with poly(4-vinyl phenol-co-methyl methacrylate) and poly(methyl silsesquioxane). All the polymeric semiconductors were deposited by solution process in ambient conditions. Chapter 5 and 6 provide the detailed procedures of solution-deposited gate, source, and drain electrodes.

2.4.2 Characterization of OTFTs

The electronic properties of the OTFT devices were evaluated using a Keithley 4200 SCS semiconductor characterization system, as shown in Figure 1, and all the devices were characterized at ambient conditions. The field-effect mobility, μ , was calculated from the data in the saturate regime according to the following equation: $I_D = \mu C_i (W/2L)(V_G - V_T)^2$, where I_{SD} is the source drain current at the saturated region, W and L are the semiconductor channel width and length respectively; V_G and V_T are the gate voltage and threshold voltage respectively, C_i represents capacitance per unit area of the gate dielectric layer.

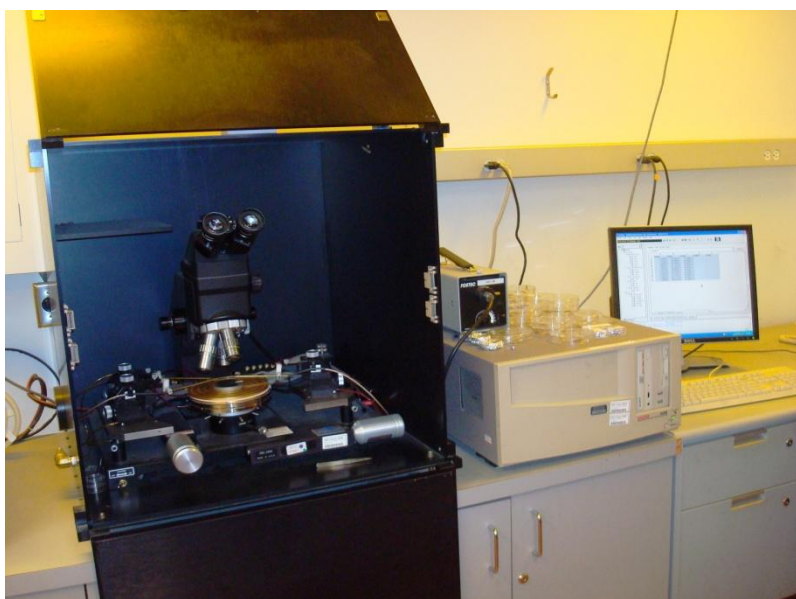


Figure 1. Photograph of Keithley 4200 SCS semiconductor characterization system.

Current on/off ratio, $I_{\text{on}}/I_{\text{off}}$, is defined as a ratio of current at “on” state (when a gate voltage applied, $V_G \neq 0$) to the current at “off” state (no gate voltage V_G applied, $V_G=0$). V_T of the device was obtained from the relationship between the square root of I_D at the saturated regime and V_G by extrapolating the measured data to I_D at 0, which was illustrated in Figure 1.2 (Chapter 1).

Chapter 3

Novel Stable Liquid Crystalline Organic Semiconductors

3.1 Introduction

Organic semiconductors play an important role in organic thin film transistors. One of the great challenges for most organic semiconductors is their stability in ambient conditions. Most previously developed high mobility organic semiconductor materials are usually not stable in air such as most pentacene-based and thiophene-based semiconductors. This chapter describes the development of a new class of stable liquid crystalline organic semiconductors for OTFT applications. The results of this research were published in *Chem. Mater.* **2009**, *21*, 2721-2732.

I was primarily responsible for the developments of these new organic semiconductors including molecular design, synthetic work and material characterization. Dr. Yiliang Wu provided assistance for OTFT characterization; Dr. Hualong Pan gave me assistance for single-crystal XRD analysis; Ms. Sandra Gardner performed XRDs for thin film semiconductor samples; Dr. Beng Ong, Dr. Shiping Zhu, and Dr. Yuning Li provided valuable discussions.

3.2 Main Text of the Paper 1

Reprinted with permission from *Chem. Mater.* **2009**, *21*, 2721-2732.

Copyright © 2009, American Chemical Society.

Novel High-Performance Liquid-Crystalline Organic Semiconductors for Thin-Film Transistors

Ping Liu,^{*,†,‡} Yiliang Wu,[†] Hualong Pan,^{†,§} Yuning Li,^{†,§} Sandra Gardner,[†] Beng
S. Ong,^{†,⊥,§} and Shiping Zhu^{*,‡}

[†] *Xerox Research Centre of Canada, Mississauga, Ontario, Canada, L5K 2L1 and*

[‡] *Department of Chemical Engineering, McMaster University, Ontario, Canada*

L8S 4L7. § Current address: Institute of Materials Research and Engineering,

Singapore 117602. ⊥ Current address: School of Materials Science &

Engineering,

Nanyang Technological University, Singapore 639798

*Email: ping.liu@xrcc.xeroxlabs.com

*Email: zhuship@mcmaster.ca

ABSTRACT: A novel class of liquid-crystalline organic semiconductors based on 2,5'-bis-[2-(4-pentylphenyl)vinyl]-thieno(3,2-*b*)thiophene and 2,5'-bis-[2-(4-pentylphenyl)vinyl]-(2,2')bithiophene were synthesized through proper structural design. The materials exhibited high field-effect mobilities up to $0.15 \text{ cm}^2 \text{ V}^{-1} \text{ s}^{-1}$ and current on/off ratio of 10^6 . The high performance is attributed to their abilities to form highly ordered structures through molecular packing, which is revealed by single-crystal and thin film X-ray diffraction (XRD). The structures were analyzed by polarized optical microscope and showed obvious changes in texture corresponding to the phase changes in DSC diagrams, indicating their abilities to form liquid crystalline structures. High environmental stabilities have been demonstrated with these new compounds, which is consistent with their low HOMO levels and large band gaps. In addition, UV-Vis spectra of the thin films formed from these compounds have showed that their absorption peaks mainly appear in the range of ultraviolet spectrum region, indicating they could be used for the application of those circuits requiring transparency such as optoelectronic devices.

Introduction

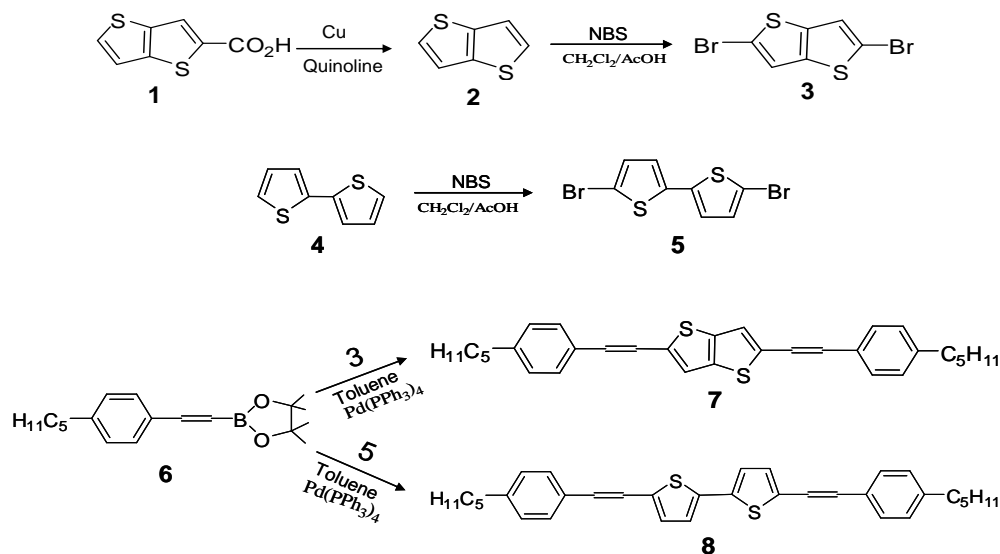
Organic thin-film transistors (OTFTs) have attracted great interests in both industrial and academic research communities as low-cost alternatives to traditional silicon-based transistors for electronic applications in the past two decades.¹⁻⁶ OTFTs are particularly attractive for large-area electronic device

applications where high processing speeds are not required such as backplane electronics for large displays, electronic paper and radio-frequency identification (RFID) tags etc. For these applications, it is critical that the organic semiconductor materials have sufficient stabilities in ambient conditions with high OTFT performance in order to achieve low-cost manufacturing processes and high OTFTs stabilities. However, very few organic semiconductor materials possess both high mobility and environmental stability. Most of high performance p-type organic semiconductors such as pentacenes, polythiophenes, and their derivatives⁷⁻⁸ have relatively high HOMOs and small band gaps, therefore they are easily oxidized when processed or operated in ambient conditions, resulting in significant degradation in performance. The lack of environmental stability of these organic semiconductor materials presents great challenges for the low cost manufacturing processes where ambient conditions are preferred. It also limits the OTFT applications where light emission such as backlight is involved. Recently, several stable and high performance organic OTFTs based on oligofluorene derivatives,^{9(a-b)} thiophene-phenylene, thiophenethiazole) oligomers^{10(a-d)} and anthracene-based compounds¹¹ have been reported. Thiophene and thienothiophene-based polythiophenes have received great attention for the OTFTs application due to their high mobilities.^{8(c-d)} However, like most highly conjugated polythiophenes, they are not very stable in air. In this article, we report our studies on a new class of semiconductors based on the molecular structures of 2,5'-bis-[2-(4-pentylphenyl)vinyl]-thieno(3,2-*b*)thiophene

7 and 2,5'-bis-[2-(4-pentylphenyl)vinyl]-2,2'-bithiophene **8**, which exhibit high OTFT performance with remarkable air stability.

Results and Discussion

New semiconductors **7** and **8** were synthesized according to the procedure shown in Scheme 1. Thieno[3,2-*b*]thiophene-2-carboxylic acid **1** was prepared accordingly by following a synthetic method published in the literature.¹² Compound **2** was obtained with 90% yield by refluxing **1** in quinoline with copper powder. Compound **3** and **5** were prepared by bromination of **2** and **4** with *N*-bromosuccinimide (NBS) in a mixture of dichloromethane and acetic acid at room temperature, respectively. Compounds **7** and **8** were synthesized via Suzuki coupling from the commercially available compound **6** with **3** and **5** respectively in good yields (>65%).



Scheme 1. Syntheses of New Organic Semiconductors **7** and **8**.

The UV-vis spectra of compound **7** and **8** in chlorobenzene solution and their thin films on glass are shown in Figure 1.

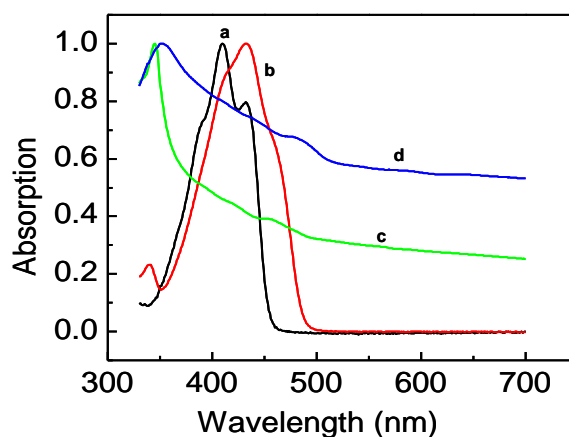


Figure 1. UV-Vis spectra of compounds **7** and **8**. **a** and **b** represent **7** and **8** in chlorobenzene solution, respectively; **c** and **d** represent their thin films of **7** and **8** on glass substrates, respectively.

The absorption spectra of **7** and **8** in chlorobenzene solution have their λ_{\max} value at 410 nm and 432 nm, respectively. The absorption spectra of vacuum-deposited thin films of **7** and **8** have the absorption maxima (λ_{\max}) at 345 and 351 nm, respectively, which indicate larger band gaps than the most organic semiconductors, especially compared to acenes and their derivatives.^{7-8,11,13} Semiconductors of this nature without absorption in the visible region are particularly suitable for transparent OTFTs which can be used in those circuits requiring transparency such as optoelectronic devices.¹⁴⁻¹⁵ The cyclic voltammetric measurements of **7** and **8** showed a reversible oxidation process with similar onset oxidation potential at 0.80-0.82 eV against Ag/AgCl electrode,

which corresponds to an estimated HOMO level (ionization potential) of 5.18 – 5.20 eV from vacuum (see Supporting Information). Thus both UV-vis and cyclic voltammetric spectra indicate their high stabilities against oxidation in ambient conditions.

Molecular packing of compound **8** was investigated with single crystal XRD. As shown in Figure 2, the two thiophene rings in the centre are co-planar with torsional angle of 180° (C3-C2-C2'-C3'). The five member ring of thiophene also has less steric hindrance to the hydrogen atom attached to C6, which results in better co-planarity with a smaller torsional angle of 8.4° (C7-C6-C4-C5), compared with a counterpart torsional angle of 10.6° in a substituted anthracene system.¹¹ The carbon (C6) in the molecule is in high planarity with maximum deviation of 0.45 Å from thiophene plane.

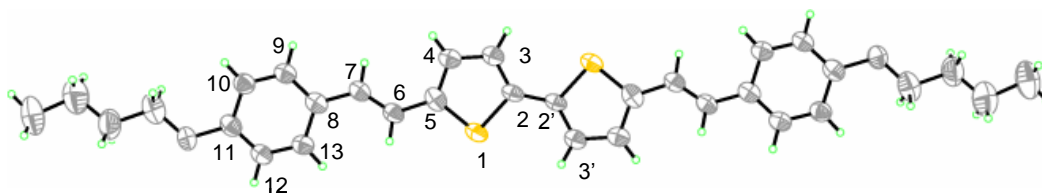


Figure 2. Thermal ellipsoid plots (prepared at the 30% probability level) of single-crystal structure of **8** (viewed down thiophene plane).

The linear structure of this class of molecules is facilitated by the trans-conformation of vinyl groups. Such elongated linear structure with a rigid segment in the central region and flexible chains in its two ends is a perfect

example of a typical liquid crystal molecule, which has been clearly observed in their three-dimensional arrangement of the molecules in the single crystal (Figure 3).

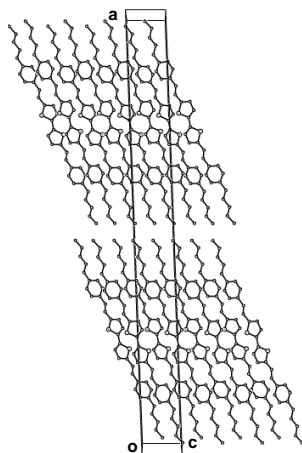


Figure 3. Schematic view of the molecular packing of compound **8** as seen down the b-axis. (Hydrogen atoms are not shown for clarity.)

The strong anisotropic intermolecular forces from the aromatic π - π interactions and the high ratio of length (~ 32.0 Å)/width (~ 3.0 Å) make the molecules align well with a lamellar structure. The interlayer distance derived from the peak at (200) is 32.1 Å, which is about the same as the molecule length. It means there is no interdigitation of alkyl chains between the layers, which favors the growth of large domain in the *b*, *c*-plane (parallel to the substrate surface). For compound **7**, where the central region of the molecule is a thieno[3,2-*b*]thiophene, the anisotropy of intermolecular force becomes larger and the relatively weak force between the layers results in poor periodicity of

atoms between the layers. So only very strong interlayer reflection points related with interlayer distance were found in the single crystal XRD measurement, indicating clear lamellar structures in the crystal, but no three dimensional molecule ordering was solved.

The molecular ordering of compounds **7**, **8** in thin film was also studied using X-ray diffraction. Figure 4 shows the diffraction patterns of the thin films prepared at different substrate temperatures.

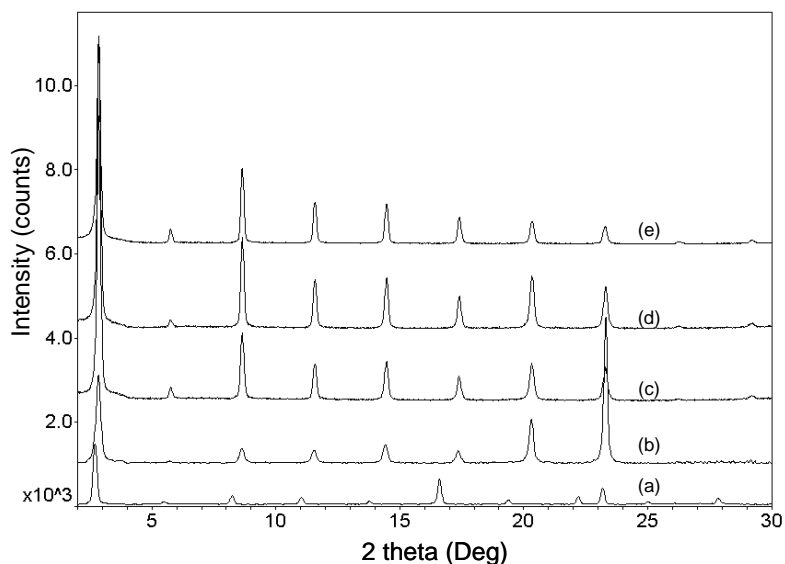


Figure 4. X-ray diffraction patterns of 100-nm thin films: (a) thin film of compound **8** at room temperature; (b) to (e) compound **7** with substrate temperature at room temperature, 40, 60, 80 °C, respectively.

The diffraction peak of compound **7** at 2θ of 2.88° corresponds to a d -spacing of 30.7 \AA , which is the same as the extended molecular length. It indicates that the molecules are aligned with their long axis normal to the substrate. The diffraction

peaks up to 8th order could be observed, revealing a highly crystalline order of the vacuum deposited film. Compound **8** shows a diffraction peak at 2θ of 2.74° , which corresponds to a d -spacing of 32.2 \AA . The d -spacing agrees to the interlayer distance obtained from the single crystal data.

The thermal properties of compound **7** and **8** were evaluated by DSC, as shown in Figure 5. The DSC thermograms show two endotherms at 152.6°C and 321.9°C for **7** (black line), and multiple peaks for **8** ($129.3, 163.0^\circ\text{C}, 214.7^\circ\text{C}, 251^\circ\text{C},$ and 275°C) (red line), indicating liquid crystalline properties of the compounds. The phases is assigned and discussed in the following together with a polarized optical microscopy. The phase transition temperature from liquid crystalline to isotropic phase transition for **7** (321.9°C) is much higher than that for **8** (214.7°C). This result is consistent with their chemical structures as compound **7** has a rigid fused thieno[3,2-*b*]thiophene in its backbone.

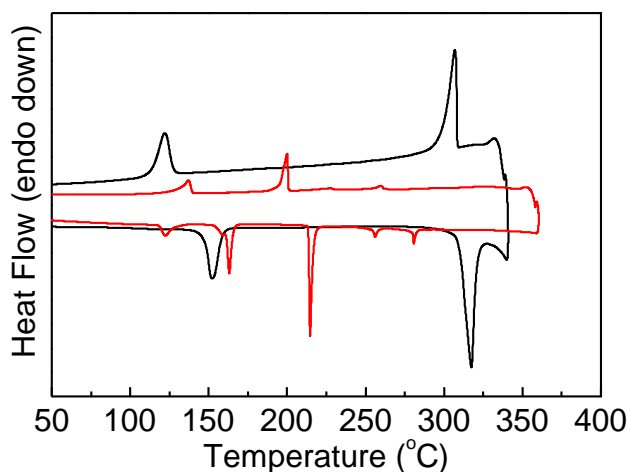


Figure .5. DSC thermograms of compound **7** and **8**. **7** (black line); **8** (red line).

The molecular organizations of both compounds **7** and **8** were further examined by polarized optical microscope. Both compounds experienced obvious texture changes at temperatures where the phase changes occurred in the DSC diagrams. For example, compound **8** gave Schlieren texture on cooling from the isotropic phase (Fig. 6e), indicating it was in a nematic phase at 260 °C. On further cooling, a typical focal conic texture revealed the formation of a smectic A phase (Fig. 6d). When cooled below 210 °C, a dramatic texture change was observed (Fig. 6c), which probably represented a smectic C phase. On further cooling, although the texture was not changed, the brightness decreased according to each phase transition (Fig. 6b and Fig. 6a). For compound **7**, a typical mosaic texture was observed in the temperature range from 150 °C to 320 °C, indicating the formation of a smectic phase of the material (Fig. 6f). Further study of these compounds using temperature-dependent X-ray diffraction will be conducted to understand the phase transitions.

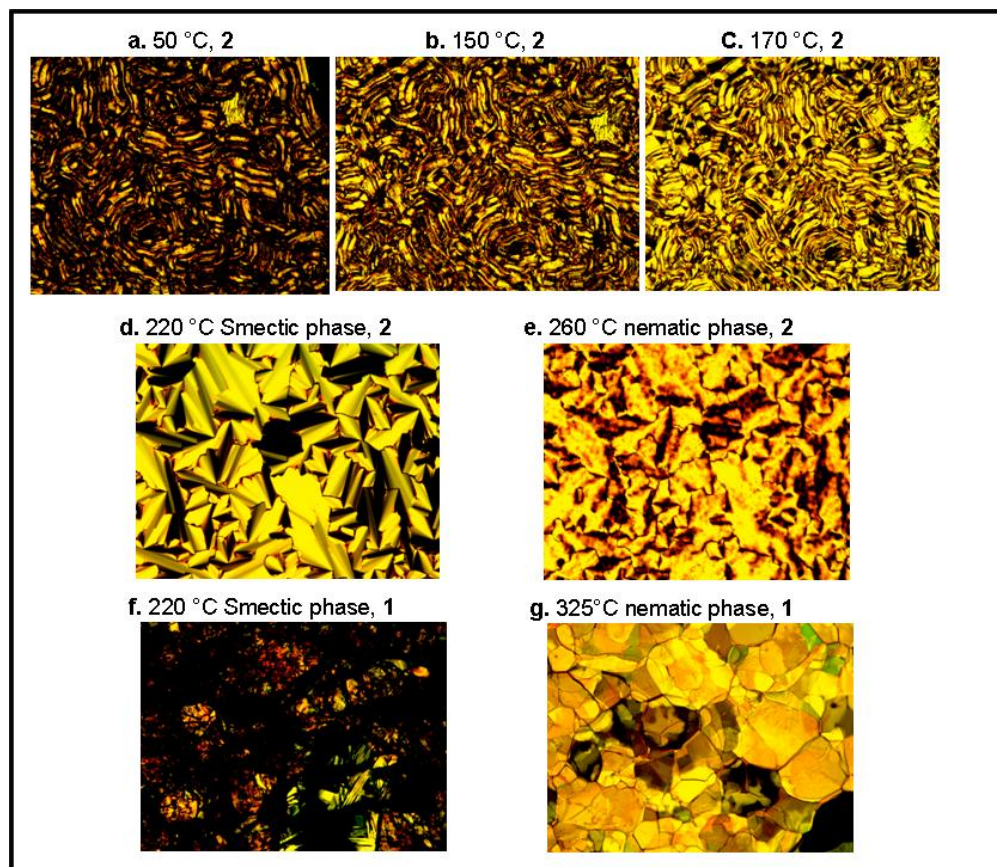


Figure 6. Polarized optical microscopic images of compound **8** at (a) 50 °C, (b) 150 °C, (c) 170 °C, (d) 220 °C, (e) 260 °C, respectively; and compound **7** at (f) 220 °C, (g) 325 °C, respectively.

To investigate their OTFT properties, thin films (~100 nm) of compounds **7** and **8** were vacuum-deposited on n^{++} -Si substrates as channel semiconductors in both top-contact and bottom-contact OTFT device configurations. The transfer and output characteristics of the devices indicated that both **7** and **8** are typical p-type semiconductors (Figure 7). The top-contact devices showed close to zero turn-on voltage and good saturation behavior with a small contact resistance. The

characteristics of top-contact OTFTs comprised from **7** and **8** as the semiconductor layer at various substrate temperatures are summarized in Table 1. It was observed that the OTFT performances for both compounds depended on the temperature of the substrate. Good performance with the mobility up to $0.15 \text{ cm}^2 \text{ V}^{-1} \text{ S}^{-1}$ and on/off ratio of 10^6 was obtained when compound **7** was deposited at a substrate temperature of $60 \text{ }^\circ\text{C}$. It was also noted that the field-effect mobility of **7** was much higher than that of **8** at both $60 \text{ }^\circ\text{C}$ and room temperature, which may be attributed to the more effective π conjugations and closer π - π overlaps of compound **7**. Bottom contact devices with compounds **7** and **8** at the optimal substrate temperature showed saturated mobilities of $0.075 \text{ cm}^2/\text{V.s}$ and $0.006 \text{ cm}^2/\text{V.s}$, respectively, which is around a factor of two lower than those in top-contact devices. The decrease of mobility in bottom-contact configuration was reported for various semiconductors including pentacene and polythiophenes, which is attributed to the increased contact resistance in the bottom-contact configuration.

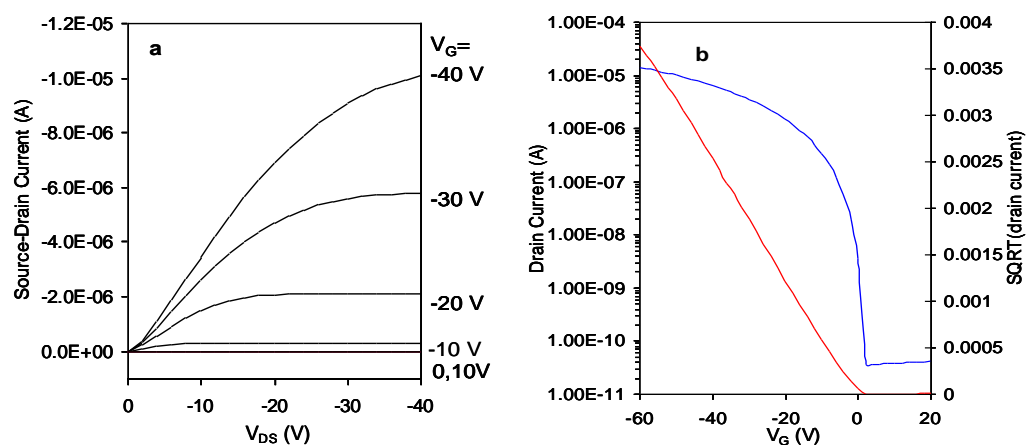


Figure 7. OTFTs characteristics of an exemplary with vacuum-deposited compounds **7** and **8** as channel semiconductors (substrate at 60 °C, channel length 90 μm and channel width 5000 μm): (a) Output curves at various gate voltages for compound **7**; (b) a transfer curve for compound **8** in the saturated regime at a constant $V_{DS} = -40$ V and the square root of the absolute value of the current as a function of the gate voltage.

Table 1 Summary of OTFT mobility and current on/off ratio with compounds **7** and **8** as semiconductor at various substrate temperatures.

Sample	Substrate temp. (°C)	Mobility ($\text{cm}^2/\text{V}\cdot\text{s}$)	On/off ratio
7	r.t.	0.05-0.06	10^5 - 10^6
7	40	0.077-0.081	10^5 - 10^6
7	60	0.1-0.15	10^6
7	80	0.0004-0.002	10^3 - 10^5
8	r.t.	0.01-0.02	10^5 - 10^6
8	40	0.01-0.02	10^6
8	60	0.039 – 0.053	10^5 - 10^6
8	80	0.023 – 0.030	10^6

The effect of the substrate temperature on the device mobility was also evident from the X-ray diffraction (XRD) data. As shown in Figure 4, the peak intensities increased gradually as the substrate temperature increased from room temperature to 60 °C, indicating that the order of molecular structure in the film was improved, and thus the increased mobility was resulted. The decrease of mobility with further increasing substrate temperature from 60 to 80 °C for both compounds was probably due to pronounced grain boundary in the thin film with large crystals in size, since the orientation of molecules in the thin film was not changed as indicated by the same diffraction patterns. It should be noted that all devices were characterized at room temperature. Studies on device performance at elevated temperatures such as the liquid crystalline phase transition temperatures are underway.

Consistent with the properties of low HOMO level and large band gaps of this class of organic semiconductor, OTFT devices with these compounds exhibited excellent air-stability. When stored in the dark in ambient air for 2 years, the device with compound 7 showed a mobility of 0.077 cm²/V.s, only a factor of 2 lower than that of the fresh device (see Figure S2 in the Supporting information). This high stability feature may enable practical application of this class of organic semiconductors.

Conclusion

In conclusion, a new class of high-performance liquid crystalline p-type organic semiconductors has been developed for OTFT applications. Our results revealed that this class of organic semiconductors has a strong tendency to form highly ordered molecular structures with liquid crystalline characteristics, which contributes to their good performance in the OTFT devices. These new organic semiconductors have both lower HOMO levels and larger band gaps than the most other p-type organic semiconductors such as acenes, polythiophenes, and their derivatives. Excellent environmental stabilities have been demonstrated for the OTFT devices comprised from these semiconductor materials. In addition, these new organic semiconductors have a great potential for those electronic device applications where transparent OTFTs are required since their thin film absorption peaks appear mainly in the range of ultraviolet spectrum region.

Experimental Procedures

Instrumentations and measurements. NMR spectra were obtained in CDCl₃ with a Bruker DPX 300 NMR spectrometer with tetramethylsilane as an internal reference. Absorption spectra were measured on a Varian Cary-5 UV-Vis-NIR Spectrophotometer for both thin films and chlorobenzene solutions. DSC thermograms were obtained on TA Instruments DSC 2910 differential scanning calorimeter with a heating rate of 10 °C per minute under nitrogen atmosphere. The single crystal of **8** for structure analysis was grown by recrystallization from a

mixture solvent of toluene and chlorobenzene at a ratio of three to one by volume. Single crystal X-ray diffraction was performed on a Bruker Smart 6000 CCD 3-circle D8 diffractometer with a Cu RA X-ray source ($\lambda=1.5418 \text{ \AA}$) at room temperature. Cyclic voltammetric measurements were carried out on a BAS 100 voltammetric system with a three electrode cell in a solution of tetrabutylammonium perchlorate, Bu_4NClO_4 , in dichloromethane (0.1 M) at a scanning rate of 40 mV/s by using Ag/AgCl as reference electrode. The HOMO levels were estimated from the following equation $E_{\text{HOMO}} = E_p + 4.38 \text{ eV}$, where E_p represents the onset potential for oxidation relative to the Ag/AgCl reference electrode.¹⁶ The properties of all the fabricated OTFT devices were evaluated using a Keithley SCS-4200 characterization system in ambient conditions.

Synthesis. All the chemicals were purchased from Sigma-Aldrich and used without further purification. Thieno[3,2-*b*]thiophene-2-carboxylic acid **1** was synthesized according to the synthetic method described in the literature.¹² 2, 2'-Bithiophene **4** and 2-[2-(4-pentylphenyl)vinyl]-4,4,5,5-tetramethyl-1,3,2-dioxaborolane **6** were obtained from Sigma-Aldrich.

*Thieno(3,2-*b*)thiophene 2.* To a mixture of thieno[3,2-*b*]thiophene-2-carboxylic acid **1** (8.80 g, 47.78 mmol) and copper powder (1.76 g, 27.78 mmol) in a 3-necked flask was added 90 mL of quinoline. The mixture was heated to reflux with stirring for 50 min and then cooled down to room temperature. The reaction mixture was diluted with ethyl ether (~300 mL) and filtered to remove solid contents. The organic solution was washed four times with aqueous HCl solution

(5 %) and 3 times with water, dried with anhydrous magnesium sulfate and filtered. The crude product, obtained after evaporation of the solvents, was purified through column chromatograph on silica gel using hexane as an eluent, and then recrystallized from 2-propanol, providing 5.5 g (yield: 82%) of thieno(3,2-*b*)thiophene **2** as a white crystalline product. ^1H NMR (CDCl_3 , 300 MHz, ppm): δ 7.28 (d, $J = 5.1$ Hz, 2H), 7.41 (d, $J=5.1$ Hz, 2H).

*2,5-Dibromothieno (3,2-*b*)thiophene 3.* To a stirred solution of thieno(3,2-*b*)thiophene **2** (1.513 g, 10.8 mmol) in a mixture of 25 mL of dichloromethane (CH_2Cl_2) and 12 mL of acetic acid (AcOH) in a 250 ml flask was slowly added NBS (3.84 g, 21.6 mmol) in small portions over a period of 40 min. After the addition, the mixture was stirred at room temperature for three hours until TLC showed no starting material left. The mixture was washed twice with aqueous NaHCO_3 solution (5 %), three times with water, dried with anhydrous magnesium sulfate and filtered. The product was obtained after evaporation of the solvent and dried in vacuo, resulting 3.10 gram (yield: 96%) of **3** as white solid. ^1H NMR (CDCl_3 , 300 MHz, ppm): δ 7.18 (s, 2H).

2,5-Dibromothiophene 5. To a stirred solution of 2, 2'-bithiophene **4** (10.00 g, 60.15 mmol) in a mixture of 100 mL of dichloromethane (CH_2Cl_2) and 50 of acetic acid (AcOH) in a 500 ml reaction flask was slowly added NBS (22.48 g, 126.30 mmol) in small portions over a period of 30 min. After the addition, the

mixture was stirred at room temperature for three hours. The solid formed during the reaction was collected by filtration, washed with distilled water, rinsed with methanol and dried in vacuo overnight, providing 17.93 grams of **5** as white flakes. Yield: 92 %. ^1H NMR (CDCl_3 , 300 MHz, ppm): δ 6.96 (d, $J = 3.9$, 2H), 6.85 (d, $J = 3.9$ Hz, 2H).

2,5-Bis[2-(4-pentylphenyl)vinyl]-thieno(3,2-b)thiophene 7. To a stirred solution of 2,5-dibromothiopheno(3,2-b)thiophene **3** (3.01 g, 10.1 mmol) and 2-[2-(4-pentylphenyl)vinyl]-4,4,5,5-tetramethyl-1,3,2-dioxaborolane **6** (7.58 g, 25.2 mmol) in 100 mL of toluene, under argon, was added a 2M aqueous sodium carbonate solution (28 mL), Aliquat 336 (2.02 g, 5.0 mmol) in 25 mL of toluene and tetrakis(triphenylphosphine)palladium(0) (0.23 g, 0.20 mmol). The mixture was heated to 90 °C and refluxed at this temperature for three days. The precipitated solid product was collected by filtration and washed with methanol. The crude product was recrystallized three times in a mixture of toluene and chlorobenzene at a ratio of three to one by volume, providing 3.57 g (yield: 73%) of 2,5-bis[2-(4-pentylphenyl)vinyl]-thieno(3,2-b)thiophene **7** as a shiny yellowish crystal. Mass spectra analysis: 484.2259 ($\text{C}_{32}\text{H}_{36}\text{S}_2$ calculated 484.2258); melting point: 320.5 °C; Elemental analysis: calculated for $\text{C}_{32}\text{H}_{36}\text{S}_2$: C, 79.29; H, 7.47; S, 13.23. Found: (C, 78.73, H, 7.49, S, 13.00). ^1H NMR (CDCl_3 , 300 MHz, ppm): δ 7.32 (dd, $J = 8.1$ Hz, 4H), 7.13 (dd, $J = 8.1$ Hz, 4H),

7.12 (s, 2H), 7.04 (br, 2H), 6.90 (br, 2H), 2.58 (t, J = 7.2 Hz, 4H), 1.61 (m, 4H), 1.32 (m, 8H), 0.90 (t, J = 6.0 Hz, 6H).

2,5-Bis[2-(4-pentylphenyl)vinyl]-2,2'-bithiophene **8**. To a stirred solution of 2,5-dibromothiophene **5** (3.25 g, 10.0mmol) and 2-[2-(4-pentylphenyl)vinyl]-4,4,5,5-tetramethyl-1,3,2-dioxaborolane **6** (7.51 g, 25.0 mmol) in 100 mL of toluene under argon, was added 2 M aqueous sodium carbonate solution (28 mL), Aliquat 336 (2.02 g, 5.0 mmol) in 25 mL of toluene and tetrakis(triphenylphosphine)palladium(0)(0.23 g, 0.20 mmol). The resulting mixture was heated to 90 °C and refluxed at this temperature for three days. The resulting precipitated solid was collected by filtration and washed with methanol. Additional product was collected from the filtrate, which was washed with water, extracted with toluene, dried with MgSO₄ and filtered. The combined crude product was recrystallized from a mixture of toluene and chlorobenzene at a ratio of three to one by volume, providing 3.4 g (yield: 66%) of 2,5-bis[2-(4-pentylphenyl)vinyl]-2,2'-bithiophene **8** as shiny orange crystals. Mass spectra analysis: 510.2411 (C₃₄H₃₈S₂ calculated 510.2415); Melting point: 214.39 °C; Elemental analysis: calculated for C₃₄H₃₈S₂: C, 79.95; H, 7.50; S, 12.55. Found: (C, 78.99, 7.27, 12.29). ¹H NMR (CDCl₃, 300 MHz, ppm): δ 7.38 (dd, J = 8.1 Hz, 4H), 7.16 (dd, J = 8.1 Hz, 4H), 7.13 (d, J = 15.9 Hz, 2H), 7.06 (d, J = 3.9 Hz, 2H), 6.94 (d, J = 3.9 Hz, 2H), 6.87 (d, J = 15.9 Hz, 2H), 2.60 (t, J = 7.5 Hz, 4H), 1.62 (m, 4H), 1.33 (m, 8H), 0.89 (t, J = 6.9 Hz, 6H).

OTFT Fabrication and Evaluation. Both top-contact and bottom-contact thin film transistors using compounds **7** and **8** as channel semiconductor were fabricated. Devices were built on an n-doped silicon wafer with a thermally grown silicon oxide layer (SiO_2 , ~ 100 nm). The silicon wafer acted as the gate electrode and the SiO_2 layer acted as gate dielectric. The wafer was cleaned with isopropanol, argon plasma, isopropanol, and dried with air. The wafer was then immersed in a 0.1M solution of octyltrichlorosilane, OTS-8, in toluene at 60°C for 20 min. The modified wafer was then washed with toluene, isopropanol, and air dried. For top-contact devices a 100-nm thick semiconductor layer of compound **7** (or **8**) was vacuum-deposited on the OTS-8 treated silicon wafer substrate at a rate of 1 \AA/s under a high vacuum of 10^{-6} torr with the substrate held at various temperatures. The gold source and drain electrodes were deposited on top of the semiconductor layer by vacuum deposition through a shadow mask with various channel lengths and widths, creating a series of OTFT transistors with various channel length (L) and width (W) dimensions. For bottom-contact device, gold electrodes were deposited through shadow mask first on OTS-8 modified silicon wafer, followed by modification with octanethiol. A semiconductor layer was subsequently deposited to complete the devices. The properties of the OTFT devices fabricated with compound **7** and **8** as channel semiconductor materials were evaluated using a Keithley 4200 SCS semiconductor characterization system at ambient conditions. Their field-effect mobility, μ , was calculated from the data in the saturated regime according to the

following equation: $I_{SD} = C_i \mu (W/2L) (V_G - V_T)^2$, where I_{SD} is the source drain current at the saturated regime, W and L are the width and length of the semiconductor channel respectively, C_i is the capacitance per unit area of the gate dielectric layer, V_G and V_T are the gated voltage and threshold voltage, respectively. V_T of the device was determined from the relationship between the square root of I_{SD} at the saturated regime and V_G was obtained by extrapolating the measured data to $I_{SD} = 0$. Devices were kept in the dark in a humidity control chamber (RH < 30%) for stability testing.

ACKNOWLEDGEMENT. We thank Dr. Jim Britten in Chemistry Department at McMaster University for single-crystal X-ray diffraction characterization.

REFERENCES

1. Garnier, F.; Hajlaoui, R.; Yassar, A.; Srivastava, P. *Science* **1994**, *265*, 1684.
2. Bao, Z. *Adv. Mater.* **2000**, *12*, 227.
3. Dimitrakopoulos, C. D.; Mascaro, D. J. *Adv. Mater.* **2002**, *14*, 99.
4. (a) Siringhaus, H.; Tessler, N.; Friend, R. H. *Science* **1998**, *280*, 1741. (b) Siringhaus, H.; Brown, P. J.; Friend, R. H.; Nielsen, M. M.; Bechgaard, K.; Langeveld-Voss, B. M. W.; Spiering, A. J. H.; Janssen, R. A. J.; Meijer, E. W.; Herwig, P.; de Leeuw, D. M. *Nature* **1999**, *401*, 685.
5. Katz, H. E. *Chem. Mater.* **2004**, *16*, 4748.
6. Singh, T. B.; Sariciftci N. S. *Annu. Rev. Mater. Res.* **2006**, *36*, 199.
7. (a) Afzali, A.; Dimitrakopoulos, C. D.; Breen, T. L. *J. Am. Chem. Soc.* **2002**, *124*, 8812. (b) Kelly, T. W.; Boardman, L. D.; Dunbar, T. D.; Muyres, D. V.; Pellerite, M. J.; Smith, T. P. J. *Phys. Chem. B* **2003**, *107*, 5877. (c) Sundar, V. C.; Zaumseil, J.; Podzorov, V.; Menard, E.; Willett, R. L.; Someya, T.; Gershenson, M. E.; Rogers, J. A. *Science* **2004**, *303*, 1644.
8. (a) Bao, Z.; Dodabalapur, A.; Lovinger, A. J. *Appl. Phys. Lett.* **1996**, *69*, 4105. (b) Siringhaus, H.; Tessler, N.; Friend, R. H. *Science*, **1998**, *280*, 1741. (c) Ong, B. S.; Wu, Y.; Liu, P.; Gardner, S. *J. Am. Chem. Soc.* **2004**, *126*, 3378. (d) McCulloch, I.; Heeney, M.; Bailey, C.; Genevicius, K.; Macdonald, I.; Shkunov, M.; Sparrowe, D.; Tierney, S.; Wagner, R.;

- Zhang, W.; Chabinyo, M. L.; Kline, R. J.; McGehee, M. D.; Toney, M. F. *Nature Materials*, **2006**, *5*, 328.
9. (a) Meng, H.; Bao, Z.; Lovinger, A. J.; Wang, B. C.; Mujcsce, A. M. *J. Am. Chem. Soc.* **2001**, *123*, 9214. (b) Locklin, J.; Ling, M. M.; Sung, A.; Roberts M. E.; and Bao, Z. *Adv. Mater.* **2006**, *18*, 2989.
- 10 (a) Hong, X. M.; Katz, H. E.; Lovinger, A. J.; Wang, B. C.; and Raghavachari, K. *Chem. Mater.* **2001**, *13*, 4686. (b) Mushrush, M.; Facchetti, A.; Lefenfeld, M.; Katz, H. E.; and Marks, T. J. *J. Am. Chem. Soc.* **2003**, *125*, 9414. (c) Katz, H. E.; Siegrist, T.; Lefenfeld, M.; Gopalan, P.; Mushrush, M.; Ocko, B.; Gang, O.; Jisrawl, N. *J. Phys. Chem. B* **2004**, *108*, 8567. (d) Sung, A.; Ling, M. M.; Tang, M. L.; Bao, Z.; Locklin, J. *Chem. Mater.* **2007**, *19*, 2342.
11. (a) Meng, H.; Sun, F.; Goldinger, M. B.; Jaycox, G. D.; Li, Z.; Marshall, W. J.; Blackman, G. S. *J. Am. Chem. Soc.* **2005**, *127*, 2406. (b) Meng, H.; Sun, F.; Goldinger, M. B.; Gao, F.; Londono, D. J.; Marshal, W. J.; Blackman, G. S.; Dobbs, K. D.; Keys, D. E. *J. Am. Chem. Soc.* **2006**, *128*, 9304.
12. Fuller, L. S.; Iddon, B.; Smith, K. A. *J. Chem. Soc. Perkin Trans.* **1997**, *1*, 3465.
13. Li, Y.; Wu, Y.; Liu, P.; Prostran, Z. Gardner, S. Ong, B. S. *Chem, Matter.* **2007**, *19*, 418.

14. Nomura, K.; Ohta, H.; Ueda, K.; Kamiya, T.; Hirano, M.; Hosono, H. *Science* **2003**, *300*, 1269
15. Wu, Y.; Li, Y.; Gardner, S.; Ong, B. S. *J. Am. Chem. Soc.* **2005**, *127*, 614.
16. Li, Y.; Ding, J.; Day, M.; Tao, Y.; Lu, J.; D'iorio, M. *Chem. Matter.* **2004**, *16*, 2165.

3.3 Supporting Materials for the paper

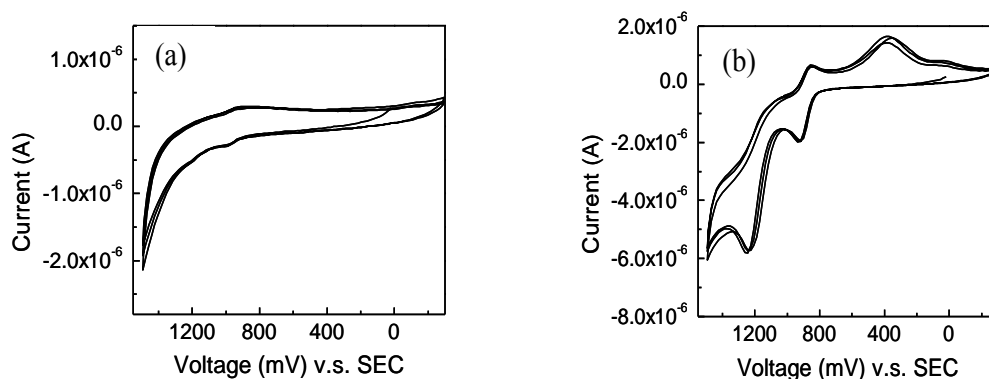


Figure S1. Cyclic voltammetric curves of **7** (a) and **8** (b)

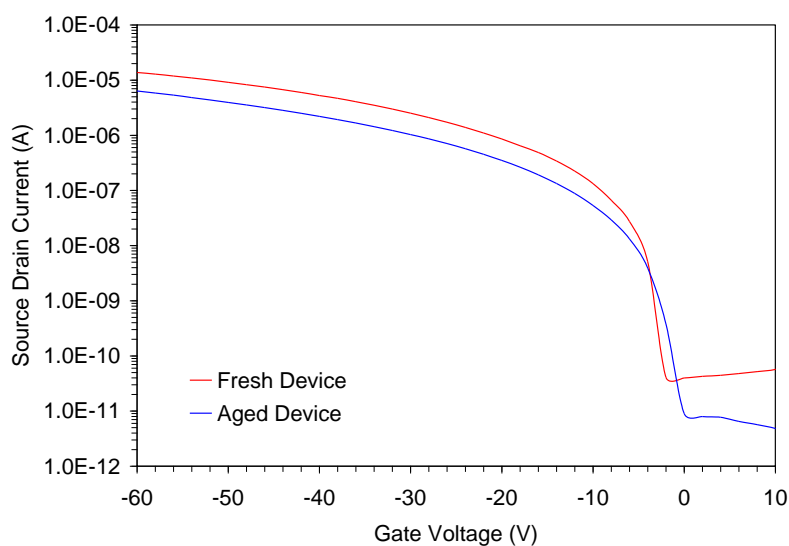


Figure S2. Transfer curves of an OTFT device with compound **7** as the semiconductor layer. The device has a channel length of $190 \mu\text{m}$ and a channel width of $1000 \mu\text{m}$. Red curve, fresh device which showed a mobility of $0.15 \text{ cm}^2/\text{V}\cdot\text{s}$; blue curve, aged device stored in the dark under ambient air for 2 years, showing a mobility of $0.077 \text{ cm}^2/\text{V}\cdot\text{s}$.

3.4 Summary

In this research, a class of liquid-crystalline organic semiconductors, 2,5'-bis-[2-(4-pentylphenyl)vinyl]-thieno(3,2-*b*)thiophene and 2,5'-bis-[2-(4-pentylphenyl)vinyl]-(2,2')bithiophene, were designed and synthesized. The structures of the developed organic semiconductors were analyzed by polarized optical microscope and showed obvious changes in texture corresponding to the phase changes in DSC diagrams. The results indicate that these organic semiconductors have abilities to form liquid crystalline structures, which facilitate the structural ordering in certain conditions. The OTFTs fabricated from this type of liquid crystalline semiconductors showed good field-effect mobility up to $0.15 \text{ cm}^2 \text{ V}^{-1} \text{ s}^{-1}$ and current on/off ratio up to 10^6 . The high performance is attributed to their abilities to form highly ordered structures through molecular packing, which is revealed by single-crystal and thin film X-ray diffraction (XRD). Furthermore, these organic semiconductors have good environmental stabilities, consistent with their low HOMO levels and large band gaps. In addition, the absorption peaks of the UV-Vis spectra from these organic semiconducting thin films appear mainly in the range of an ultraviolet spectrum region, indicating their potential applications for the electronic circuits requiring transparency.

Chapter 4

Novel Copolythiophene Semiconductors

4.1 Introduction

Polythiophene-based organic semiconductors have been studied extensively over the last two decades. However, most solution-processable polythiophenes with good field-effect mobility require chlorinated solvents such as chloroform, chlorobenzene and dichlorobenzene in their device fabrication process due to their poor solubility. It is known that chlorinated organic solvents are ozone depleting or possible carcinogenic. A general trend of device fabrication processes is to replace chlorinated solvents with more environmentally friendly non-chlorinated solvents.

More specifically, a great number of published papers have pointed out the importance of developing organic semiconductors that can be processed in more environmentally friendly non-chlorinated solvents in the recent years. The research objective presented in this chapter was focused on the development of new polymeric semiconductors that could be processed in more environmentally friendly non-chlorinated solvents. The detailed results of this research were published in *Macromolecules* **2010**, *43*, 2721-2732.

I was primarily responsible for the molecular design, synthetic work and material characterizations. Dr. Yiliang Wu provided assistance for OTFT

evaluations; Dr. Hualong Pan helped for single-crystal and thin film XRD analyses; Dr. Beng Ong and Dr. Shiping Zhu provided valuable discussions.

4.2 Main Text of Paper 2

Reprinted with permission from *Macromolecules* **2010**, *43*, 6368–6373.

Copyright © 2010, American Chemical Society.

High-Performance Polythiophene Thin-Film Transistors Processed with Environmentally Benign Solvent

Ping Liu,^{*,†,‡} Yiliang Wu,[†] Hualong Pan,^{†,§} Beng S. Ong,^{†,||} Shiping Zhu,^{*,‡}

[†]*Xerox Research Centre of Canada, Mississauga, Ontario, Canada, L5K 2L1 and*

[‡]*Department of Chemical Engineering, McMaster University, Ontario, Canada*

L8S 4L7. §Current address: Polyera, 4855 Carol Street, Unit F, Skokie, IL

60077. ||Current address: School of Chemical and Biomedical Engineering,

Nanyang Technological University, Singapore 637459

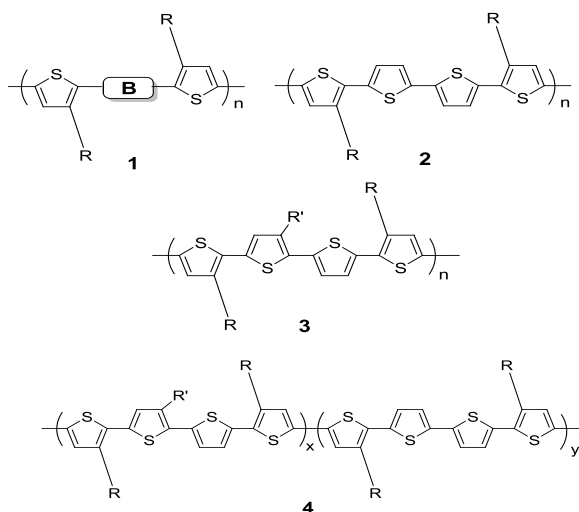
*Email: ping.liu@xrcc.xeroxlabs.com

*Email: zhuship@mcmaster.ca

Introduction

Printed organic thin-film transistors represent an appealing low-cost alternative to their amorphous silicon counterparts for applications in large-area, flexible and ultra low-cost electronics.¹⁻¹⁷ This emerging technology requires stable organic semiconductors which can be readily solution-processed in an environmentally friendly solvent to enable low-cost mass-manufacturing of thin-film transistor (TFT) arrays/circuits under ideally ambient conditions. However, most solution processable high performance organic semiconductors such as polythiophenes and their derivatives suffer from either extreme sensitivity to air or requiring chlorinated solvents for their device fabrications to achieve optimal OTFT performances.¹⁸⁻²⁷

Earlier, we reported the design principle for high-performance polythiophene semiconductors for OTFTs based on structure **1**.



In this structural design, the long pendant alkyl side-chains would impart solution processability and self-assembly capability to the system, while the intervening bridge, **B**, serves to provide stability against photo-induced oxidative doping. Using this design principle, a high-performance polythiophene semiconductor, poly(3,3''-dialkylquaterthiophene), (**2**, **PQT**), with enhanced air stability was developed. Excellent field effect transistor (FET) properties have been achieved in OTFTs using this polythiophene semiconductor system (**2**, $R = n-C_{12}H_{25}$) fabricated entirely at ambient conditions.¹⁹ However, like most high-performance solution-processable polymeric semiconductors, **2** self-assembles readily even in solution and exhibits a great tendency to gel out of solution at room temperature. This has presented some practical difficulties in OTFT fabrications until the recent development of structurally ordered PQT nanoparticles, which effectively resolves the gelling complications.²⁸ Nevertheless, this approach still requires the use of chlorinated solvents for its device fabrication to achieve the optimum performance, thus severely limiting its general applicability in manufacturing environments.⁵ In this article, we describe a facile approach to tuning the solution properties of high mobility polythiophene **2** (**PQT**) system of this nature. Our results reveal that both significantly improved solution processability in environmentally benign solvents such as xylene and high field-effect mobility up to $0.18 \text{ cm}^2/\text{V}\cdot\text{s}$. can be simultaneously achieved via judicious structure modification, thus circumventing a general and formidable challenge currently

besetting solution-processable polymeric semiconductors for low-cost TFT array/circuit manufacturing.

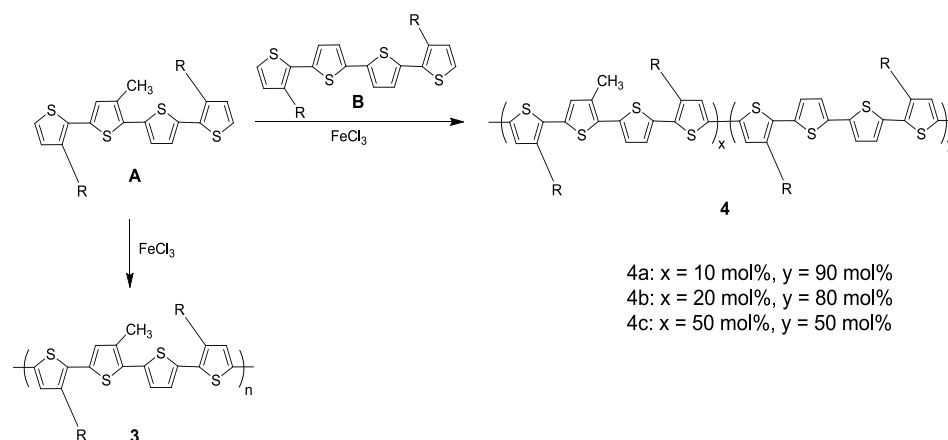
The strong self-assembly ability of **2** stems from the strategically regioregular placement of long pendant side-chains, R's, along its backbone, which promotes intermolecular side-chain interdigitation leading to extensive lamellar ordering in solution. We envisioned that this facile self-organization in solution could be greatly suppressed or even eliminated by slight perturbation to the structural regioregularity of **2** via incorporation of a small substituent (e.g., methyl) in the intervening thienylene moiety as in polythiophene **3** (R = long n-alkyl; R' = CH₃) or copolythiophene **4** (R = long n-alkyl; R' = CH₃), in which the structural regioregularity of long side-chains, R's, of parent polythiophene **2** could still preserve. It was anticipated that this weak structural perturbation, while rendering the polythiophene system disordered when in solution, could be overcome in a great extent by the strong self-assembly tendency associated with the regioregularity of long pendant side-chains via intermolecular interdigitation when in solid state such that highly ordered semiconductor channels could be created in TFTs.

Results and Discussion

Polythiophene **3** (R = C₁₂H₂₅; R' = CH₃), PQT-CH₃, was prepared readily by FeCl₃-mediated oxidation coupling polymerization of 3,3''-didodecyl-3'-methylquaterthiophene (**A**) in good yields; while **4** (R = C₁₂H₂₅; R' = CH₃) was

prepared by copolymerization of 3,3''-didodecyl-3'-methylquaterthiophene (**A**) and 3,3''-didodecylquaterthiophene (**B**) in various stoichiometries under analogous conditions (**Scheme 1**). The final content of monomer A in the copolymer **4** was calculated from NMR data. The results showed that the copolymers have a similar molar ratio as the feeding ratio of the monomers, which is anticipated by the similar reactivity of the monomers.

Scheme 1. Syntheses of polythiophene **3** and copolythiophene **4**



As expected, **3** (**PQT-CH₃**) showed much better solubility in organic solvents than **2** (**PQT**) not only in chlorinated solvents but also in non-chlorinated environmentally benign solvents such as THF, toluene and xylene at room temperature. More specifically, a hot solution of **2** (**PQT**) in dichlorobenzene with 0.3 wt% was gelled upon cooling to room temperature within several minutes due to its poor solubility, on the other hand, a much more concentrated solution of **3** (**PQT-CH₃**) up to 2.0 wt% in dichlorobenzene was very stable

without gelling at room temperature. Furthermore, a comparison of their solubility in a non-chlorinated solvent such as o-xylene was also examined. The solubility of **2 (PQT)** in o-xylene was very poor, which could not be dissolved in o-xylene even with very low concentration of 0.1 wt%, while a ten times more concentrated solution of **3 (PQT-CH₃)** in o-xylene (1.0 wt%) was stable at room temperature in a period of over two weeks. It should be noted that such 1 to 2 wt% concentration is sufficient for OTFT fabrications.^{3,19,21,22} It is interesting that such a dramatic solubility improvement in organic solvents can be achieved by this strategic structure modification. As a result, copolythiophene **4** showed much better solubility in common organic solvents than PQT. As shown in **Figure 1**, a hot coating solution of **2 (PQT)** in dichlorobenzene with 0.3 wt% was gelled upon cooling to room temperature within several minutes due to its poor solubility, while the coating solutions prepared from polythiophene **3** and copolymer **4a** even in a non-chlorinated solvent such as o-xylene were much more stable at room temperature for much longer time (e.g. a couple of hours for copolymer **4a** and a few weeks for polymer **3**), providing sufficient time for their device fabrications. In general, the solution stability of the new polymers increases with the increase of mole ratio of monomer **A**.

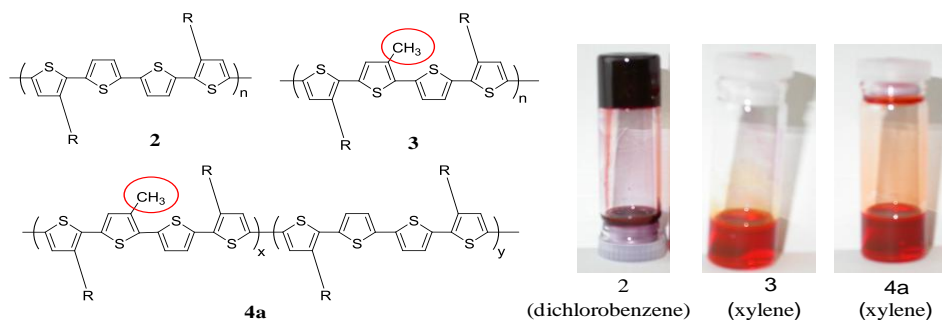


Figure 1. Coating solution stability of **2** (PQT) in dichlorobenzene (0.3 wt%), **3** (PQT-CH₃) and copolythiophene **4a** (x=10 mol%, y=90 mol%) in xylene (1.0 wt%).

Nevertheless, the ability to order in their thin-films has been preserved even with y approaching zero as in the case of **3** (i.e., **4**, $y=0$). This can be readily understood from the single-crystal data of the corresponding quaterthiophene monomers as depicted in **Figure 2**. As can be noted, the two pendant dodecyl side-chains in methyl-substituted didodecylquaterthiophene in the single crystal structure assume a coplanar conformation, which is similar to its unsubstituted didodecyl-quaterthiophene counterpart.²⁹ Thus it is reasonable to assume that the conformational structures of **3** (PQT-CH₃) and copolythiophene **4** would be similar to that of **2** (PQT) in their solid states. Therefore, the ability of forming lamellar structural order of polythiophene **2** (PQT)¹⁹ has been preserved for both **3** (PQT-CH₃) and copolythiophene **4** (a-c) in their thin films, which leads to the high mobility. The significantly improved solubility characteristics of **3** (PQT-CH₃) and copolythiophene **4** (a-c) in common organic solvents could be attributed

to the random nature of their compositions with respect to the regiochemistry of the methyl substituent.

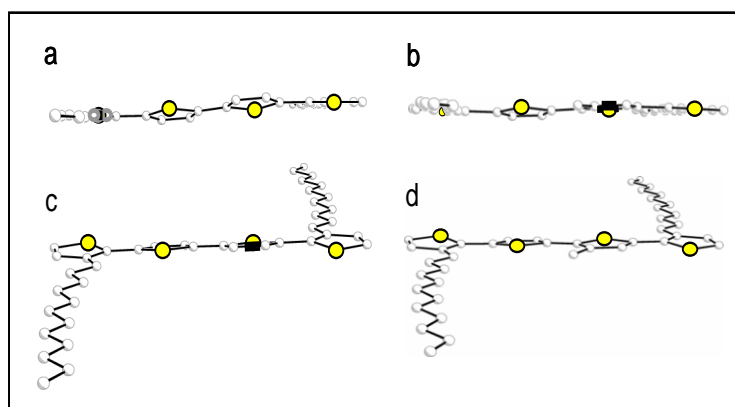


Figure 2. Single crystal structures of **monomer B** (a, c) and **monomer A** (b, d) (a, b: view along outer thiophene plane; c, d: view along inner thiophene plane.)

UV-visible absorption spectra of thin films spin cast from solution of **2** (**PQT**), **3** (**PQT-CH₃**) and copolythiophene **4a** (x=10 mol%) in chlorobenzene on glass slides (**Figure 3**) have shown that all of the polythiophenes exhibited well-defined vibronic splitting characteristic of high structural ordering at $\lambda_{\text{max}} \sim 510$ nm (shoulder), 548 nm, and 587 nm, indicating that the thin-film spectral properties of polythiophene **3**(**PQT-CH₃**) and copolythiophene **4** are similar to those of polythiophene **2** (**PQT**) with 3D lamellar π -stacking structural ordering in the thin film.^{19,28}

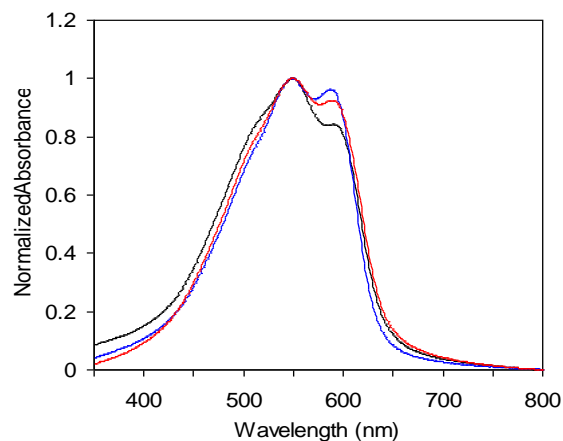


Figure 3. UV-Vis absorption spectra of thin films spin cast from **2** (blue), **3** (black), and **4a** (red).

The structural order of **3** (PQT-CH₃) and copolythiophene **4a** in their thin films were further established by X-ray diffraction (XRD) studies. XRD of a 0.2 μm thin film spin cast from **3** and **4a** on an octyltrichlorosilane (OTS-8)-modified silicon wafer showed very similar three distinctive diffraction peaks after annealing. The diffraction peaks of the annealed thin films are at $2\theta = 5.2^\circ$ (100), 10.8° (200), and 16.2° (300) for **3** and at $2\theta = 5.3^\circ$ (100), 10.6° (200), and 16.0° (300) for **4a**, respectively, as shown in **Figure 4**. These diffraction peaks correspond to d spacing for the inter-chain distance between two neighbouring polythiophene chains within the lamellar structure, which showed essentially similar lamellar structural orders of polythiophene **2** (PQT).^{19,28} Comparing to **4a**, the slightly increased d spacing of **3** might be due to the present of methyl group.

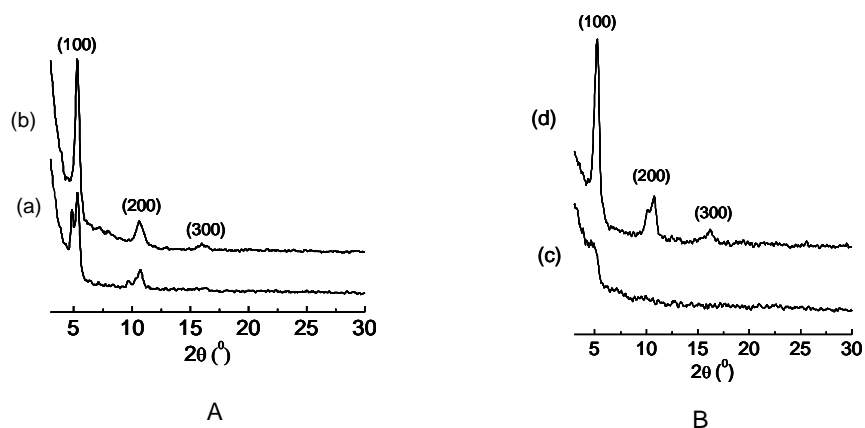


Figure 4. **A.** XRDs of **4a**, (a) 0.2 μm thin film without annealing; (b) 0.2 μm thin film annealed at 140°C; **B.** XRDs of **3**, (c) 0.2 μm thin film without annealing; (d) 0.2 μm thin film annealed at 120°C.

Thermal properties of **2** (**PQT**), **3** (**PQT-CH₃**) and **4(a-c)** were characterized by DSC measurements and their phase transition temperatures on heating are shown in **Figure 5**. Two endothermic peaks were observed on heating curves for all of them, indicating liquid crystalline properties of these polymeric semiconductors. The first peak on heating can be assigned to melting of the long alkyl side chain, and the second peak can be assigned to melting of the polythiophene backbone. In general, the phase transition temperature increases slightly with the increase of the monomer content of **2** (**PQT**). The slight variation might be due to the difference of molecular weight.

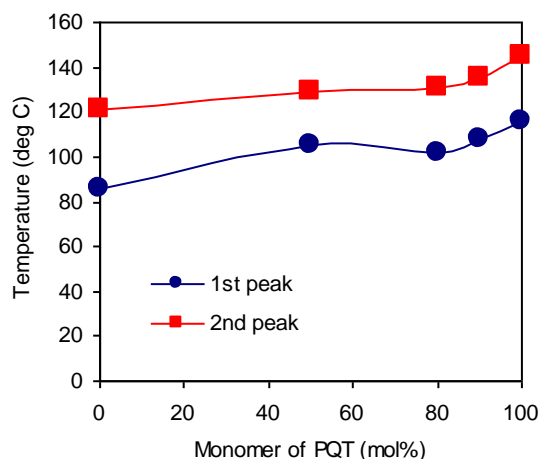


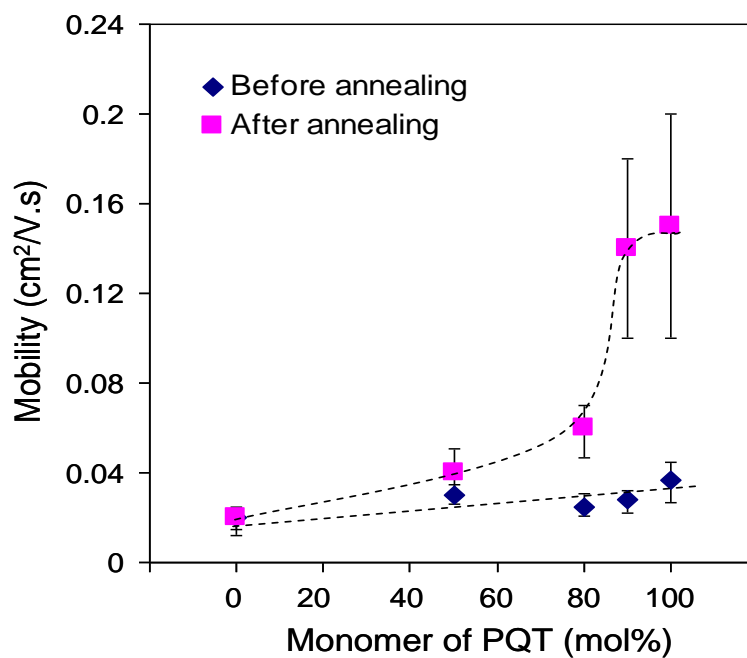
Figure 5. Phase transition temperatures of **2** (PQT), **3** (PQT-CH₃) and **4(a-c)** on heating.

Electronic properties of thin-film transistors fabricated from **3** (PQT-CH₃) and **4(a-c)** as a semiconductor layer were evaluated from both dichlorobenzene and o-xylene solvents, and their mobilities in both solvents were at the similar level. The results of OTFTs fabricated from **3** (PQT-CH₃) and **4(a-c)** in o-xylene by spin coating were compared with those OTFTs fabricated from semiconductor **2** (PQT) in dichlorobenzene, as it was not soluble in o-xylene at room temperature. All the fabrication and characterization of organic thin-film transistors (OTFTs) were done under ambient conditions without taking any precautions to isolate the materials and devices from exposure to air, moisture, and light. Bottom-gate TFT devices were built by spin-coating solutions of **2**, **3** and **4(a-c)** on n-doped silicon wafer as the gate electrode with a 110-nm thermal silicon oxide (SiO₂) as the dielectric layer. The dielectric surface was modified with octyltrichlorosilane as reported before for better compatibility with

polythiophene semiconductor.³⁰ The values of mobility and current On/Off ratio for the OTFTs were summarized in **Table 1** and illustrated in **Figure 6**. The results show that mobility increases with increasing the composition of polythiophene **2 (PQT)**. The result is consistent with their enthalpy values which were obtained from DSC measurement. Also shown in **Table 1**, the enthalpy value decreased with increasing the content of monomer **A**, indicating a gradually decreased crystallinity with increasing the content of monomer **A**. The incorporation of methyl group does cause a slight perturbation of solid state crystallinity. However, even with 100 mol% of monomer **A**, polymer **3 (PQT-CH₃)** not only showed excellent stability in coating solution for over several weeks, but also reached a reasonable field-effect mobility up to $0.03 \text{ cm}^2 \text{ V}^{-1} \text{ s}^{-1}$, which is consistent with our assumption that by strategically attaching a small substituent, the methyl group, in PQT system, the structural regioregularity of long side-chains of **PQT** would not be significantly disturbed and, therefore both polymer **3** and copolymer **4 (a-c)** can still form ordered molecular structures and give good mobility values.

Table 1. Summary of enthalpy data, OTFT mobility, and current on/off ratio with **2** (PQT), **3** (PQT-CH₃) and **4(a-c)** as a semiconductor layer.

Polythiophenes	Mw/Mn	solvent	enthalpy (J/g)	Mobility (cm ² /V.s), (current On/Off)	
				Before annealing	after annealing
2 (PQT)	22.9K/17.3K	dichlorobenzene	7.30	0.03 - 0.047 (10 ⁶)	0.10 - 0.2 (10 ⁷)
4a (x=10 mol %)	30.6k/17.4k	<i>o</i> -xylene	5.53	0.024-0.035 (10 ⁶)	0.10 - 0.18(10 ⁷)
4b (x=20 mol %)	21.5k/10.9k	<i>o</i> -xylene	5.42	0.021-0.03 (10 ⁶)	0.05 - 0.07(10 ⁶)
4c (x= 50mol %)	21.6k/10.9k	<i>o</i> -xylene	4.77	0.025-0.035 (10 ⁶)	0.03 - 0.05(10 ⁶)
3 (PQT-CH ₃)	29.2k/14.8k	<i>o</i> -xylene	1.79	0.015-0.022 (10 ⁶)	0.015 - 0.03(10 ⁶)

**Figure 6.** Mobility as a function of the molar percentage of the monomer for **2** (PQT) in the copolythiophene.

Furthermore, it was observed that the OTFTs fabricated from the solution of copolythiophene **4a** in xylene showed high TFT performance with mobility up to $0.18 \text{ cm}^2 \text{ V}^{-1} \text{ s}^{-1}$ and current On/Off $> 10^7$ (**Figure 7**), which reached similar mobility of **2 (PQT)** fabricated in dichlorobenzene. The results demonstrated that the solubility characteristics of high performance semiconductor **2 (PQT)** system of this nature were significantly improved, and in the same time a small amount of steric perturbation effect in solid state has little effect on charge carrier mobility. Therefore, an optimum TFT performance, fabricated from an environmentally benign solvent, was obtained by this strategic judicial structure modification.

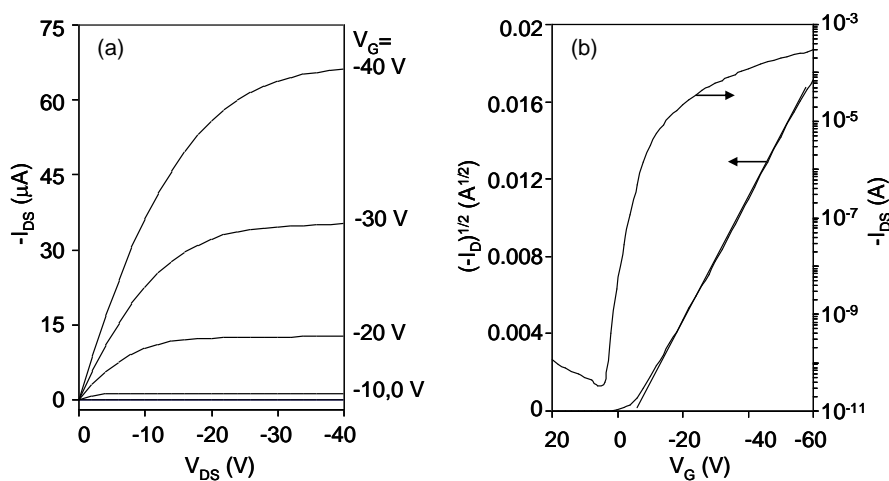


Figure 7. I-V characteristics of exemplary copolymer **4a** TFT device with 90- μm channel length and 5000- μm channel width: (a) output curves at different gate voltages; (b) transfer curve at linear regime.

Conclusion

In conclusion, we have developed a facile approach to tuning the solubility characteristics of a high mobility polythiophene system, **2 (PQT)**, of this nature. The results demonstrated that significantly improved solution processability in an environmentally benign solvent with high field effect mobility could be simultaneously obtained through the judicious structure modification. Solution processed OTFTs comprised with newly developed **3 (PQT-CH₃)** and copolythiophene **4 (a-c)** were fabricated using an environmentally benign solvent and excellent TFT characteristics with high field-effect mobility up to $0.18 \text{ cm}^2 \text{ V}^{-1} \text{ s}^{-1}$ and current On/Off ratio up to 10^7 were obtained. Thus they are suitable for OTFT applications in low-cost solution process manufacturing environments.

Experimental Procedures

All the synthetic works, material characterizations and OTFT device fabrications were done at Xerox Research Centre of Canada, excepting that X-ray diffraction analyses were done at McMaster University, Ontario, Canada.

Instrumentation and measurements. NMR spectra were obtained in CDCl_3 with a Bruker DPX 300 NMR spectrometer with tetramethylsilane as an internal reference. Absorption spectra were measured on a Varian Cary-5 UV-Vis-NIR spectrophotometer for the thin films of polymeric semiconductors. Gel permeation chromatography (GPC) was conducted using Waters 2690 Separation Module to obtain molecular weights and molecular weight distributions (relative

to polystyrene standards). Thermal properties of polymeric semiconductors were measured using Differential Scanning Calorimeter (DSC) (TA instrument, DSC2910) with a scanning rate of 10 °C/min. The film X-ray diffractions were performed at room temperature on a Rigaku MiniFlex Diffractometer using Cu K α radiation ($\lambda = 1.5418 \text{ \AA}$) with a θ -2 θ scans configuration. Single crystal X-ray diffractions were performed on a Bruker Smart 6000 CCD 3-circle D8 diffractometer with a Cu RA X-ray source ($\lambda=1.5418 \text{ \AA}$) at room temperature. OTFTs were characterized using a Keithley SCS-4200 characterization system under ambient conditions.

Synthesis. All the chemicals were purchased from Sigma-Aldrich and used without further purification. Polythiophene **2 (PQT)** was synthesized according to the synthetic method reported in the literature.¹⁹

5,5'-bis(3-dodecyl-2-thienyl)-3-methyl-2,2'-dithiophene (monomer A). A solution of 2-bromo-3-dodecylthiophene (15.36 g, 46.36mmol) in anhydrous tetrahydrofuran (30 mL) was added slowly over a period of time (~20 minutes) to a magnetically stirred suspension of magnesium turnings (1.69 g, 69.52 mmol) in anhydrous tetrahydrofuran (10 mL) under an inert argon atmosphere. The resulting mixture was stirred at room temperature for 2.5 hours, and then at 50°C for 30 minutes before cooling down to room temperature. Then, the freshly prepared Grignard solution was added slowly via a cannula to a mixture of 5,5'-dibromo-3-methyl-2,2'-dithiophene (6.27 g, 18.54 mmol) and [1,3-

bis(diphenylphosphinoethane)dichloronickel (II) (0.48 g, 0.91 mmol) in anhydrous tetrahydrofuran (50 mL) and the resulting mixture was refluxed for 48 hours under inert argon atmosphere. Subsequently, the reaction mixture was diluted with ethyl acetate (200 mL), washed with water and dried with magnesium sulphate. After removing the solvent by a rotary evaporator, the resulting dark brown crude solid was purified by column chromatography on silica gel with hexane. The final product was obtained from recrystallization in a mixture of methanol and isopropanol, giving 5,5'-bis(3-dodecyl-2-thienyl)-3-methyl-2,2'-dithiophene as an orange yellow crystalline solid (8.61g, 68 % yield). ^1H NMR (CDCl_3): δ 7.19 (m, 2H), 7.10 (dd, 2H), 6.96(m, 2H), 6.93 (s, 1H), 2.80 (t, 4H), 2.45 (s, 3H), 1.67 (q, 1.65, 4H), 1.27 (bs, 36H), 0.89 (m, 6H); mp:34 °C; elemental analysis: C, 71.99 %; H, 9.06 %, S, 20.24 %.

Polythiophene 3 (PQT-CH₃). A solution of 5,5'-bis(3-dodecyl-2-thienyl)-3-methyl-2,2'-dithiophene (monomer A, 1.0 g, 1.47 mmol) in chlorobenzene (20 mL) was added slowly to a well stirred mixture of FeCl₃ (1.0 g, 6.16 mmol) and chlorobenzene (10 mL) and the resulting mixture was stirred at 60°C under an argon atmosphere for 48 hours. After the resulting mixture was cooled to room temperature, it was diluted with methylene chloride (50 mL) and washed with water (~200 mL) three times. The combined organic layer was stirred in an aqueous ammonia solution (150 mL, 7.5 wt%) for 1 hour and then washed with water (~200 mL) three times. The washed organic layer was poured into methanol (~ 300 mL) with good stirring and the crude product was collected by

filtration. Then, the crude product was purified by soxhlet extraction with methanol, hexane, and chlorobenzene respectively. After the soxhlation, the resulting product in chlorobenzene solution was precipitated in methanol (~300 mL) and collected by filtration, giving the final product as a dark red solid (0.57 g, 57%) with following molecular weight properties: M_w 29.2 K and M_n 14.8 K. $^1\text{H NMR}$ (CDCl_3): δ 7.13 (m, 2H), 7.03(m, 2H), 6.96 (s, 1H), 2.80 (t, 4H), 2.47 (s, 3H), 1.70 (q, 4H), 1.28 (bs, 36H), 0.89 (m, 6H).

Copolythiophene 4a (x=10 mol%): A solution of mixed 5,5'-bis(3-dodecyl-2-thienyl)-2,2'-dithiophene (monomer B, 500 mg, 0.75 mmol) and 5,5'-bis(3-dodecyl-2-thienyl)-3-methyl-2,2'-dithiophene (monomer A, 57 mg, 0.084 mmol) in 10 mL of chlorobenzene was added slowly to a well stirred mixture of FeCl_3 (500 mg, 3.08 mmol) in 5 mL of chlorobenzene. The resulting mixture was stirred at 60°C under an argon atmosphere for 48 hours. After the polymerization, the resulting mixture was cooled to room temperature, diluted with methylene chloride (~50 mL) and washed with water (~200 mL) three times. The collected organic layer was stirred with an aqueous ammonia solution (150 mL, 7.5 wt%) for 1 hour and then washed with water (~200 mL) three times. The collected organic layer was poured into methanol (~300 mL) with good stirring and the crude product was collected by filtration. The crude product was purified by soxhlet extraction with methanol, heptane, and chlorobenzene respectively. After the soxhlation the resulting product in chlorobenzene solution was precipitated in methanol (~300 mL), collected by filtration and then dried in a vacuum oven. The

content of monomer A in the copolymer was determined from NMR results by integration of the peak area of the methyl group in monomer A at 2.47 ppm (chemical shift) and the ethylene groups attached to the thiophene atoms in both monomer A and monomer B at 2.80 ppm (chemical shift). The result is consistent with the starting monomer ratio. The final product as dark red solid with a yield of 86% (0.48g) showed the following molecular weight properties: $M_w=30.6K$ and $M_n=17.4K$. 1H NMR ($CDCl_3$): δ 7.16 (m, 2H), 7.07(m, 1.6H), 7.04 (s, 1H), 6.98 (s, 0.1H), 2.80 (t, 4H), 2.47 (s, 0.3H), 1.71 (q, 4H), 1.28 (bs, 36H), 0.89 (t, 6H).

Copolythiophene 4b (x=20 mol%) and **4c** (x=50 mol%) were prepared in the similar manner as described in **4a**. The content of monomer A in the copolymer **4b** and **4c** is 19.7 mol% and 50.4 mol%, respectively, calculated from NMR results using the same method as described for copolymer **4a**. The results are consistent with the starting monomer ratios as well. The molecular weights of **4b** and **4c** were $M_w=21.5K$ ($M_n=15.4K$) and $M_w=21.6K$ ($M_n:10.9K$) respectively. The yields of **4b** and **4c** were 79% and 68% respectively. 1H NMR ($CDCl_3$) for **4b**: δ 7.16 (m, 2H), 7.08(m, 1H), 6.97 (s, 0.2H), 2.80 (t, 4H), 2.47 (s, 0.6H), 1.71 (q, 4H), 1.28 (bs, 36H), 0.89 (m, 6H); 1H NMR ($CDCl_3$) for **4c**: δ 7.13 (m, 2H), 7.03 (bS, 2H), 6.96 (s, 0.5H), 2.80 (t, 4H), 2.47 (s, 1.5H), 1.71 (q, 4H), 1.28 (bs, 36H), 0.89 (m, 6H).

OTFT Fabrication and Evaluation. All the fabrication and characterization of organic thin-film transistor device (OTFTs) were done under ambient conditions without taking any precautions to isolate the material and device from exposure to air, moisture, and light. Bottom-gate TFT devices were built on n-doped silicon wafer as the gate electrode with a 110-nm thermal silicon oxide (SiO_2) as the dielectric layer. The SiO_2 surface was modified with octyltrichlorosilane (OTS-8) by immersing a cleaned silicon wafer substrate in 0.1 M OTS-8 in toluene at 60 °C for 20 min. The wafer was subsequently rinsed with toluene and isopropanol, and then dried with an air stream. Semiconductor layer was first deposited on the OTS-8-modified SiO_2 layer by spin coating a semiconductor solution in o-xylene (1.0 wt%) for **3 (PQT-CH₃)** and **4(a-c)**, and the semiconductor layer of **2 (PQT-12)** was deposited by spin coating its solution in dichlorobenzene (0.3 wt%) at 1000 rpm for 120 seconds, and vacuum dried to give a 20-50 nm-thick semiconductor layer. Subsequently, the gold source and drain electrodes were deposited by vacuum evaporation through a shadow mask, thus creating a series of TFTs with various channel length (L) and width (W) dimensions. All the devices were annealed by heating the dried TFT devices in a vacuum oven at 120-140 °C for 15 to 30 minutes and then cooled down to room temperature. Patterned transistors with channel length of 90 or 190 μm and channel width of 1 or 5 mm were used for I-V measurements. The mobilities in the linear and saturated regimes were extracted from the following equation:

$$\text{Saturated regime } (V_D > V_G): \quad I_D = C_i \mu (W/2L) (V_G - V_T)^2$$

Where I_D is the drain current, C_i is the capacitance per unit area of the gate dielectric layer, and V_G and V_T are respectively the gate voltage and threshold voltage. V_T of the device was determined from the relationship between the square root of I_D at the saturated regime and V_G of the device by extrapolating the measured data to $I_D = 0$.

ACKNOWLEDGEMENT. We thank Dr. Jim Britten in Chemistry Department at McMaster University for X-ray diffraction characterizations.

References

1. Bao, Z.; Feng, Y.; Dodabalapur, A.; Raju, V. R.; Lovinger, A. J. *Chem. Mater.* **1997**, *9*, 1299-1301.
2. Sirringhaus, H.; Tessler, N.; Friend, R. H. *Science* **1998**, *280*, 1741-1744.
3. Sirringhaus, H.; Brown, P. J.; Friend, R. H.; Nielsen, M. M.; Bechgaard, K.; Langeveld-Voss, B. M. W.; Spiering, A. J. H.; Janssen, R. A. J.; Meijer, E. W.; Herwig, P.; de Leeuw, D. M. *Nature* **1999**, *401*, 685-688.
4. Bao, Z.; Lovinger, A. J.; *Chem. Mater.* **1999**, *11*, 2607-2612.
5. Bao, Z. *Adv. Mater.* **2000**, *12*, 227-230.
6. Sirringhaus, H.; Kawase, T.; Friend, R. H.; Shimoda, T.; Inbasekaran, M.; Wu, W.; Woo, E. P. *Science* **2000**, *290*, 2123-2126.
7. Katz, H. E.; Bao, Z. *J. Phys. Chem. B* **2000**, *104*, 671-678.
8. Dimitrakopoulos, C. D.; Malenfant, P. R. L. *Adv. Mater.* **2002**, *14*, 99-117.
9. Mushrush, M.; Facchetti, A.; Lefenfeld, M.; Katz, H. E.; and Marks, T. J. *J. Am. Chem. Soc.* **2003**, *125*, 9414-9423.
10. Meng, H.; Zheng, J.; Lovinger, A. J.; Wang, B. C.; Patten, P. G. V.; Bao, Z. *Chem. Mater.* **2003**, *15*, 1778-1787.
11. Forrest, S. R. *Nature* **2004**, *428*, 911-918.
12. Katz, H. E. *Chem. Mater.* **2004**, *16*, 4748-4756.
13. Ling, M. M.; Bao, Z. *Chem. Mater.* **2004**, *16*, 4824-4840.
14. Singh, T. B.; Sariciftci N. S. *Annu. Rev. Mater. Res.* **2006**, *36*, 199-210.

15. Lu, G.; Usta, H.; Risko, C.; Wang, L.; Facchetti, A.; Ratner, M. A.; Marks, T. J. *J. Am. Chem. Soc.* **2008**, *130*, 7670–7685.
16. Mauldin, C. E.; Puntambekar, K.; Murphy, A. R.; Liao, F.; Subramanian, V.; Fréchet, J. M. J.; DeLongchamp, D. M.; Fischer, D. A.; Toney, M. F. *Chem. Mater.* **2009**, *21*, 1927-1938.
17. Yan, H.; Chen, Z.; Zheng, Y.; Newman, C.; Quinn, J. R.; Dötz, F.; Kastler, M.; Facchetti, A. *Nature*, **2009**, *457*, 679-686.
18. Bao, Z.; Dodabalapur, A.; Lovinger, A. J. *Appl. Phys. Lett.* **1996**, *69*, 4108-4110.
19. Ong, B. S.; Wu, Y.; Liu, P.; Gardner, S. *J. Am. Chem. Soc.* **2004**, *126*, 3378-3379.
20. Wu, Y.; Liu, P.; Gardner, S.; Ong, B. S. *Chem. Mater.* **2005**, *17*, 221-223.
21. McCulloch, I.; Heeney, M.; Bailey, C.; Genevicius, K.; Macdonald, I.; Shkunov, M.; Sparrowe, D.; Tierney, S.; Wagner, R.; Zhang, W.; Chabynyc, M. L.; Kline, R. J.; McGehee, M. D.; and Toney, M. F. *Nat. Mater.* **2006**, *5*, 328-333.
22. Pan, H.; Li, Y.; Wu, Y.; Liu, P.; Ong, B. S.; Zhu, S.; Xu, G. *J. Am. Chem. Soc.* **2007**, *129*, 4112-4113.
23. Osaka, I.; Sauv e, G.; Zhang, R.; Kowalewski, T.; McCullough, R. D. *Adv. Mater.* **2007**, *19*, 4160-4165.

24. Liu, J.; Zhang, R.; Sauv, G.; Kowalewski T.; McCullough, R. D. *J. Am. Chem. Soc.* **2008**, *130*, 13167-13176.
25. Li, J.; Qin, F.; Li, C. M.; Bao, Q.; Chan-Park, M. B.; Zhang, W.; Qin, J.; Ong, B. S. *Chem. Mater.* **2008**, *20*, 2057-2059.
26. He, M.; Li, J.; Sorensen, M. L.; Zhang, F.; Hancock, R. R.; Fong, H. H.; Pozdin, V. A.; Smilgies D. M.; Malliaras, G. G. *J. Am. Chem. Soc.*, **2009**, *131*, 11930-11938.
27. Kim, D. H.; Lee, B. L.; Moon, H.; Kang, H. M.; Jeong, E. J.; Park, J.; Han, K. M.; Lee, S.; Yoo, B. W.; Koo, B. W.; Kim, J. Y.; Lee, W. H.; Cho, K.; Becerril, H. A.; Bao Z. *J. Am. Chem. Soc.*, **2009**, *131*, 6124-6132.
28. Ong, B. S.; Wu, Y.; Liu, P.; Gardner, S. *Adv. Mater.* **2005**, *17*, 1141-1144.
29. Pan, H.; Liu, P.; Li, Y.; Ong, B. S.; Zhu, S.; Xu, G. *Adv. Mater.* **2007**, *19*, 3240-3243.
30. Wu, Y.; Liu, P.; Ong, B.S.; Srikumar, T.; Zhao, N.; Botton, G.; Zhu, S. *Appl. Phys. Lett.* **2005**, *86*, 142102-142104.

4.3 Supporting Materials for the Paper

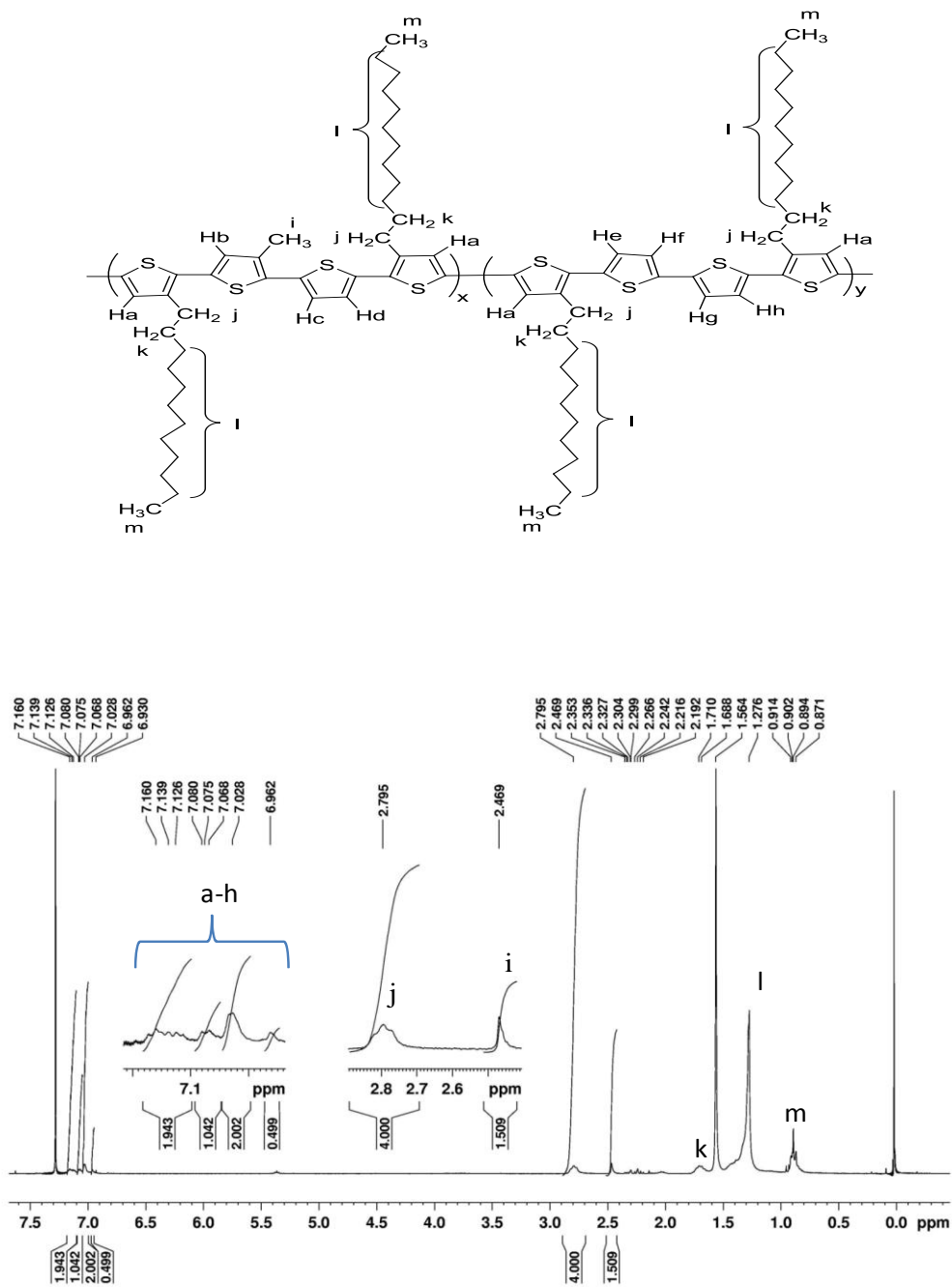


Figure S1 ^1H NMR (CDCl₃) spectrum for copolymer 4c (x=50 mol%, y=50 mol%).

4.4 Summary

In this work, a simple approach was developed to improve the solubility characteristics of a high mobility polythiophene system by strategic structure modification. The developed copolythiophenes showed significantly improved solubility in environmentally benign solvents. The OTFT devices with this type of copolythiophenes gave excellent electrical properties with field-effect mobility of $0.18 \text{ cm}^2 \text{ V}^{-1} \text{ s}^{-1}$ when fabricated from more environmentally friendly solvent such as xylene. The results obtained from this study could help better understanding the relationship between the molecular structure and their properties including the solubility, molecular ordering and OTFT performance. Thus better performance organic semiconductors with desired material properties can be developed for electronic device applications.

Chapter 5

Robust Gate Dielectric Design

5.1 Introduction

This chapter describes a robust gate dielectric design for OTFT applications. In addition to semiconductor materials, the property of gate dielectrics also plays an important role in the performance of OTFTs. In the last two decades, most researches in the area of OTFTs have been focused their efforts on developing organic semiconductors and thus most OTFTs were fabricated on silicon wafers with a thin layer of thermally grown SiO₂ as dielectric layer for the convenience. Therefore, fewer solution-processable high performance dielectric materials have been developed for the applications in solution processed flexible OTFTs. The major challenges for a gate dielectric layer include robustness with little pinholes to prevent current leakage; good compatibility with the semiconductor layer to enhance field-effect mobility; and excellent solution processability for low cost and flexible OTFT applications.

The research work presented in this chapter was focused on developing a robust gate dielectric structure for OTFT applications by solution processes. Furthermore, the developed dielectric must have good compatibility with most polythiophene-based semiconductors to enhance the performance of OTFTs.

I was primarily responsible for this dual-layer dielectric structure design, material synthesis, and device fabrication. Dr. Yiliang Wu provided guidance for the device fabrication and characterization. Dr. Yuning Li provided gold

nanoparticles for the fabrication of electrodes. Dr. Beng Ong and Dr. Shiping Zhu provided valuable suggestions and discussions.

5.2 Main Text of Paper 3

Reprinted with permission from *J. Am. Chem. Soc.* 2006, 128, 4554-4555.

Copyright © 2006, American Chemical Society.

Enabling Gate Dielectric Design for All Solution-Processed, High-Performance, Flexible Organic Thin-Film Transistors

Ping Liu^{a,b}, Yiliang Wu^a, Yuning Li^a, Beng S. Ong^{a}, Shiping Zhu^b*

^aMaterials Design & Integration Laboratory, Xerox Research Centre of Canada,
Mississauga, Ontario, Canada

^bDepartment of Materials Science & Engineering, McMaster University,
Hamilton, Ontario, Canada

Solution processabilities of both active and passive materials (conductor, semiconductor and dielectric) for organic thin-film transistors (OTFTs) are crucial to the fabrication of printed integrated transistor circuits. The possibility of using low-cost solution patterning and deposition techniques, coupled with such salient OTFT circuit features of being physically compact, lightweight, and flexible, has fuelled the current surge in organic electronics research.¹ While there exist many printable and functionally capable semiconductors^{2,3} and conductors,⁴ few

solution processable and electrically satisfactory dielectric materials⁵ are available to enable design of flexible electronics.

The interfacial interactions of organic semiconductor layer with gate dielectric are often very specific and play a decisive role in the functioning of field effect transistor (FET) devices. Optimum device performance generally requires synergistic interactions at the semiconductor/dielectric interface. For example, while the octyltrichlorosilane (OTS-8) self-assembled monolayer (SAM) on thermal SiO₂ surface enhances the semiconductor performance of regioregular polythiophene, PQT-12,^{2a} utilization of untreated native SiO₂ surface has led to reductions in mobility and on/off ratio by as much as up to three orders of magnitude.⁶ A great variety of other alkyl silylating agents have also been explored with the objective of optimizing the dielectric/semiconductor interactions, often with satisfactory performance results.⁷⁻¹¹ Specifically, hexamethyldisilazane (HMDS) surface treatment has been employed to promote segregation of regioregular polythiophenes for improved mobility,⁷ while perfluorosilane modification, for manipulating threshold voltages of OTFTs.^{8,9} More recently, alkylphosphonic acid SAM on alumina has been demonstrated to be effective in achieving hitherto best FET performance of evaporated pentacene semiconductor.¹¹ However, all these modifications have two limiting characteristics. First, the creation of synergistic dielectric surface requires appropriate chemical reactions between the modification agent and the dielectric surface. Second, if SAMs are utilized, their qualities, which depend critically on

the surface chemistry of dielectric and the methods through which they are formed, would greatly affect the final FET performance. These modification approaches may thus be difficult to implement reproducibly in high throughput manufacturing processes, particularly on such chemically inert surfaces as those of common plastic substrates to enable flexible electronic design.

In this communication, we report an effective approach to a solution processed dielectric design to enable all-solution processed, high-performance OTFTs for flexible electronic applications. This is through a dual-layer dielectric structure comprising of a UV-crosslinked poly(4-vinyl phenol)-co-poly(methyl methacrylate) (PVP-PMMA) bottom layer and a thermally crosslinked polysiloxane top layer of for example poly(methyl silsesquioxane) (pMSSQ) which can be readily generated from methyltrialkoxysilane.¹² The partially crosslinked pMSSQ in an appropriate solvent is solution processable and its solution viscosity can be adjusted to suit various solution deposition techniques such as spin coating, stamping, flexography, and inkjet printing to name a few. After deposition, the pMSSQ layer can then be fully crosslinked thermally at a temperature which is compatible with common commercial plastic substrates for fabrication of flexible integrated circuits.

Figure 1 schematically depicts the preparation of pMSSQ and its use in modifying the PVP-PMMA surface for an all solution-processed OTFT on a polyester plastic substrate (PET) such as Mylar[®]. A thin gold film serving as the

gate electrode was first formed on a PET substrate by spin coating a gold nanoparticle dispersion, followed by annealing at 150 °C.^{4a} A solution of PVP-PMMA in DMF was spin cast on top of this gold film and crosslinked via exposure to a 254 nm-UV light. Thereafter, a 50-nm pMSSQ layer was laid on top of crosslinked PVP-PMMA by spin coating a solution of pMSSQ in methyl isobutyl ketone, followed by curing at 140-160 °C. This was followed by patterning an array of gold source/drain electrode feature pairs via stencil printing using a gold nanoparticle dispersion, followed by annealing at 150 °C.^{4a} Finally, a semiconductor layer was deposited using the PQT-12 nanoparticle dispersion via spin coating or inject printing,¹³ thus creating a series of OTFTs of different channel length/width dimensions. For comparison, OTFT devices without pMSSQ top layers were also fabricated. All the devices were annealed at 140 °C to achieve optimum molecular ordering in the PQT-12 semiconductor layer for best OTFT performance.

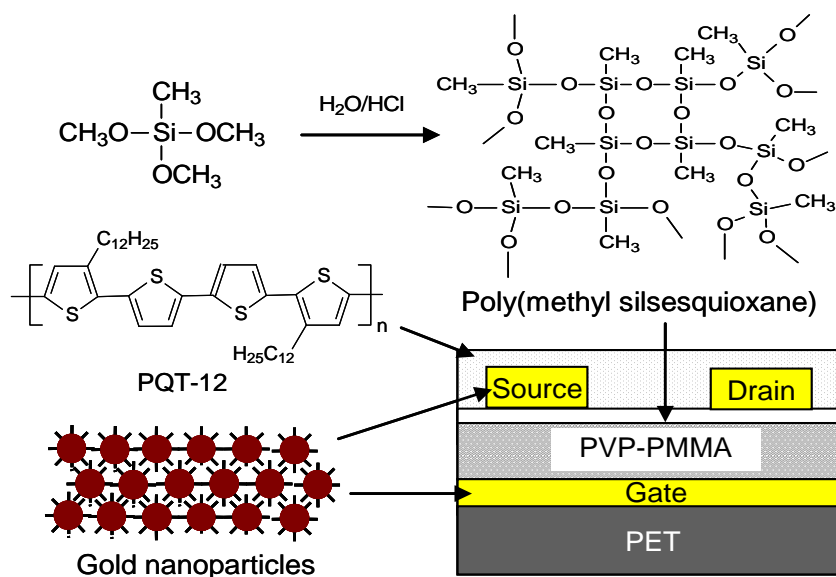


Figure 1. Schematic depiction of formation of poly(methyl silsesquioxane) from methyltrimethoxysilane and its incorporation as a dielectric top layer in an all-solution processed organic thin film transistor device on PET.

The surface properties of dielectrics were characterized by water advancing contact angle measurement. The uncoated PVP-PMMA surface, with a high concentration of surface hydroxy groups, was hydrophilic and exhibited a water contact angle of $\sim 78^\circ$. After treatment with pMSSQ, a hydrophobic surface with a water contact angle of $\sim 98^\circ$ was obtained (Table 1).

Table 1. Water contact angle and device performance of the OTFTs with different dielectrics.

Gate Dielectric	Contact angle	Mobility (cm ² /V.s)	On/off ratio	V _{th} (V)
PVP-PMMA	78±3°	0.003	10 ⁴	-4
PVP-PMMA/OTS-8	95±3°	0.003	10 ⁴	-4
PVP-PMMA/pMSSQ	98±2°	0.15	10 ⁶	-2

This contact angle is identical to the case when a hydrophilic native SiO₂ surface is modified with octyltrichlorosilane (OTS-8).⁶ Modification of the PVP-PMMA dielectric surface with OTS-8 gave a water contact angle of ~ 95°, but the contact angle decreased to about 80° in a few hours, indicative of the instability of OTS-8 SAM on PVP-PMMA surface.

All the OTFT devices were fabricated under ambient conditions and evaluated using a Keithley SCS-4200 in a black metal box in air. Figure 2 shows the output and transfer curves of all-solution processed OTFTs on PET substrates. The devices with the non-modified, UV-cured PVP-PMMA dielectric showed a mobility of 0.003 cm² V⁻¹ s⁻¹ and current on/off ratio of 10⁴. With OTS-8 modification, the devices gave similar results.

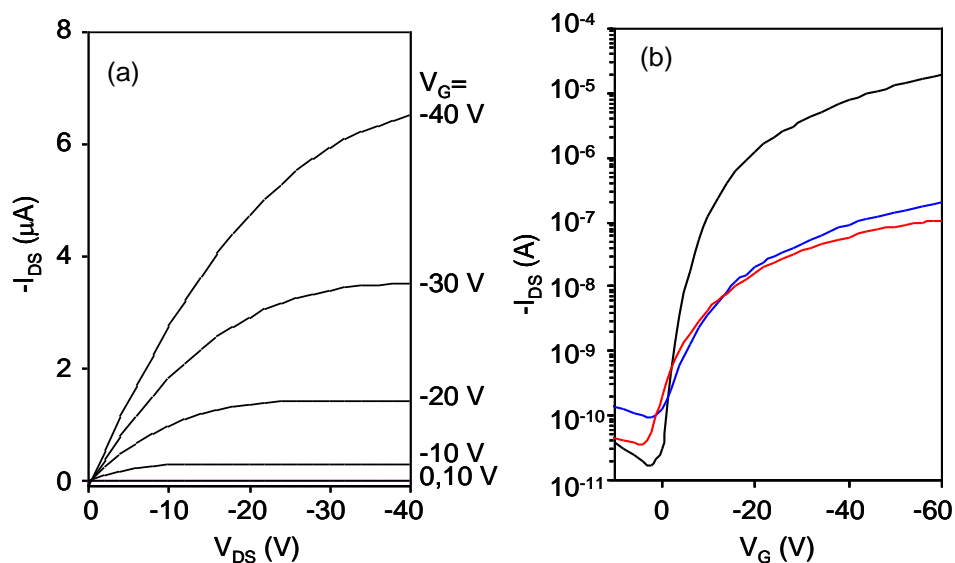


Figure 2. (a) Source-drain current versus source drain voltage at different gate voltages for an OTFT with dual-layer gate dielectric. (b) Source-drain current versus gate voltage at a source-drain voltage of -60 V for OTFTs with different gate dielectrics: dual-layer dielectric, black line; OTS-8-modified UV cured-PVP-PMMA dielectric, blue line; UV-cured PVP-PMMA dielectric, red line. (Channel length = 90 μm ; channel width = 1000 μm).

All the OTFT devices were fabricated under ambient conditions and evaluated using a Keithley SCS-4200 in a black metal box in air. Figure 2 shows the output and transfer curves of all-solution processed OTFTs on PET substrates. The devices with the non-modified, UV-cured PVP-PMMA dielectric showed a mobility of $0.003 \text{ cm}^2 \text{ V}^{-1} \text{ s}^{-1}$ and current on/off ratio of 10^4 . With OTS-8 modification, the devices gave similar results. However, with the present dual-layer gate dielectric i.e., UV-cured PVP-PMMA modified with pMSSQ (dielectric constant = 4.0; Capacitance = 9.0 nF cm^{-2}), the OTFTs exhibited ideal FET behaviors, conforming well to the conventional transistor models in both the

linear and saturated regimes. The output characteristics showed no observable contact resistance, very good saturation behavior, and clear saturation currents which were quadratic to gate bias. The devices switched on at ~ 0 V, displayed subthreshold slopes of ~ 2 V dec⁻¹, and exhibited small hysteresis effect. Compared with the devices with the non-modified or OTS-8 modified UV-cured PVP-PMMA dielectrics, the improvements were phenomenal, with mobility by as much as 50 times to 0.15 cm² V⁻¹ s⁻¹ and on/off ratio by 2 orders of magnitude to 10^6 (Table 1). The performance characteristics of these OTFTs were very consistent and reproducible, with little transistor-to-transistor variations, which would be critically important for large-area electronic device fabrication where large OTFT circuits with hundreds of thousands of transistors may be involved.

The use of just pMSSQ as gate dielectric gave very low device yields, and its coupling with a chemically crosslinked PVP-PMMA dielectric led to high gate leakage currents. The observed low gate leakage with the UV-crosslinked PVP-PMMA gate dielectric is attributable to a much higher crosslink density.

The current pMSSQ/UV-cured PVP-PMMA dual-layer gate dielectric is robust and extremely resistant to common organic coating solvents including alcohol, toluene, chlorinated solvents such as chloroform, chlorobenzene, dichlorobenzene, etc. Subsequent liquid deposition of semiconductor layer followed by annealing did not lead to its dimensional and structural damages or adverse electrical performance consequences.

In conclusion, we have concretely demonstrated that the pMSSQ/UV-cured PVP-PMMA dielectric is a solution processable, high-performance dielectric that is suitable for all-printed OTFT circuits on flexible substrates.

Acknowledgement. Partial financial support of this work is provided by the National Institute of Standards and Technology through an Advanced Technology Grant (70NANB0H3033).

References

1. For reviews see (a) Sirringhaus, H. *Adv. Mater.* **2005**, *17*, 2411-2425. (b) Ling, M. M.; Bao, Z. *Chem. Mater.* **2004**, *16*, 4824-4840. (c) Chabynyc, M. L.; Salleo, A. *Chem. Mater.* **2004**, *16*, 4509-4521. (d) Dimitrakopoulos, C. D.; Malenfant, P. R. L. *Adv. Mater.* **2002**, *14*, 99-117. (e) Katz, H. E. *Chem. Mater.* **2004**, *16*, 4748-4756.
2. (a) Ong, B. S.; Wu, Y.; Liu, P.; Gardner, S. J. *Am. Chem. Soc.* **2004**, *126*, 3378-3379. (b) Wu, Y.; Liu, P.; Gardner, S.; Ong, B. S. *Chem. Mater.* **2005**, *17*, 221-223. (c) Wu, Y.; Li, Y.; Gardner, S.; Ong, B. S. *J. Am. Chem. Soc.* **2005**, *127*, 614-618. (d) Li, Y.; Wu, Y.; Gardner, S.; Ong, B. S. *Adv. Mater.* **2005**, *17*, 849-853.
3. (a) Meng, H.; Bao, Z.; Lovinger, A. J.; Wang, B.; Mujcsce, A. M. *J. Am. Chem. Soc.* **2001**, *123*, 9214-9215. (b) Afzali, A.; Dimitrakopoulos, C. D.; Breen, T. L. *J. Am. Chem. Soc.* **2002**, *124*, 8812-8813. (c) Murphy, A. R.; Frechet, J. M. J.; Chang, P.; Lee, J.; Subramanian, V. *J. Am. Chem. Soc.* **2004**, *126*, 1596-1597. (d) Payne, M. M.; Parkin, S. R.; Anthony, J. E.; Kuo, C.-C.; Jackson, T. N. *J. Am. Chem. Soc.* **2005**, *127*, 4986-4987. (e) Katz, H. E.; Lovinger, A. J.; Johnson, J.; Kloc, C.; Siegrist, T.; Li, W.; Lin, Y.-Y.; Dodabalapur, A. *Nature*, **2000**, *404*, 478-480. (f) Pappenfus, T.M.; Chesterfield, R. J.; Frisbie, C. D.; Mann, K. R.; Casado, J.; Raff, J. D.; Miller, L. L. *J. Am. Chem. Soc.* **2002**, *124*,

- 4184-4185. (g) Yoon, M.-H.; DiBenedetto, S. A.; Facchetti, A.; Marks, T. J. *J. Am. Chem. Soc.* **2005**, *127*, 1348-1349.
4. Wu, Y.; Li, Y.; Ong, B.S.; Liu, P.; Gardner, S.; Chiang, B. *Adv. Mater.* **2005**, *17*, 184-187. (b) (b) Huang, D.; Liao, F.; Molesa, S.; Redinger, D.; Subramanian *J. Electrochem. Soc.* **2003**, *150*, 412-417. (c) Li, Y.; Wu, Y.; Ong, B. S. *J. Am. Chem. Soc.* **2005**, *127*, 3266-3267. (d) Lefenfeld, M.; Blanchet, G.; Rogers, J. A. *Adv. Mater.* **2003**, *15*, 1188-1191. (e) Gray, C.; Wang, J.; Duthaler, G.; Ritenour, A.; Drzaic, P. *Proceedings of SPIE* **2001**, *4466*, 89-94.
5. (a) Bao, Z. ; Kuck, V. ; Rogers, J. A.; Paczkowski, M. A. *Adv. Funct. Mater.* **2002**, *12*, 1-6. (b) Facchetti, A.; Yoon, M.; Marks, T. J. *Adv. Mater.* **2005**, *17*, 1705-1725. (c) Veres, J.; Ogier, S.; Lloyd, G. *Chem. Mater.* **2004**, *16*, 4543-4555.
6. Wu, Y.; Liu, P.; Ong, B. S.; Srikumar, T.; Zhao, N.; Botton, G.; Zhu, S. *Appl. Phys. Lett.* **2005**, *86*, 142102.
7. Sirringhaus, H.; Tessler, N.; Friends, R.H. *Science* **1998**, *280*, 1741-1744.
8. Salleo, A.; Chabinyc, M. L.; Yang, M. S.; Street, R. A. *Appl. Phys. Lett.* **2002**, *81*, 4383-4385.
9. Kobayashi, S.; Nishikawa, T.; Takenobu, T.; Mori, S.; Shimoda, T.; Mitani, T.; Shimotani, H. ; Yoshimoto, N.; Ogawa, S. ; Iwasa, Y. *Nat. Mater.* **2004**, *3*, 317-322.

10. Gundlach, D. J.; Lin, Y. Y.; Jackson, T. N.; Nelson, S. F.; Schlom, D. G. *IEEE Electron Device Lett.* **1997**, *18*, 87-89.
11. Kelley, T. W. ; Boardman, L. D.; Dunbar, T. D. ; Muyres, D. V. ; Pellerite, M. J. ; Smith, T. P. *J. Phys. Chem B.* **2003**, *107*, 5877-5881.
12. Lee, L.-H.; Chen, W.-C.; Liu, W.-C. *J. Polym. Sci.: Part A: Polym. Chem.* **2002**, *40*, 1560-1571.
13. (a) Ong, B.S.; Wu, Y.; Liu, P.; Gardner, S. *Adv. Mater.* **2005**, *17*, 1141-1144.
(b) Arias, A. C.; Ready, S. E.; Lujan, R.; Wong, W. S.; Paul, K. E.; Salleo, A.; Chabynyc, M. L.; Wu, Y.; Liu P.; Ong, B. *Appl. Phys. Lett.* **2004**, *85*, 3304-3306.

5.3 Supporting Materials for the Paper

1. Instrumentation

Advancing water contact angle was measured on a DAT 1100-Fibro System using deionized water. Capacitance was measured with a BK Precision 820 capacitance meter (Dynascan Corporation). Thickness of thin film was measured with a Dektak 6M Stylus Profiler. OTFTs were characterized using Keithley SCS-4200 Characterization System under ambient conditions.

2. Synthesis of poly(methyl silsesquioxane).

Poly(methyl silsesquioxane) was prepared using methyltrimethoxysilane as precursor as follows: A mixture of 0.88 grams of 0.1 wt% aq. hydrochloric acid solution and 5.13 grams of tetrahydrofuran was added dropwise over a period of 30 minutes to a rigorously stirred mixture of 4.08 grams of methyltrimethoxysilane and 9.24 grams of methylisobutylketone in a 3-necked flask cooled with an ice bath under a dry atmosphere. The resulting mixture was allowed to warm to room temperature and then stirred at 60° C for 24 hours before subsequent use as the modification agent.

3. Deposition of Gate electrode.

Polyester substrate was first subject to heating at 160 °C for 10 min, cooled to room temperature and cleaned with isopropanol before use. A 7 wt% dispersion

of butanethiol-stabilized gold nanoparticles [Ref. Wu, Y.; Li, Y.; Ong, B.S.; Liu, P.; Gardner, S.; Chiang, B. *Adv. Mater.* **2005**, *17*, 184-187] in cyclohexane was filtered through 0.2 μm syringe filter, and then spin coated on the polyester substrate at 1000 rpm for 30 s. The coated gold nanoparticle layer was air dried and annealed in a vacuum oven at 150 $^{\circ}\text{C}$ for 30 min, resulting in a 90 nm-thick conductive gold layer on the polyester substrate. The surface of the gold layer was cleaned with air plasma for 30 seconds before subsequent deposition of gate dielectric.

4. Preparation of dual-layer gate dielectric layer.

A 13 wt% of poly(vinyl phenol-co-methyl methacrylate) (PVP-co-PMMA) (obtained from Aldrich, 51 mol % vinyl phenol) in DMF solution was filtered through a 0.2 μm syringe filter, and then deposited by spin coating on top of the above gold layer on the polyester substrate. The resultant 420-nm PVP-co-PMMA thin film was dried at 60 $^{\circ}\text{C}$ for 30 min and then annealed at 140 $^{\circ}\text{C}$ for 10 min. After cooling to room temperature, the PVP film was irradiated with an UV light ($\lambda = 254 \text{ nm}$) for 20 min, and then immersed in n-butanol at 60 $^{\circ}\text{C}$ to remove the unreacted polymer, giving a 380-nm crosslinked PVP-co-PMMA film after drying. Thereafter, a thin layer of poly(methyl silsesquioxane) ($\sim 50 \text{ nm}$) was spin coated on top of the PVP-co-PMMA layer and then cured by heating at 160 $^{\circ}\text{C}$ for 1 hour on a hot plate. The capacitance of the resulting dual-layer dielectric

was measured to be 9.0 nF/cm^2 with a BK Precision 820 capacitance meter (Dynascan Corporation) at room temperature. The dielectric constant of the dielectric layer was calculated to be 4.0.

5. Fabrication of source/drain electrodes and deposition of semiconductor.

A 7 wt% dispersion of gold nanoparticles in cyclohexane was deposited on the dielectric surface via a mask-assisted microcontact printing as follows. A stainless steel mask (thickness $\sim 13 \text{ }\mu\text{m}$) with an array of source/drain electrode feature apertures was placed on top of the dual-layer dielectric. A PDMS rubber sheet spin coated with a thin film of gold nanoparticles was laid on top of the mask. A gentle pressure was applied to the PDMS sheet to force the gold nanoparticle film to make contact with the dielectric surface through the apertures of the mask. After about 2 min, both the mask and the PDMS sheet were lifted, leaving the gold nanoparticle electrode features on the dielectric surface. The printed features of gold nanoparticles were annealed in a vacuum oven at $150 \text{ }^\circ\text{C}$ for 30 min, resulting in the formation of gold source/drain electrode pairs with channel lengths of 90 to $400 \text{ }\mu\text{m}$ and channel widths of 1000 to $5000 \text{ }\mu\text{m}$. Finally, a 30-nm thick of PQT-12 semiconductor layer was deposited by spin coating a dispersion of PQT-12 nanoparticles in dichlorobenzene, and annealed at $140 \text{ }^\circ\text{C}$ for 20 min. [Ref. Ong, B. S.; Wu, Y.; Liu, P.; Gardner, S. *Adv. Mater.* **2005**, *17*, 1141-1144].

6. Characterization of OTFTs.

The OTFTs were characterized in air using a Keithley 4200 Semiconductor Characterization System. The mobility in the linear and saturated regimes was extracted from the following equations:

$$\text{Linear regime } (V_D \ll V_G): I_D = V_D C_i \mu (V_G - V_T) W/L$$

$$\text{Saturated regime } (V_D > V_G): I_D = C_i \mu (W/2L) (V_G - V_T)^2$$

where I_D is the drain current, C_i is the capacitance per unit area of the gate dielectric layer, and V_G and V_T are respectively the gate voltage and threshold voltage. V_T of the device was determined from the relationship between the square root of I_D at the saturated regime and V_G of the device by extrapolating the measured data to $I_D = 0$.

Figure S1 shows the I-V characteristics for both forward (positive to negative) and reverse (negative to positive) scans at a source-drain voltage of -40V. The device exhibited only small hysteresis effect.

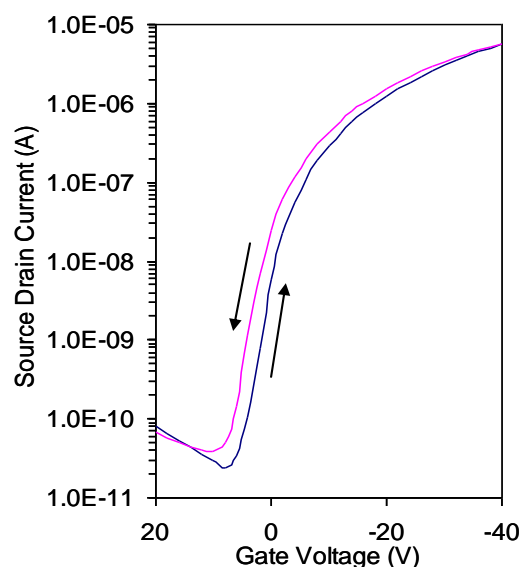


Figure S1. Forward and reverse scans of I-V characteristics at a source-drain voltage of -40 V for a typical OTFT with the dual-layer gate dielectric.

5.4 Summary

In this work, a novel solution-processable robust dual-layer gate dielectric was developed with a crosslinked poly(4-vinyl phenol)-co-poly(methyl methacrylate) bottom layer and a crosslinked poly(methyl silsesquioxane) top layer for the applications of organic thin-film transistors. This gate dielectric design, coupled with compatible solution-processable semiconductor and conductor materials, allowed for the fabrication of all solution-processed high performance organic thin-film transistors on flexible substrates.

Chapter 6

Integration of Solution Processed Flexible OTFTs in Non-Chlorinated Solvents

6.1 Introduction

This manuscript describes all solution processed flexible organic thin-film transistors (OTFTs) on plastic substrates. Semiconductor channels were deposited by solution processes with the developed copolythiophenes in non-chlorinated solvents. The dual-layer polymeric gate dielectric structure composed from a solution-processed crosslinked poly(vinyl phenol-co-methyl methacrylate) bottom layer and a solution-processed crosslinked organosiloxane top layer.

All flexible OTFTs with the developed semiconductors were fabricated on polyester films, which contained a thin layer of alumina functioned as a gate electrode. Source and drain (S/D) electrodes were obtained from a silver nanoparticle ink by inkjet printing. Vacuum-evaporated gold source and drain electrodes were also used for comparisons. All solution fabricated flexible OTFTs showed excellent thin-film transistor characteristics with field-effect mobility (μ) up to $0.1 \text{ cm}^2/\text{V}\cdot\text{s}$ and on/off current ratio to 10^4 , demonstrating that flexible OTFTs could be integrated from these solution-processable organic functional materials including semiconductors and dielectrics.

I was primarily responsible for the material synthesis, device fabrication, and characterization of the flexible OTFTs fabricated from the copolythiophenes and dual-layer dielectrics developed in this thesis. Dr. Yiliang Wu, Dr. Shiping Zhu, and Dr. Nanxing Hu provided valuable discussion and support.

6.2 Manuscript

All solution Processed Flexible Organic Thin-Film Transistors from Non-Chlorinated Solvents

To be submitted for the journal of *Materials Science and Engineering B*

1. Introduction

Organic thin-film transistors have attracted great interest from researchers in the recent years due to their potential to reduce the manufacturing costs in fabrication processes for flexible and large-area electronic device applications.¹⁻⁴ Unlike silicon transistor technologies that require sophisticated equipment and facility such as high temperature, high vacuum system and ultra clean room for device fabrication, OTFTs can usually be fabricated by low-cost liquid deposition techniques such as spin coating, dip coating, stamping, and printing. Such low-cost solution deposition technologies can be used in manufacturing processes to fabricate low-cost large-area integrated circuits, electronic sensors, radio

frequency identification tags, etc. on flexible substrates effectively. Significant progresses have been made in the recent years although challenges regarding the performance of OTFTs still remain because most organic semiconductors usually have lower field-effect mobility and are less stable in air than silicon counterparts. Many solution-processable organic materials including semiconductors,⁵⁻⁷ conductors,⁸⁻⁹ and dielectrics¹⁰⁻¹² have been developed for the flexible OTFTs applications. However, the fabrication of flexible OTFTs with all solution-processed materials including gate dielectrics, semiconductor channels, and source/drain electrodes with a good performance still presents a great challenge. This is one of the main reasons for most OTFTs still being fabricated on n-doped silicon wafer substrates with a top thin layer of thermally grown SiO₂ dielectric and vacuum-evaporated gold as source/drain electrodes.

In this article, we report a simple and low-cost material integration process for the fabrication of flexible OTFTs on plastics from all solution-processable semiconductors, dielectrics and source/drain electrodes. Solution-processed copolythiophenes (PQT-CH₃-*co*-PQT) [13] were used as semiconductor. A dual-layer dielectric structure composed of poly(4-vinyl phenol-*co*-methyl methacrylate) (PVP-*co*-PMMA) bottom layer and cross-linked poly(methyl silsesquioxane) top layer [12] was used as gate dielectrics. Silver nanoparticle inks [14] were printed as source and drain electrodes, as illustrated in Figure 1 for both top-contact and bottom-contact OTFTs.

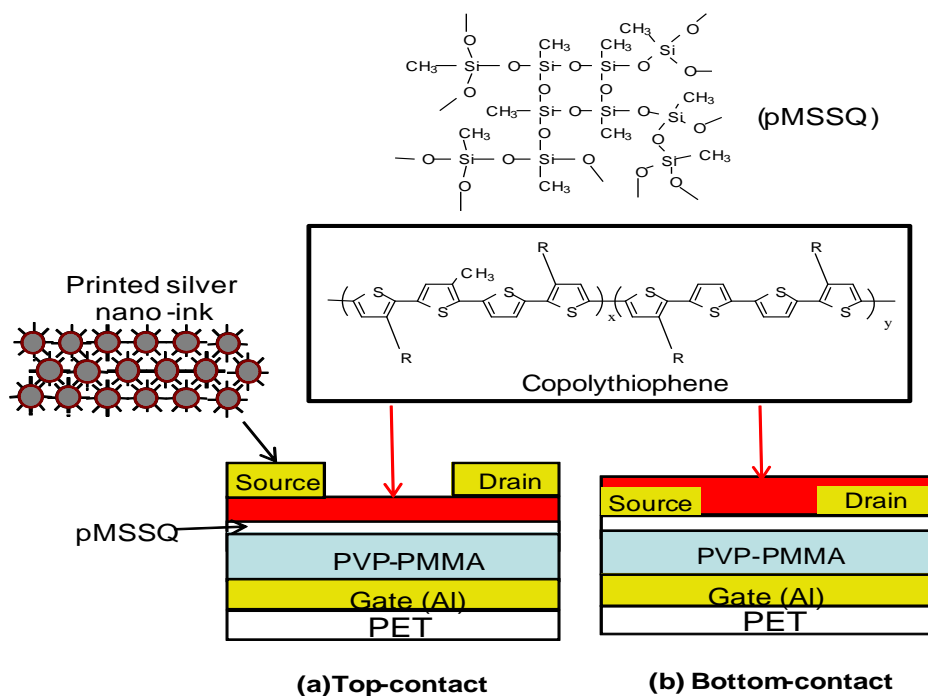


Figure 1. Schematic configurations of flexible OTFTs: (a) top-contact; (b) bottom-contact.

Evaporated gold source/drain electrodes were used as reference for comparison with printed silver electrodes from the silver nanoparticle inks.¹⁴ The performance of all solution processed flexible OTFTs with printed silver nano-ink source/drain electrodes achieved a similar level as those with evaporated gold source/drain electrodes. The field-effect mobility reached 0.07 to 0.1 cm²/V.s for top-contact configuration OTFTs. Furthermore, the semiconductor channels were obtained from solution-processable polythiophenes, processed from a more environmentally friendly non-chlorinated solvent system.

2. Experimental

2.1 Fabrications of flexible top-contact OTFTs

2.1.1 Dual-layer dielectric fabrications

An aluminized polyester (PET) film with ~200 nm aluminum top layer was used as a flexible substrate for OTFT fabrications. The thin aluminum layer on the top of PET functioned as the gate electrodes.

A dual layer gate dielectric was prepared by a previously published method with a little modification.¹² The first layer was obtained from a solution of poly(PVP-*co*-PMMA) in DMF (13 wt%) by spin-coating on the top of the aluminized PET substrate. The deposited film (~485 nm) was dried at 60 °C for 30 min and then at 140 °C for 10 min. The resulting film was then irradiated with a UV light ($\lambda=254$ nm) for 20 min, yielding a crosslinked polymeric film with a thickness of 430 nm. Then a 60 nm thin layer of poly(methyl silsesquioxane) was spin coated on the top of the poly(PVP-*co*-PMMA) layer and cured at 160 °C for one hour in an oven. The capacitance of the resulting dual-layer dielectric was 7.8 nF/cm², measured with a BK Precision 820 capacitance meter (Dynascan Corporation).

2.1.2 Depositions of source/drain electrodes and semiconductors

A semiconductor thin layer (30 nm) was deposited by spin coating directly on the top of the prepared dual layer dielectric using the solution-processable

copolythiophenes (PQT-CH₃-*co*-PQT)¹³ shown in Figure 1, containing 10 mol% of PQT-CH₃ (x=10) and 50 mol% of PQT-CH₃ (x=50) from their xylene solutions (~0.4 wt%) respectively. The spin coated semiconductor layer was annealed at 125-135 °C for about 20 min in a vacuum oven to improve the mobility of the semiconductor.

After the semiconductor layer was annealed, silver source/drain electrodes were printed using a solution-processable silver nanoparticle ink developed by Xerox Research Centre of Canada. The silver nanoparticles in the ink were stabilized by organoamine such as hexadecylamine by a reduction method with an average diameter of 5 nm.¹⁵ The silver nanoparticle ink was prepared by dispersing the silver nanoparticles (4 g) in a mixed solvent of dodecane (4 g) and terpineol (2 g), which was then filtered with 1µm syringe filter. A series of paired thin lines as the source/drain electrodes were printed with the silver nanoparticle ink directly on the prepared dielectric layer on the flexible PET substrate (see section 2.1.1) with a Dimatix (2800) inkjet printer at a substrate temperature of 50 °C. A 10 picoliter (pL) print head was used and a drop velocity of 5 m/s was set by adjusting the nozzle voltage. Highly conductive electrodes were obtained after the printed features were annealed at about 135 to 140 °C for 10 min. For the purpose of comparison with the printed silver electrodes, gold source/drain electrodes were also prepared by vacuum deposition on the top of the semiconductor layer.

2.2 Fabrications of flexible bottom-contact OTFTs

Bottom-contact flexible OTFTs were fabricated by the deposition of printed silver nanoparticle ink or vacuum-evaporated gold source/drain electrodes directly on the top of the prepared dual-layer dielectric layer using a similar method described in section 2.1.1, followed by the deposition of semiconductor layer. For bottom-contact OTFTs, semiconductor channels were deposited by both spin coating and inkjet printing techniques. The spin coated semiconductor layer was formed by the same method as described for the top contact OTFTs with both copolythiophenes containing 10 mol% and 50 mol% PQT-CH₃.

All printed flexible bottom-contact OTFTs including both printed silver nanoparticle source/drain electrodes and printed semiconductor channel were fabricated. The printed semiconductor channels were formed by printing a solution of the 50 mol% PQT-CH₃ copolythiophene in xylene (~ 0.4 wt%) into the channels of printed source/drain electrodes. The semiconductor channels were printed using the same Dimatix inkjet printer as used for the printed silver source/drain electrodes. The printed semiconductor channels were annealed at 125 °C in a vacuum oven for 10 min.

2.3 Characterization of OTFTs

All the fabricated OTFTs were characterized using Keithley 4200 Semiconductor Characterization System in ambient conditions. Both output curves (drain current versus drain voltage) and transfer curves (drain current versus gate voltage) for the flexible OTFTs were examined. The field effect mobility of OTFTs was extracted in the saturate region according to the following equation:

$$\text{Saturated regime } (V_D > V_G): I_D = C_i \mu (W/2L)(V_G - V_T)^2$$

where I_D is the drain current, C_i is the capacitance per unit area of the gate dielectric layer, and V_G and V_T are the gate voltage and threshold voltage respectively. V_T of the device was determined from the relationship between the square root of I_D at the saturated regime and V_G of the device by extrapolating the measured data to $I_D = 0$.

3. Results and discussions

The top-contact flexible OTFTs with the spin-coated copolythiophenes were fabricated in xylene solution. The main advantage of this type of copolythiophenes is their improved solubility, while maintaining high performance.¹³ Unlike other high performance polythiophene-based semiconductors such as poly(dialkylquaterthiophene) PQT,⁵ poly(2,5-bis(3-

alkylthiophene-2-yl)thieno[3,2-*b*]thiophene), PBTTT,¹⁶ and poly(4,8-dialkyl-2,6-bis-(3-alkylthiophene-2-yl)-benzo[1,2-*b*:4,5-*b'*]dithiophene),¹⁷ this type of copolythiophenes does not require chlorobenzene or dichlorobenzene in the deposition process because it can be dissolved in non-chlorinated solvent such as xylene, which is a much more environmentally friendly solvent.¹³ The source/drain electrodes were deposited from the silver nanoparticle ink by printing the conductive features directly on the top of the semiconductor layer. Vacuum-evaporated gold electrodes were used as a reference to compare with the printed silver electrodes. As shown in Figure 2, such all solution processed flexible top-contacted OTFTs showed excellent transfer characteristics (a) and output characteristics (b) with the copolythiophene containing 10 mole% of PQT-CH₃ and printed silver source/drain electrodes. The device can be turned on at a gate voltage close to zero with very a small threshold voltage, as shown in 2b. The mobility of the device reached 0.08 cm²/Vs with an on/off current ratio of 10⁴.

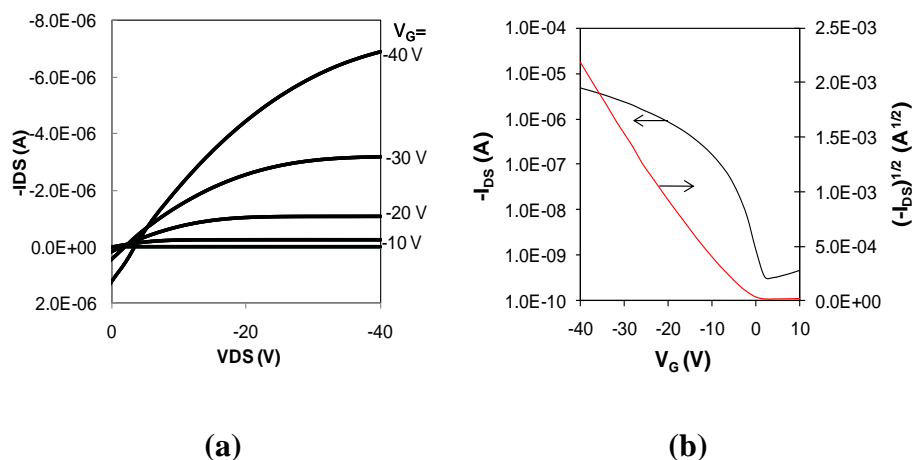


Figure 2 (a) Source-drain current versus source-drain voltage at different gate voltages; (b) Source-drain current versus gate voltage at a source-drain voltage of -40 v for OTFTs with the 10 mol% of PQT-CH₃ copolythiophene.

The output characteristics showed non-observable contact resistance with well behaved linear and saturate regions (2a). A small current leakage observed at a high gate voltage might be caused by coating defects of the dielectric dual-layer such as pinholes and roughness in the film.

Bottom-contact flexible OTFTs were also fabricated from both copolythiophenes, as described in the experimental section. In addition to the fabrication of bottom-contact OTFTs with evaporated gold source/drain electrodes, all printed bottom-contact flexible OTFTs were successfully fabricated on the PET substrates with the dual-layer dielectric structure using both printable silver nanoparticles as the source/drain electrodes and the printable

copolythiophene containing 50 mol% of PQT-CH₃ composition as the semiconductor.

The performances of both top and bottom-contact flexible OTFTs fabricated from the solution-processed copolythiophenes with the evaporated gold and printed silver source/drain electrodes are summarized in Table 1.

Table 1. Mobility and current on/off ratio for both top and bottom-contact OTFTs from the copolythiophenes containing 10 mol% and 50 mol% of PQT-CH₃ with both evaporated-gold and printed-silver source/drain electrodes.

Device Configuration	Copolythiophene (PQT-CH ₃) _x -co-(PQT) _y	Source/Drain Electrodes	Mobility (cm ² /V.s)	Current On/Off
Top-contact	x=10 mol% (spin coated)	Au (evaporated)	0.07 – 0.1	10 ⁴
	x=50 mol% (spin coated)	Au (evaporated)	0.04- 0.06	10 ⁴
Top-contact	x=10 mol% (spin-coated)	Ag (printed)	0.07 – 0.08	10 ⁴
	x=50 mol% (spin-coated)	Ag (printed)	0.04 - 0.06	10 ⁴
Bottom-contact	x=10 mol% (spin-coated)	Au (evaporated)	0.01- 0.03	>10 ²
	x=50 mol% (spin-coated)	Au (evaporated)	0.008 – 0.02	>10 ²
Bottom-contact	x=50 mole% (printed)	Ag (printed)	0.007 – 0.02	>10 ²

The OTFTs fabricated from the 10 mol% PQT-CH₃ copolythiophene showed higher mobility than the 50 mol% PQT-CH₃ copolymer. The decreased mobility with the higher PQT-CH₃ content was caused by the reduced crystallinity from the methyl groups in the PQT chain and it was consistent with the previous

result where OTFTs were fabricated from the same copolythiophenes on the n-doped silicon wafers with thermally grown SiO₂ as the dielectric layer.[13] It was also noticed that the top-contact OTFTs showed significantly better performance with a higher mobility and a higher on/off current ratio. This may be attributed to more efficient charge injections from the semiconductor channels to the source/drain electrodes with the top-contacted OTFTs. Furthermore, all printed flexible bottom-contact OTFTs were successfully integrated with both printed copolythiophene (x=50 mol%) and printed gold source/drain electrodes. The printed OTFTs functioned well with OTFT characteristics, showing mobility up to 0.02 cm²/V.s and on/off current ratio up to 10³. The relative lower mobility and on/off current ratio were mainly attributed to the unfavorable bottom-contact OTFT configuration. It was also found that the mobility values of both top and bottom-contact OTFTs with the printed silver source/drain electrodes were similar to those with the evaporated gold source/drain electrodes for both copolythiophenes. These excellent properties indicated that by replacing commonly used evaporated gold with the printed silver nanoparticles as the source/drain electrodes, cheaper OTFTs could be effectively fabricated from all solution-processed materials through the inkjet printing technologies, which would be more desirable for large-area and low-cost electronic applications.

4. Conclusions

In summary, both top and bottom-contact flexible OTFTs were integrated with all solution-processable materials on PET substrates without using environmentally unfriendly chlorinated solvents such as chlorobenzene or dichlorobenzene. The fabricated flexible devices showed good characteristics of OTFTs with mobility up to 0.1 and on/off current ratio up to 10^4 for the top-contact OTFTs. Furthermore, all printed flexible OTFTs were successfully integrated with bottom-contact configuration from the solution-processable copolythiophene as semiconductor channels and the silver nanoparticle ink as source/drain electrodes through inkjet printing. It was observed that OTFTs with the printed silver source/drain electrodes showed similar performance as those with the evaporated gold source/drain electrodes for both top and bottom-contact devices. With this solution-processable silver nanoparticle inks, the source/drain electrodes could be directly printed on various substrates such as silicon wafers, glass and flexible plastics without using any shadow masks, which would be much more convenient and cost effective for low-end, large-area, and flexible electronic device applications.

References

1. H. Sirringhaus, T. Kawase, R. H. Friend, T. Shimoda, M. Inbasekaran, W. Wu, E. P. Woo, *Science* 290 (2002) 2123-2126.
2. S. A. Jenekhe, *Chem. Mater.* 16 (2004) 438-4382, the special issue on organic electronics.
3. H. Sirringhaus, *Adv. Mater.* 17 (2005) 2411-2425.
4. J. Locklin, Z. Bao, *Anal Bioanal Chem.* 384 (2006) 336-342.
5. B. S. Ong, Y. Wu, P. Liu, S. Gardner, *J. Am. Chem. Soc.* 126 (2004) 3378-3379.
6. M. M. Payne, S. R. Parkin, J. E. Anthony, C.- C. Kuo, T. N. Jackson, *J. Am. Chem. Soc.* 127 (2005) 4986-4987.
7. Y. Li, S. P. Singh, P. Sonar, *Adv. Mater.* 22 (2010) 4862-4866.
8. Y. Li, Y. Wu, B. S. Ong, *J. Am. Chem. Soc.* 127 (2005) 3266-3267.
9. Y. Wu, Y. Li, B. S. Ong, *J. Am. Chem. Soc.* 129 (2007) 1862-1863.
10. M.-H. Yoon, H. Yan, A. Facchetti, and T. J. Marks, *J. Am. Chem. Soc.* 127 (2005) 10388-10395.
11. Y. Wu, P. Liu, B. S. Ong, *Appl. Phys. Lett.* 89 (2006) 013505.
12. P. Liu, Y. Wu, Y. Li, B. S. Ong, S. Zhu, *J. Am. Chem. Soc.* 128 (2006) 4554-4555.
13. P. Liu, Y. Wu, H. Pan, B. S. Ong, S. Zhu, *Macromolecules* 43 (2010) 6368-6373.

14. J. Doggart, Y. Wu, P.Liu, S. Zhu, *Appl. Mater. Interfaces*, 2 (8), (2010) 2189-2192.
15. Y. Li, Y. Wu, B. S. Ong, *J. Am. Chem. Soc.* 127, [2005] 3266-3267.
16. I. Mcculloch, M. Heeney, C. Bailey, K. Genevicius, I. Macdonald, M. Shkunov, D. Sparrowe, S. Tierney, R. Wagner, W. Zhang, M. L. Chabinyc, R. J. Kline, M. D. Mcgehee, M. F. Toney, *Nature Materials*, 5 [2006] 328-333.
17. H. Pan, Y. Li, Y. Wu, P. Liu, B. S. Ong, S. Zhu, G. Xu, *J. Am. Chem. Soc.* 129 [2007] 4112-4113.

6.3 Summary

In this chapter, the efforts were directed in the integration of flexible OTFTs on PET substrates with previously developed solution processed materials including the copolythiophene semiconductors in chapter 3 and the dual-layered dielectric in chapter 5. The integrated flexible OTFTs with both top and bottom-contact configurations with these materials developed in this work showed good properties of OTFTs with mobility up to $0.1 \text{ cm}^2/\text{V}\cdot\text{s}$ and current on/off ratio up to 10^4 for the top-contact OTFTs. Furthermore, non-environmentally friendly chlorinated solvents such as chloroform, chlorobenzene, and dichlorobenzene were eliminated during the fabrication of semiconductors by utilizing the developed copolythiophene semiconductors in the flexible OTFTs. In this work, solution processed silver source/drain electrodes were fabricated by inkjet printing using silver nanoparticles, which showed similar performance to vacuum evaporated gold source/drain electrodes. Thus costly high temperature and high vacuum deposition process with shadow masks could be eliminated by direct printing techniques. The results of this study demonstrated that all solution processed flexible OTFTs could be fabricated with solution processable functional materials and they have great potential applications for large area, low-end, and flexible electronic devices.

Chapter 7

Summary and Outlook

7.1 Summary

The research work presented in this thesis was focused on developing novel organic materials including semiconductors and dielectrics for organic thin film transistor applications. In addition to developing new functional organic materials, great efforts were made in the integration of flexible OTFTs using the developed organic semiconductors and dielectric materials. The main contributions of this thesis research include the following:

(1) Several new organic semiconductors were developed and their electronic properties were carefully characterized for the application of OTFTs. Chapter 3 described a material design and synthetic work for a class of new liquid crystalline small organic semiconductors and their OTFTs applications. The semiconductors 2,5'-bis-[2-(4-pentylphenyl)vinyl]-thieno(3,2-*b*)thiophene (**7**) and 2,5'-bis-[2-(4-pentylphenyl)vinyl]-2,2'-bithiophene (**8**) showed excellent air stability and OTFT performance. Furthermore, they are promising for the application of electronic devices where transparent OTFTs are required as their thin film absorption peaks appear mainly in the range of ultraviolet region.

(2) A facile approach was developed to improve the solubility of a high performance polythiophene (PQT) system through a judicious structure modification. A series of new copolythiophene semiconductors were synthesized and evaluated for OTFT applications. The copolythiophenes showed excellent

solubility and they were able to be solution-processed in more environmentally friendly solvents such as xylene while excellent OTFT properties were still maintained. Environmentally hazardous chlorinated solvents such as chlorobenzene and dichlorobenzene could thus be eliminated in OTFT fabrication processes. The details were described in Chapter 4.

(3) The development of solution-processable dielectric materials and a robust dielectric structure design for flexible OTFT applications was described in Chapter 5. A robust dual-layer dielectric composed from a crosslinked poly(4-vinyl phenol)-co-poly(methyl methacrylate) bottom layer and a crosslinked poly(methyl silsesquioxane) top layer was developed. This gate dielectric, together with compatible solution-processable semiconductors and conducting materials, allowed a low-cost solution fabrication for low-end flexible electronic device applications.

(4) Chapter 6 described OTFT integrations through solution process techniques such as spin coating and inkjet printing using the developed copolythiophene semiconductors and the dual-layer dielectric in this thesis work. Flexible OTFTs were successfully fabricated on PET substrates with solution depositions in non-chlorinated solvents. The fabricated top-contact OTFTs showed good characteristics of OTFTs with mobility up to about $0.1\text{cm}^2/\text{V}\cdot\text{s}$. Furthermore, in order to integrate all solution processed flexible OTFTs, source/drain electrodes were fabricated from the organoamine stabilized silver nanoparticle ink by inkjet printing techniques. In this study, a similar level of

OTFT performance was achieved compared to the results from the OTFTs with vacuum-evaporated gold source/drain electrodes. Thus much more expensive gold electrodes fabricated with costly high vacuum evaporation process at high temperature could be eliminated.

In conclusion, this thesis research made significant contributions in the areas of developing organic semiconductors, gate dielectrics, and solution fabrication process for the application of organic thin film transistors. The developed copolythiophene semiconductors and crosslinked dual-layer dielectric structure allowed a solution fabrication process for flexible OTFTs on plastic substrates without using environmentally hazardous chlorinated solvents such as chloroform, chlorobenzene and dichlorobenzene. In addition, the research results obtained from this thesis could help us better understand the effect of semiconductor structures and conformations on the solution processability and the OTFT performance.

7.2 Outlook

Over the last two decades, significant progresses have been made in the material development and the fabrication process for the organic thin film transistor applications. Particularly, great efforts have been made on developing high performance solution processable organic semiconductors, which are one of the key elements for solution processed OTFTs. At present, high performance

organic thin film transistors have been fabricated on various substrates such as glasses and plastics, and the mobility of some thiophene-based organic semiconductors has reached up to about $1 \text{ cm}^2/\text{V.s.}$ In addition, potential applications of OTFTs for low-end electronic devices such as electronic sensors, RFID tags, and even flexible displays have been demonstrated. However, significant challenges still remain to realize the practical electronic applications for OTFTs.

First of all, an improvement in the device performance and robustness is crucial in order to achieve practical electronics applications for OTFTs. The improvement can be achieved through optimizations of material structures, formulations, and device fabrications including solution processable semiconductors, dielectrics, and conductive metal nanoparticle inks. For example, the mobility and solubility of the copolythiopenes (PQT-CH₃-co-PQT), developed in this thesis study, could be further improved through the optimizations of their molecular structures and coating solutions. Higher mobility could be likely achieved through incorporating more conjugated thiophene or aromatic moieties in the main polymer chain and better solubility could be likely obtained through incorporating longer alkyl side chains. To prevent electrical current leakage, the robustness of the dual-layer dielectric structure could be further improved by increasing the crosslink network in the dielectric structure. Furthermore, the properties of the interface between the solution deposited semiconductor layer and the gate dielectric layer have significant impacts on the OTFT performance. More

consistent field effect mobility and current on/off ratio could be obtained by reducing the roughness of the solution deposited films through optimizations of the coating solutions and thickness of the films.

Second, it still remains a big challenge to obtain sustained high performance OTFTs currently. So far, most high performance OTFTs can be only obtained from their initial device evaluations and their performance such as mobility and current on/off ratio are usually degraded very fast, compared to traditional silicon TFTs. This is because most high mobility organic semiconductors are air sensitive and they can be easily oxidized at ambient conditions. To realize electronic applications for OTFTs, the device lifetime should be improved significantly. The stability of OTFTs can be improved by using organic semiconductor materials with large band gap and low HOMO energy level to improve the air stability against oxidations. Furthermore, lifetime of OTFTs can be improved by optimizations of the device configurations such as adding an overcoat layer to prevent or slow down the process of oxidizations.

Third, organic materials with the ability for large scale manufacturing production such as roll to roll solution processes play an important role in realizing the advantages of solution processed OTFTs for low cost electronic device applications. To enable roll to roll solution processing, functional organic materials with good solubility in non-chlorinated solvents are desired. However, most high performance organic semiconductor materials still require chlorinated solvents during the OTFT fabrications.

In summary, continued efforts on functional material developments including both solution processable organic semiconductors and gate dielectrics are essential for the integration of OTFTs into low-end and large area electronic devices. Organic semiconductors with high mobility, air stability, and good solubility in non-chlorinated solvents play a key role for OTFTs in practical electronic applications.